AN ABSTRACT OF THE THESIS OF

Jonathan W. Huggins for the degree of Master of Science

in Department of Geology presented on September 9, 1977

Title: Geology of a Portion of the Painted Hills Quadrangle, Wheeler County, North-Central Oregon

Redacted for privacy

Abstract approved: _____
Dr. E.M. Taylor

The thesis area is located in north-central Oregon approximately 15 kilometers northwest of the town of Mitchell. Painted Hills State Park is located at the southeast corner of this area. Two major geologic formations are found within this thesis area; the Clarno Formation and the John Day Formation. The dominant rock types of the Clarno Formation include lava flows of basaltic andesite, andesite, dacite and rhyodacite and cover approximately 70 percent of the study area. In addition to lava flows, the Clarno Formation is composed of interbedded tuffs, minor mudflows and rare intrusive rocks. Mineralogically the lava flows are very similar and most contain three phenocrystic phases. These phases are plagioclase, clinopyroxene and orthopyroxene. In addition, several have phenocrysts of quartz which are commonly surrounded by reaction rims of clinopyroxene and glass. Alteration

products of the flow rocks include calcite, several zeolites, smectite, chlorite, kaolinite, magnetite, celadonite, nontronite and very minor sericite. The interbedded tuffs are composed predominantly of the smectite montmorillonite although one contains abundant kaolinite and another minor clinoptilolite. The John Day Formation is a thick sequence of layered air fall pyroclastics and an ignimbrite comprised of two cooling units. This formation is divided into three members.

The chemical variation diagrams (Harker) as well as AFM and KCN plots of 60 analyzed samples of Clarno rocks follow typical calc-alkaline trends. However, when plotted on a Peacock diagram the rocks of this area are found to be calcic. This calcic nature is probably due to abundant plagioclase phenocrysts and alteration effects.

Most of this thesis area lies on the northwestern flank of the northeast trending Sutton Mountain syncline. All of the dips in the area are gentle with measurements difficult because of slumping. Faulting in the area is of the normal type with only minor displacements. Two fault trends are recognized with one north-south and the other east-west.

Geology of a Portion of the Painted Hills Quadrangle, Wheeler County, North-Central Oregon

by

Jonathan Wayne Huggins

A THESIS

submitted to

Oregon State University

in partial fulfillment of
the requirements for the
degree of

Master of Science

June 1978

APPROVED:

Redacted for privacy

Professor of Geology (in charge of major)

Redacted for privacy

Chairman of the Department of Geology

Redacted for privacy

Dean of Graduate School

Date thesis is presented: September 9, 1977

Typed by Janell Huggins for: Jonathan W. Huggins

ACKNOWLEDGEMENTS

I wish to extend my thanks to Dr. E.M. Taylor for his help in the laboratory and in the preparation of this paper. I would also like to thank Dr. Harold Enlows for his help with the petrography and Dr. Alan Niem for critically reading this manuscript.

My special appreciation is extended to my wife, Janell, for her long hours at the typewriter, her emotional and financial support and through it all, her sense of humor.

TABLE OF CONTENTS

TABLE OF CONTENTS (continued)

LIST OF FIGURES

LIST OF FIGURES (continued)

LIST OF FIGURES (continued)

LIST OF TABLES

LIST OF PLATES

Geology of a Portion of the Painted Hills Quadrangle, Wheeler County, North Central Oregon

INTRODUCTION

Location

The area of this investigation is located along the eastern margin of Wheeler County in north-central Oregon. This is approximately 12 to 20 km northwest of the town of Mitchell in the Painted Hills Quadrangle. The mapped area comprises approximately 64 km^2 and includes sections 1-4, 9-16, 21-28 and 33-36, T. 10 S., R. 20 E. (Fig. 1). The northern boundary of this area is the westward flowing John Day River, the eastern boundary is the western flank of Sutton Mountain and the southern boundary is marked by Painted Hills State Park. No distinctive geographic feature marks the western boundary.

Geography and Climate

With the exception of the John Day River on the north, there are only two small perennial streams. Bridge Creek flows from the southeast corner of the area toward the northwest, joining the John Day River and Bear Creek flows toward the northeast joining Bridge Creek (Fig. 1). These streams are fed by drainage from the Ochoco Mountains to the south. In addition, there are numerous canyons and gullies carved by ephemeral streams which contain water only in the early spring and in the summer following thunderstorms.

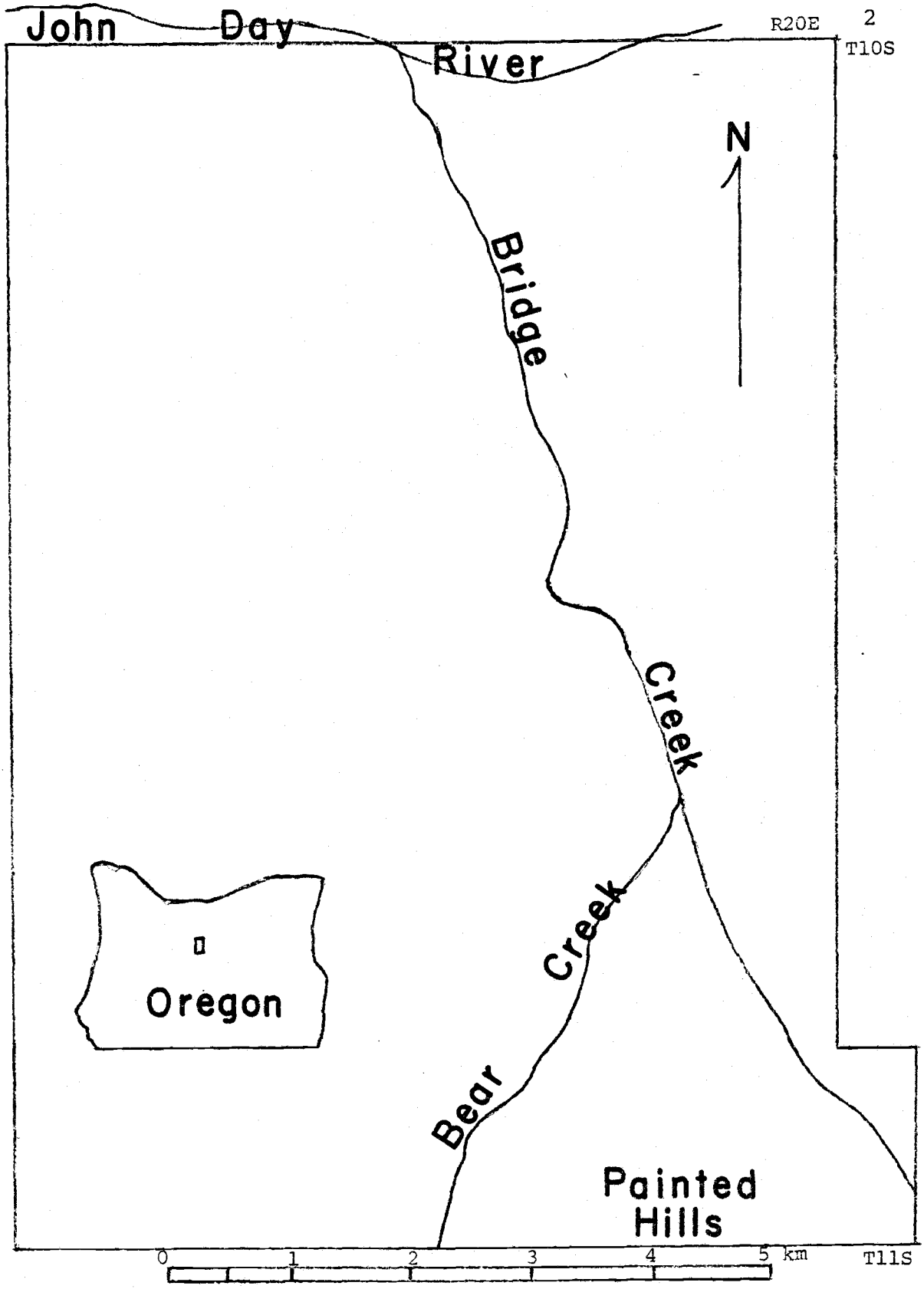

Figure 1. Location of thesis area, north-central, Oregon.

The relief of the area is 650 m. The highest elevation is 1110 m at the southwest corner of the area and the lowest elevation is 460 m along the John Day River. The topography consists of deep, steep-sided valleys, hogback ridges with gently dipping dip-slopes, flat-topped mesas and in many areas gently rolling hills.

Because this area is located approximately 100 km east of the north-south trending Cascade Range, the climate is semi-arid. The local vegetation consists mostly of sagebrush, juniper and range grass.

Accessibility and Exposure

The area can be reached by U.S. Highway 26 which is the major east-west thoroughfare through this part of Oregon. Bridge Creek road, which cuts across the thesis area in a northwesterly direction, forms a junction with U.S. 26 approximately 6.5 km west of Mitchell. The southern boundary of the thesis area is reached after traveling 9.6 km northward along Bridge Creek road. This is also the location of Painted Hills State Park. In addition to Bridge Creek road, there is one other improved but unpaved road which joins it and leads to Twickenham, a small community along the John Day River about 15 km to the northeast. Other roads in the area are unimproved or simple jeep paths and are accessible for the most part only by four-wheel-drive vehicles.

Because of the semi-arid nature of the climate, exposures are excellent throughout the area. The only difficulty in finding exposures occurs in two small areas where landslides have covered the bedrock.

Purpose and Methods of Investigation

The main purpose of this investigation is to construct a geologic map and describe in detail the mineralogical and chemical composition of the rocks in this area. Previously very little work has been done on the Clarno Formation and none in the area of this thesis. Several square kilometers of John Day Formation crop out in this area. Studies by other writers (Hay 1962b, 1963 and Fisher 1966) give adequate descriptions of the John Day Formation in this thesis area, therefore, the author has concentrated his studies on the Clarno Formation.

Initially it was believed that an unconformable contact within the Clarno, which has been identified to the south, would extend into the thesis area and a close study of this contact was planned. It was soon discovered, however, that this unconformity is not present and it is now thought that the contact will be found further to the southeast (Taylor, 1977 personal communication). It is hoped that this study will contribute to a better understanding of the Clarno Formation. This Formation may become important in deciphering the geologic and tectonic history of the Pacific Northwest during the Eocene and Oligocene periods.

Field work was conducted during the summer of 1976. Mapping was completed on a 7.5 minute topographic map of the Painted Hills Quadrangle published by the United States Geologic Survey in 1968 and with the aid of aerial photos flown in 1968 by the United States Department of Agriculture. Additional high altitude, Earth Resources Technology Satellite (ERTS) photos, provided by Dr. R.D. Lawrence, were examined to help identify large structural features in this area. The scale of the map is 1:24,000. All contacts and sample locations were drawn directly on the map while in the field and all recognizable faults were mapped.

The colors of all samples, both fresh and weathered, were described according to the Rock Color Chart published by the Geological Society of America (Goddard, 1970). Attitudes of beds were measured with a Brunton compass.

Approximately 200 samples were collected and after examination with a binocular scope about half this number were examined in greater detail in the laboratory. These studies included the examination of 85 thin sections in which modal analysis were performed on phenocrystic phases using 600 counts and groundmass phases using 450 counts. Plagioclase compositions were determined by the statistical method of Michael-Levy (Kerr, 1959).

Whole rock chemical analysis was performed on 60 samples. Weight percentages of FeO (total iron), TiO_2, CaO, K_2O and Al_2O_3 were determined by x-ray fluorescence spec-

trometry, Na_2O and MgO were determined by atomic absorption spectrometry and SiO_2 was determined both by x-ray fluorescence and visible light spectrometry. H_2O determinations were not made since all water was removed from the samples during their preparation. A brief explanation of procedures followed can be found in Appendix A. Although all sample preparation was performed by the author, the analytical runs were performed by Ruth L. Lightfoot and Dr. E.M. Taylor, Department of Geology, Oregon State University.

Clay mineral analysis of four tuff beds was performed using magnesium and potassium saturation, glycolation and heating techniques (Harward, 1977). X-ray diffraction patterns were obtained for identification. This method will be described in detail in a later section. X-ray diffraction was also used to help in the identification of alteration products of sixteen different flow rocks and one mudflow. Again this method will be described in a later section. Some zeolite identification was also possible using x-ray diffraction.

The volcanic rocks in this study will be classified on the basis of weight percent SiO_2 modified after Nockolds (1954) as suggested by Taylor (1977, personal communication). Rocks with an SiO_2 content of between 53 and 58 percent will be classified as basaltic andesite, between 58 and 63 percent as andesites and between 63 and 68 percent as dacite. Rhyodacites will be defined as those rocks with an SiO_2

weight percent greater than 68.

Geologic Setting

This thesis area contains the lower two of a succession of continentally deposited Cenozoic volcanic and volcaniclastic rocks of north-central Oregon. The earliest of the Cenozoic formations is the Clarno and this is unconformably overlain by the John Day Formation. A general stratigraphic column for the region of north-central Oregon is shown in Figure 2.

Considered in a regional sense, the Clarno is composed of lava flows ranging in composition from basalt to rhyolite, minor ash-flow tuffs, large amounts of tuffs and mudflows, minor epiclastic sandstones, breccias, conglomerates, minor agglomerates and a variety of intrusives including dikes, sills and small piston intrusions. The intrusions, as with the lava flows, show a wide range of chemical composition. Within a few miles of the thesis area are intrusions of melabasalt, andesite and rhyolite. These include Marshall Butte, White Butte and Sargent Butte (Oles and Enlows 1971). The regional stratigraphic sequence of the Clarno Formation is not well known because of the rapid lateral variations in the lithologic types. Abundant minor slumps and faults also complicate the sequence.

In this thesis area the Clarno is composed predominately of lava flows ranging in composition from basaltic andesite to rhyodacite. There is also some minor reworked tuff in

Figure 2. Generalized stratigraphic column for the area around the thesis area in north-central Oregon modified from Rogers and Novitsky-Evans (1977). Sources for potassium-argon dates as follows:

Deschutes Fm.	Armstrong and others (1975) Walker and others (1974)
Rattlesnake Fm.	Davenport (1971)
Mascall Fm.	Davenport (1971)
Picture Gorge Basalts	Watkins and Baksai (1969) Walker and others (1974)
John Day Fm.	Evernden and James (1964) Evernden and others (1964) Swanson and Robinson (1968) Walker and others (1974)
Clarno Fm.	Evernden and James (1964) Evernden and others (1964) Swanson and Robinson (1968) Enlows and Parker (1972) Dalrymple and Lamphere (1974) Walker and others (1974)

AGE		FORMATION	LITHOLOGY	K-Ar AGE
QUARTERNARY	PLEISTOCENE	QUATERNARY DEPOSITS	ALLUVIUM	
TERTIARY	PLIOCENE	DESCHUTES AND RATTLESNAKE	FLUVIAL SANDSTONE SILTSTONES, MUDFLOWS CONGLOMERATES, TUFFS BASALT, ANDESITE, IGNIMBRITES IGNIMBRITE FANGLOMERATE	4.5 5.3 6.4 12.0
	UPPER MIOCENE	MASCALL	FLUVIAL SANDSTONE, ASH, TUFF, CONGLOMERATE IGNIMBRITE	15.8
		COLUMBIA RIVER GROUP PICTURE GORGE BASALT	THOLEIITIC BASALT	14.5 14.6 15.2
	LOWER MIOCENE TO MIDDLE EOCENE	JOHN DAY	TUFF, IGNIMBRITE RHYOLITE ALKALI BASALT TRACHYANDESITE	23.3 24.9 25.3 29.4 31.1 32.0 36.1
	LOWER OLIGOCENE TO MIDDLE EOCENE	CLARNO	BASALT, ANDESITE, DACITE, RHYODACITE TUFF, MUDFLOW INTRUSIVE ROCKS	36.5 37.5 40.5 41.0 43.1 43.3 46.1
CRETACEOUS	ALBIAN TO CENOMANIAN	HUDSPETH GABLE CREEK	MARINE MUDSTONE GRAYWACKE, CONGLOMERATE	
PERMIAN		METASEDIMENTS	GLAUCOPHANE-LAWSONITE SCHIST, PHYLLITE	

small areas between flows and very minor epiclastic sands and gravels. Except for one small locality (NW¼, Sec. 11) all of the mudflow deposits are found in the extreme northwest corner of the area (NW¼, Sec. 4). Thick mudflow deposits can be seen on the north side of the John Day River just out of this study area. This thesis area shows an unusual lack of intrusive rocks compared to most areas of the Clarno with only one small east-west trending andesite dike.

Oles and Enlows (1971) have divided the Clarno into two informal members in the Mitchell Quadrangle 8 to 24 km to the east and southeast, calling them the lower and upper Clarno. According to this division all of the rocks of this area would be assigned to the lower Clarno. Much remains to be learned concerning the unconformity between the two, however, and because their division has not yet been formalized, the rocks in this study will be referred to as the Clarno Formation and not the lower member of the Clarno group.

All or parts of the John Day Formation in this area have been studied in some detail (Hay 1962, 1963 and Fisher 1963). Hay (1962) divided this formation into three members. The lower member is made up predominately of tuffaceous claystones with some intercalated vitric tuffs and two alkali olivine basalt flows. The middle member is a rhyolitic ash-flow tuff which serves as the

basis for the three part division and can be traced over an extensive area (Fisher 1966). The upper member is composed of more tuffaceous claystones and tuffs with some tuffaceous conglomerates and sandstones. In this area the formation ranges from 300 m to 900 m in thickness.

To the west-northwest the John Day Formation was divided into nine different members all lying conformably on one another as is the case in the Painted Hills area (Peck 1964). This area to the west, between Ashwood and Willowdale, shows some differences in lithology relative to the Painted Hills since it is composed mostly of lapilli tuff, numerous ash-flow tuffs, some flows of trachyandesite and rhyolite and many alkali olivine basalt flows. The thickness of the John Day in this area is approximately 1220 m.

Later work has shown that most of the section in the Ashwood-Willowdale area, up to the lower welded tuff of Peck's member H, correlates to the lower member described in the Painted Hills areas (Robinson 1968, 1973). This correlation was possible because of a distinctive soda sanidine rich layer forming a welded tuff in the west and an air-fall tuff at Painted Hills (Hay 1963). The middle member welded tuff at Painted Hills correlates to the basal welded tuff of member H near Ashwood. Robinson (1968, 1973) has chosen to refer to the John Day rocks near Ashwood and Willowdale as the western facies and those in Painted Hills and further east around Picture Gorge as the eastern facies, retaining

the original subdivisions of Peck and Hay respectively. In this paper these subdivisions will also be used.

The structural pattern of the region surrounding this thesis area consists of a few large scale and several small scale northeast-southwest trending anticlines and synclines. In addition there are several large east-west trending folds, the largest of which is the Ochoco Mountain anticline. Further to the east the Monument Dike Swarm shows a northwest-southeast trend (Fisher 1967).

The trend of the fold structures found in and immediately around this thesis area are northeast-southwest. The largest of these structures is the Blue Mountain anticline (Fisher, 1967), the axis of which is found a few kilometers to the northwest. This structural high appears to have been present since pre-Clarno time and has greatly influenced the deposition of most of the formations of this area, especially the John Day (Hay 1962, Fisher 1967 and Robinson 1968). Today this anticline still forms a topographic high. Just to the south of the thesis area the Cretaceous and Clarno rocks are strongly deformed into another northeasterly trending structure, the Mitchell anticline. The Clarno and John Day rocks found in the thesis area form the limbs of a gently dipping syncline which plunges to the northeast. This syncline is a continuation of the Sutton Mountain syncline of Oles and Enlows (1971).

Most of the faulting in this region is normal. A few

faults, such as the Mitchell fault several kilometers to the south, have had strike-slip movement of up to 6.7 km (Oles and Enlows, 1971).

Previous Work

The John Day Formation was originally named by Marsh (1875). Later, Merriam (1901) used this name to describe some of the volcanic strata in the vicinity of Picture Gorge. Calkins (1902) further studied the petrography of this formation.

In this thesis area, the John Day Formation has been studied in considerable detail by Hay (1962b, 1963) and Fisher (1966). In areas to the west and east some of the major studies include Coleman (1949), Fisher and Wilcox (1960), Peck (1961 and 1964), Robinson (1968 and 1973) and Swanson and Robinson (1968).

The fossil beds of the John Day Formation are world famous for their mammalian as well as abundant floral fossils. Because of this many people have studied and published on the paleontological aspects of this formation and no listing of previous work will be attempted here.

The Clarno Formation was named by Merriam (1901) in an area to the northwest along the John Day River at Clarno Ferry. The following year Calkins (1902) studied the petrography of Clarno rocks. Little work was done with the Clarno Formation until 1942 when E.T. Hodge published the results of his many years of study of the geology of north-central

Oregon. A few years later a brief report by Wilkinson (1950) and an important work by Waters and other (1951) was published. More recently the Clarno was studied by Oles and Enlows (1971). From 1939 to the present many students have worked in parts of the Clarno Formation. A few of the theses which deal in part or in whole with the Clarno are listed below:

Wilkinson (Ph.D.)	1939	Snook (M.S.)	1957
Dobell (M.S.)	1949	Lindsley (Ph.D.)	1960
Taubeneck (M.S.)	1950	Taylor (M.S.)	1960
Dawson (M.S.)	1951	Lukanuski (M.S.)	1963
Swarbrick (M.S.)	1953	White (M.S.)	1964
Bowers (M.S.)	1953	Patterson (M.S.)	1965
McIntyre (M.S.)	1953	Wilson (M.S.)	1973
Bedford (M.S.)	1954	Novitsky-Evans (M.S.)	1974
Irish (M.S.)	1954	Owen (M.S.)	1977
Howard (M.S.)	1955	Barnes (In Progress)	

Paleontological studies involving the Clarno began in 1902 with Knowlton. Since then many papers from various authors dealing with the flora and fauna have appeared in the literature. A few of the floral studies include Chaney (1927 and 1952), Arnold (1945), Scott (1954), Hergert (1961), Gregory (1970) and McKee (1970). Significant faunal assemblages were not discovered until 1954 by Lon Hancock which has limited published work. However, a few include Stirton (1944), Brogan (1960) and Hansen (1973). These different fossil assemblages have helped greatly in determining the age and paleoclimate of the Clarno Formation.

Other geochronologic studies using potassium-argon dating techniques have been done by Evernden and James (1964)

and Evernden and others (1964) in which they dated samples from both the John Day and Clarno Formations in this area and to the south. More recently Enlows and Parker (1972) have dated additional Clarno rocks from the Mitchell Quadrangle adjacent to and south-east of this area.

Geologic maps of this area include a U.S. Geological Survey reconnaisance map made by Swanson (1969) and a slightly more detailed map made by Robinson (1975).

STRATIGRAPHY

Clarno Formation

Introduction

The Clarno lavas, although found to be chemically variable, are megascopically very similar. The author was unable to divide and map the majority of these rocks from hand sample identification. Therefore, most of these lavas were mapped as a single inclusive unit.

Laboratory studies show a significant range in composition of the Clarno lavas with a variation in silica weight percent of 55 to around 70. These rocks will be described in three major groups based on their chemistry; basaltic andesite, andesite and dacite comprise the main divisions. These lavas cover approximately 44 km^2 and encompass close to 70 percent of this study area. Eighty thin sections were made for the petrographic study of these rocks.

Distinctive mappable units within the Clarno Formation include interbedded tuffs, mudflows and two lava flows. The lava flows will be given informal names using related geographic features in accordance with the Code of Stratigraphic Nomenclature (American Association of Petroleum Geologists-1961).

I. Basaltic Andesite

General Statement

The basaltic andesites are found on the northern and

eastern edge of this area, as well as in a small area of about 2 km^2 in sections 11 and 14. The outcrops of easiest accessibility are found above Bridge Creek road in the SW¼, SE¼, Sec. 11, T. 10 S., R. 20 E. and along the John Day River in the NE¼, NW¼, Sec. 2 T. 10 S., R. 20 E.

These flows are extremely variable in thickness, ranging from 3 m to around 70 m. The thickness appears to be related to the underlying topography with the thinner flows deposited upon flat ground and the thicker flows forming in small narrow canyons. Platy fracture predominates in the basaltic andesite flows but blocky fracture is also found. In addition columns of varying size and form are seen in some flows.

On fresh surfaces, the color in these lavas is dark gray (N3) to medium dark gray (N4) while the weathered surfaces show many shades of brown and yellow. Pale yellowish brown (10 YR 6/2) is the most common color on weathered surfaces.

Petrography

The basaltic andesite lavas are all porphyritic and contain two pyroxene phases. The three major phenocrystic phases include plagioclase, hypersthene and augite. In addition a few flows contain a small amount of quartz phenocrysts. The discussion of the quartz-bearing flows will be found in the following section dealing with the lavas of andesitic composition. The groundmass of the basaltic

andesite flows consist of plagioclase, hypersthene, augite and magnetite. In addition many flows contain biotite, apatite and glass as primary groundmass phases. Alteration products include zeolites, clay minerals, hematite, carbonate and an unidentified material which is colorless, has low relief and birefringence and is interstitial to the groundmass microlites. This material is most likely alkali-rich feldspar from the last melt to crystallize in the lava or devitrification products which might include cristobalite as well as feldspar. A volumetric modal analysis of a few selected basaltic andesites is presented in Table 1.

Pilotaxitic and glomeroporphyritic texture are very common although not ubiquitous in these rocks. Of the 14 samples examined only 20 percent did not have pilotaxitic and 20 percent did not have glomeroporphyritic textures although all samples had at least one or the other. Intergranular texture is also common with pyroxene and magnetite found between the plagioclase microlites (Figure 3). In a few samples the glomeroporphyritic clumps of pyroxene and plagioclase show poorly developed ophitic texture.

The plagioclase phenocrysts are found up to 4.0 mm in length, averaging 2.5 mm, and are subhedral to annhedral in form with rare crystals which are euhedral. Commonly these phenocrysts are composed of two or more crystals in a synneusis relationship. Compositionally they were found to be calcic labradorite with a range of An_{59} to An_{66} and

Table 1. Volumetric modes of selected Clarno basaltic andesite.

Sample*	JWH-141	JWH-91	JWH-64	JWH-14	JWH-138
Phenocryst Phases:					
Labrodorite	12.8	6.0	T	T	15.0
Augite	3.8	T	T	3.0	3.7
Hypersthene	2.2	T	-	1.0	5.7
Quartz	-	T	-	-	T
(T = less than 0.1%)					
Groundmass Phases:					
Labrodorite	68.9	68.0	63.1	52.2	60.9
Augite	27.8	24.0	16.4	26.7	18.4
Hypersthene	-	7.1	6.2	-	12.5
Magnetite	3.1	0.9	11.8	6.5	5.5
Biotite	0.2	T	-	T	T
Apatite	T	T	-	T	T
Glass	T	-	2.5	-	2.7
Clay	T	T	T	0.2	T
Zeolite	T	-	-	14.4	T
Hematite	T	-	-	-	T
(T = less than 0.2%)					

* See Appendix A for chemical analysis and sample location.

Figure 3. Photomicrograph of basaltic andesite showing intergranular and pilotaxitic texture with crossed nicols. Minerals include labradorite, augite, hypersthene and magnetite. Note also abundant interstitial glass. (Sample JWH-64 from SW¼, SE¼, Sec. 11, T. 10 S., R. 20 E.)

an average of An_{63}. The abundance in the different flows differs from a trace to 15 volumetric percent and averages 11 percent.

Several varieties of zoning were observed including normal, oscillatory and patchy zoning. Patchy zoning was studied by Vance (1965). He believed this type of zoning is due to partial resorption of an early formed plagioclase followed by crystallization of more sodic plagioclase in the areas of resorption and around the rim. These he called "included plagioclase" and "rim plagioclase" respectively.

Some basaltic andesites as well as other rocks of this thesis area have this type of zoning. However, the majority of the plagioclase with this partial resorption does not show the more sodic "included plagioclase" but instead have pockets of clear glass. This is due to rapid crystallization after extrusion to the surface. In addition, a relatively rapid ascent from depth to the surface is indicated by the fact that resorption is not very complete. These glass inclusions are very common in volcanic rocks and have been described by Kuno (1950). The "rim plagioclase" is found on most of the resorbed phenocrysts in the rocks of this area. Vance discussed several theories for the cause of the resorption but favors a decrease in confining pressure on the melt as the leading cause. This requires that the melt be water deficient which may be contrary to other

mineralogical evidence (quartz phenocrysts) which is discussed later. Taylor (1960) stated that the oscillatory zoning, which is very common in the flows of this area (Figures 4 and 5), was also due to periodic decreases in pressure. He believed the decrease was rapid and related to surface eruptions. These pressure fluctuations cause fluctuations in the liquidus temperature and thus alternating crystallization of more and then less sodic material. A feature in most of these rocks which indicates a possible mixing of magmas is seen in Figure 6. Three plagioclase phenocrysts occur together but each shows different degrees of resorption. The middle phenocryst is very fresh while others less than a millimeter away are partly and almost completely resorbed.

A feature which seems to be more characteristic of the basaltic andesites than the other lavas of this area is the abundant inclusions in the plagioclase phenocrysts. These inclusions are augite, hypersthene, magnetite and minor apatite (Figures 7 and 8).

Twinning is predominately of the albite type in both the groundmass and phenocrystic plagioclase. Pericline and Carlsbad twinning are also observed.

The groundmass plagioclase are mostly lath shape euhedral to subhedral crystals. They are sodic labradorite ranging in composition from An_{49} to An_{59} and averaging

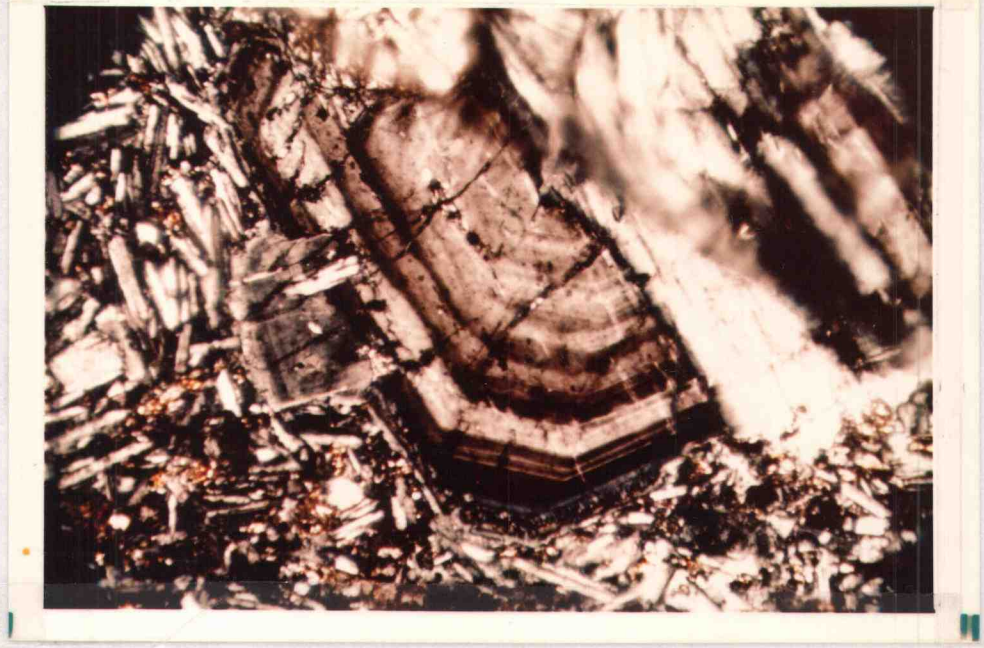

Figure 4. Photomicrograph of oscillatory zoning in andesite plagioclase phenocryst. (Sample JWH-102 from NE¼, NW¼, Sec. 16, T. 10 S., R. 20 E.)

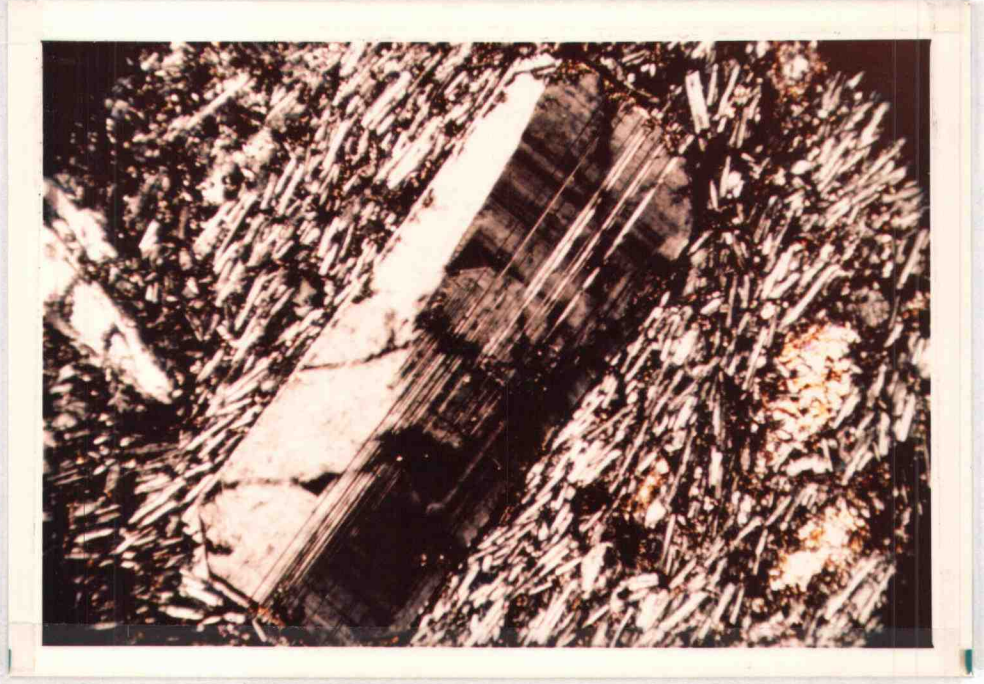

Figure 5. Photomicrograph of oscillatory zoning in an andesite plagioclase phenocryst. Note Carlsbad and albite twins. (Sample JWH-103 from SE¼, NE¼, Sec. 16, T. 10 S., R. 20 E.)

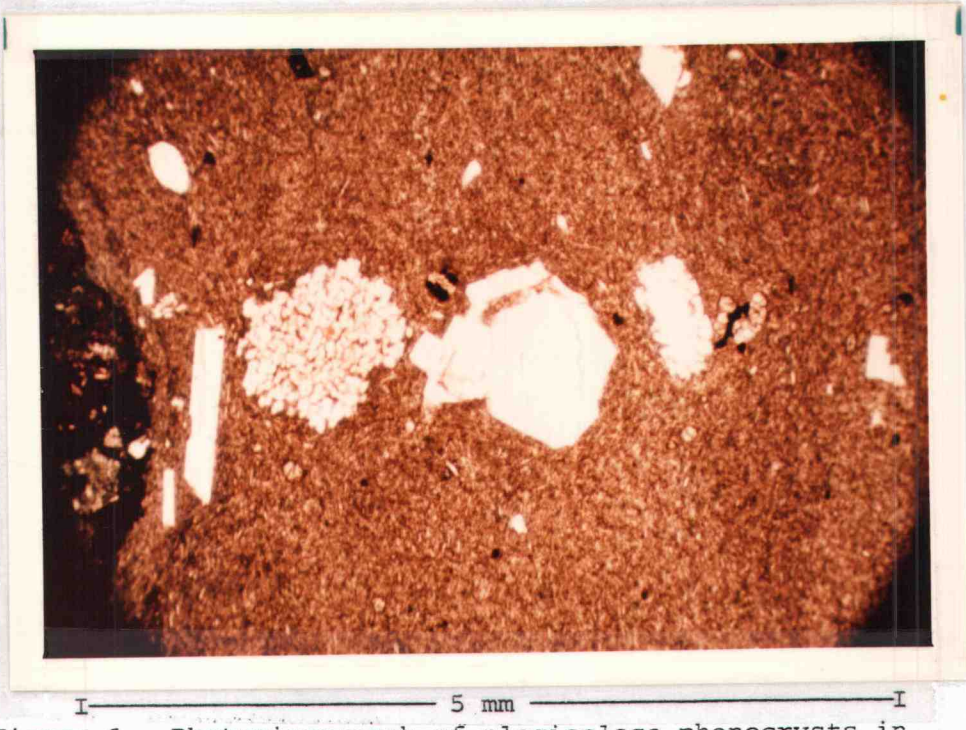

Figure 6. Photomicrograph of plagioclase phenocrysts in dacite showing varying stages of resorption. (Sample JWH-16 from NW¼, SE¼, Sec. 2, T. 10 S., R. 20 E.)

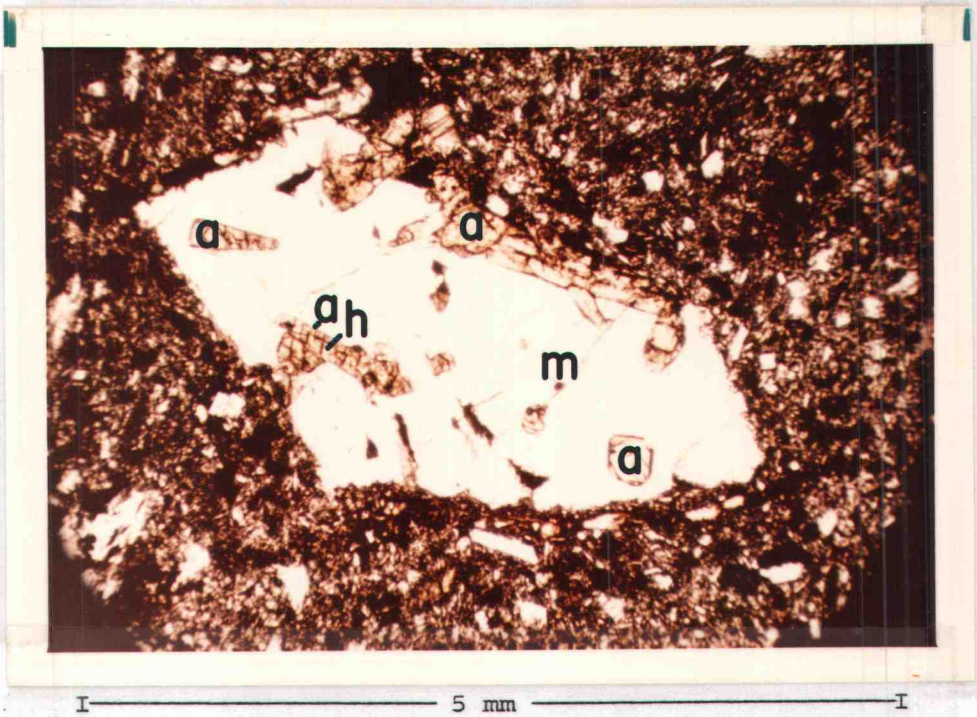

Figure 7. Photomicrograph of inclusions in basaltic andesite plagioclase. a = augite, h = hypersthene, m = magnetite. (Sample JWH-90 from SW¼, NW¼, Sec. 9, T. 10 S., R. 20 E.)

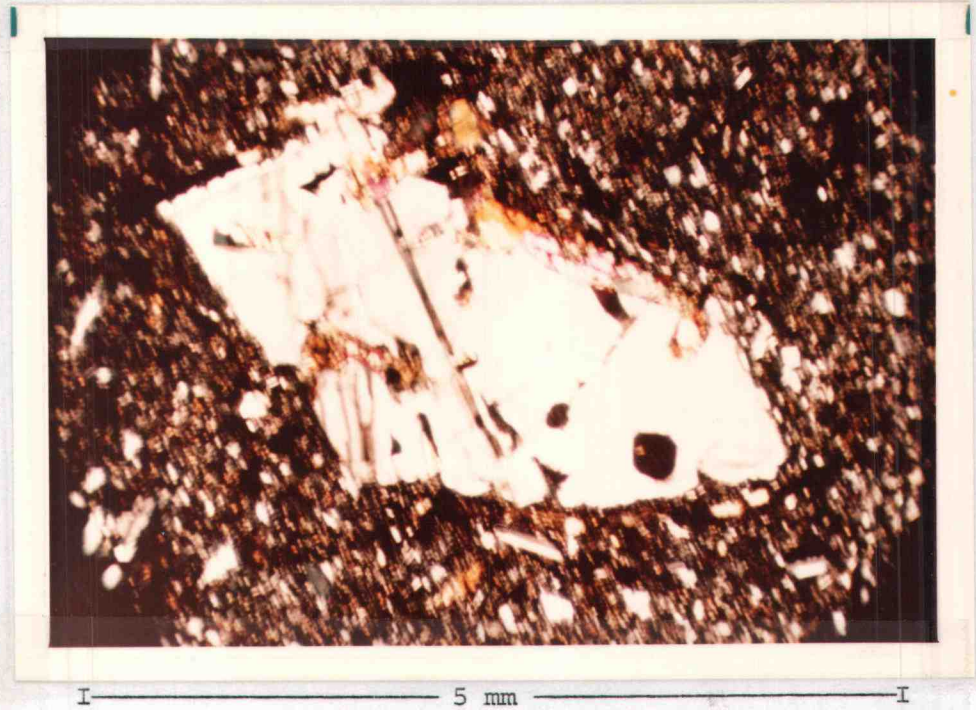

Figure 8. Same as Figure 7 above but with crossed nicols. Note rim of augite on hypersthene.

An_{53}. As seen in Table 1, they generally comprise between 50 to 70 volumetric percent of the rock.

The clinopyroxene phenocrysts are found up to 1.7 mm in diameter and average 1.0 mm. These crystals are euhedral to anhedral in form. Their colors are neutral to very pale brown. The 2V of these crystals varies between 50 and 60 degrees. The range of 2V suggests that this clinopyroxene is probably an augite with slight variations in the amount of calcium in the crystal structure. As seen in Table 1, the volumetric modal abundances of the augite phenocrysts varies from a trace to 3.8 percent. The average from 14 samples was 2.4 percent. In the groundmass, augite is found from 16.4 to 27.8 percent by volume. Augite is usually the most abundant pyroxene phase in the groundmass and in several samples it is the only type. Twinning is common in many of the clinopyroxene phenocrysts but is rarely seen in the groundmass.

The orthopyroxene phenocrysts are faintly to distinctly pleochroic from pale green to pink. The 2V varies from 70 to 80 degrees and is negative, indicating hypersthene as the variety of orthopyroxene. The hypersthene is found up to 3.0 mm in length, with an average of 1.2 mm. It is euhedral to anhedral in form and generally occurs as lath-shaped crystals. The phenocrysts comprise an average of 2.2 volume percent which varies from a trace to 5.7 percent. In the groundmass it can account for up to 12.5 percent

but in many samples is completely lacking.

Kuno (1936, 1950) noted in the rocks of Hakone Volcano the presence of granular pigeonite surrounding orthopyroxene phenocrysts. In addition, he described the groundmass pyroxene as pigeonitic augite. The rocks of this thesis area also show a granular rim of clinopyroxene surrounding many of the hypersthene phenocrysts but they were too small to identify with the equipment available to the author. This is also true of the groundmass clinopyroxene and for convenience will simply be called augite. Kuno also illustrated what he believed to be intergrowths of clinopyroxene in an orthopyroxene host and intergrowths of orthopyroxene in a clinopyroxene host. This was also noticed in the rocks of this area (Figures 9 and 10) although it appears to be more of a reaction relationship with orthopyroxene changing to clinopyroxene or visa versa. Late magmatic or deuteric reactions are probably responsible for these changes.

The volumetric percentage of both pyroxene phases together range from a trace to 9.4 percent. The average abundance is 4.6 percent.

Magnetite occurs in two ways. It is always found disseminated throughout the groundmass with euhedral to subhedral form and is often about the same size everywhere in the rock. This includes magnetite commonly seen as inclusions in other minerals, especially plagioclase. The

Figure 9. Photomicrograph of hypersthene changing to augite. (Sample JWH-15A from middle of Sec. 2, T. 10 S., R. 20 E.)

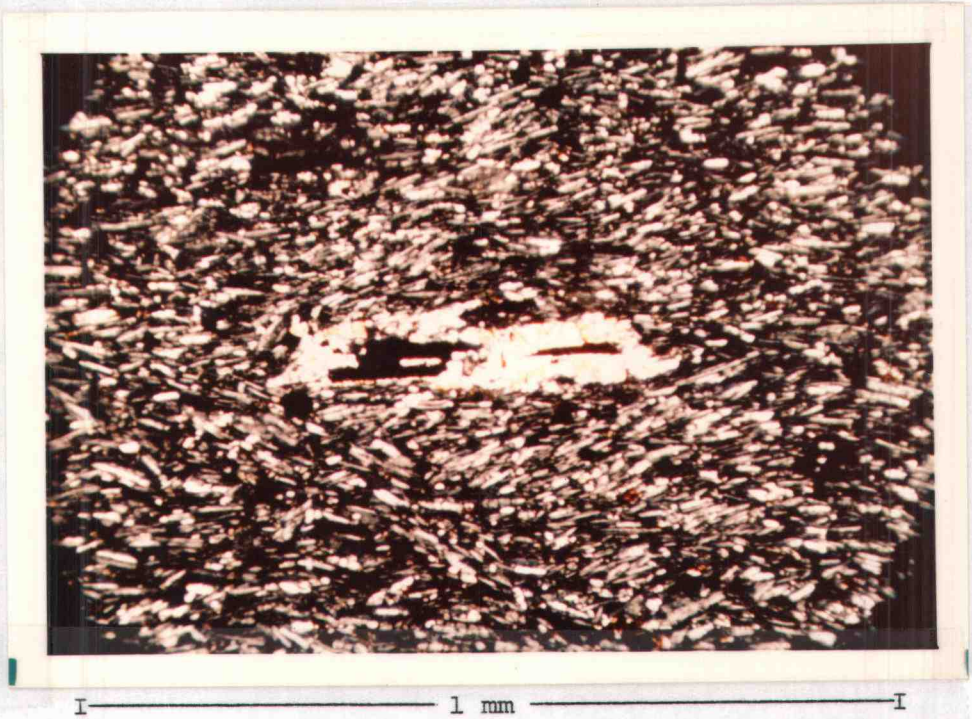

Figure 10. Same as Figure 9 above but with crossed nicols.

second way in which magnetite is found is as irregular patches and psuedomorphic replacements after pyroxene.

II. Andesites

General Statement

Outcrops of andesite lavas are found throughout this thesis area. In a very general sense they seem to be higher stratigraphically than the basaltic andesites. This is best observed in the northern part of the area in Sec. 1 and Sec. 2, T. 10 S., R. 20 E. along the John Day River. At this locality a large north-facing antidip slope composed of gently dipping flows changes from basaltic andesite along the river to andesite above and finally the ridge is capped by a succession of dacite flows.

The andesite flows show a variable thickness similar to the basaltic andesites. One flow interpreted to have filled a small canyon reaches a thickness of about 100 m (Figure 11). This flow can be seen from Bridge Creek Road and has an unusual mineralogy which will be discussed below. The andesite flows fracture in a platy fashion. Poorly developed columns and irregular blocks are also found and two flows have areas of well-formed four- to five-sided columns. These columns were generally from 10 cm to 15 cm in diameter.

The andesite flows show a much greater variation in colors than the basaltic andesites, ranging from grayish

Figure 11. Thick valley-filling flow of andesite. Location in NW¼, SW¼, Sec. 11, T. 10 S., R. 20 E.

black (N2) to yellowish gray (5Y 7/2). Overall the andesites seem to be lighter in color but many flows are the same as the basaltic andesites.

Petrography

In most respects the mineralogy and textures of the andesites are very similar to that of the basaltic andesites. Although some flows contain no clinopyroxene phenocrysts and others have no orthopyroxene phenocrysts, most could be called porphyritic two-pyroxene-bearing andesites. Only one andesite flow lacks pyroxene phenocrysts altogether. The single most distinctive feature of these lavas is the common occurrence of quartz phenocrysts. In addition a few samples contain magnetite crystals that have developed large enough to be considered a phenocrystic phase. This was observed in the more siliceous andesites. The groundmass constituents are the same as those observed in basaltic andesites with the exception of less common biotite and glass and the rare occurrence of hornblende or uralite. Although many of these andesite flows are more altered than basaltic andesites, the alteration products are very similar. Table 2 shows a volumetric modal analysis of some selected andesites.

The dominant textures are again pilotaxitic and glomeroporphyritic. Only rarely does an andesite not show some pilotaxitic texture and often the microlites form a swirling pattern around phenocrysts (Figure 12). Although

Table 2. Volumetric modes of selected Clarno andesites.

Sample*	JWH-78	JWH-38	JWH-184	JWH-110	JWH-159	JWH-102
Phenocryst Phases:						
Labrodorite	4.7	2.7	10.2	9.3	14.5	7.8
Augite	0.7	0.2	2.2	2.8	5.5	1.0
Hypersthene	0.5	1.1	2.5	2.4	3.3	2.8
Quartz	-	0.8	-	-	-	-
Groundmass Phases						
Labrodorite	66.6	61.1	63.3	62.0	-	-
Andesine	-	-	-	-	64.9	61.4
Augite	0.6	16.6	19.5	29.0	25.8	16.5
Hypersthene	17.1	11.0	2.7	2.3	-	8.4
Magnetite	2.0	2.4	7.3	4.4	3.1	3.3
Biotite	-	-	-	T	-	T
Apatite	-	-	T	-	T	T
Glass	-	8.9	0.3	-	-	-
Clay	4.3	T	3.8	2.3	1.0	2.4
Zeolite	T	T	3.1	T	4.2	5.5
Carbonate	9.4	-	-	-	-	-
Hematite	T	-	T	T	1.0	0.5

(T = Less than 0.2%)

* See Appendix A for sample location and chemical analysis.

a smaller percentage of andesites show glomeroporphyritic texture than basltic andesites, those that do have larger and better developed clumps (Figure 13). Intergranular texture is less common and no ophitic texture was seen.

The phenocryst phases show the same characteristics as those described and discussed in the section on basaltic andesites and only exceptional features will be described here. The plagioclase phenocrysts are observed up to 5 mm in length and average 2.3 mm. They range in composition from An_{54} to An_{66} and average An_{61}. In abundance they make up a trace to 15 percent by volume of the rock. The average volumetric percent is 7. The clinopyroxene was again determined to be augite. The colors and form are the same as in the basaltic andesites but the 2V is consistently around 60 degrees. Augite phenocrysts are sometimes missing but may account for up to 5.5 percent of the rock and average only 1.3 percent. With the exception of one very large (2.8 mm) crystal, the augite reaches a diameter of 1.5 mm and averages 0.8 mm. The orthopyroxenes show all of the characteristics of hypersthene described earlier. They are found up to 2.3 mm in length and average 1.2 mm. Like the clinopyroxenes they may be missing as a phenocrystic phase but can form up to 3.3 percent by volume and average 1.6 percent. Together the pyroxenes form a maximum of 8.8 percent and average 2.6 percent.

Figure 12. Photomicrograph of the flow texture around phenocrysts in andesite. Crossed nicols. (Sample JWH-103 from SE¼, NE¼, Sec. 16, T. 10 S., R. 20 E.)

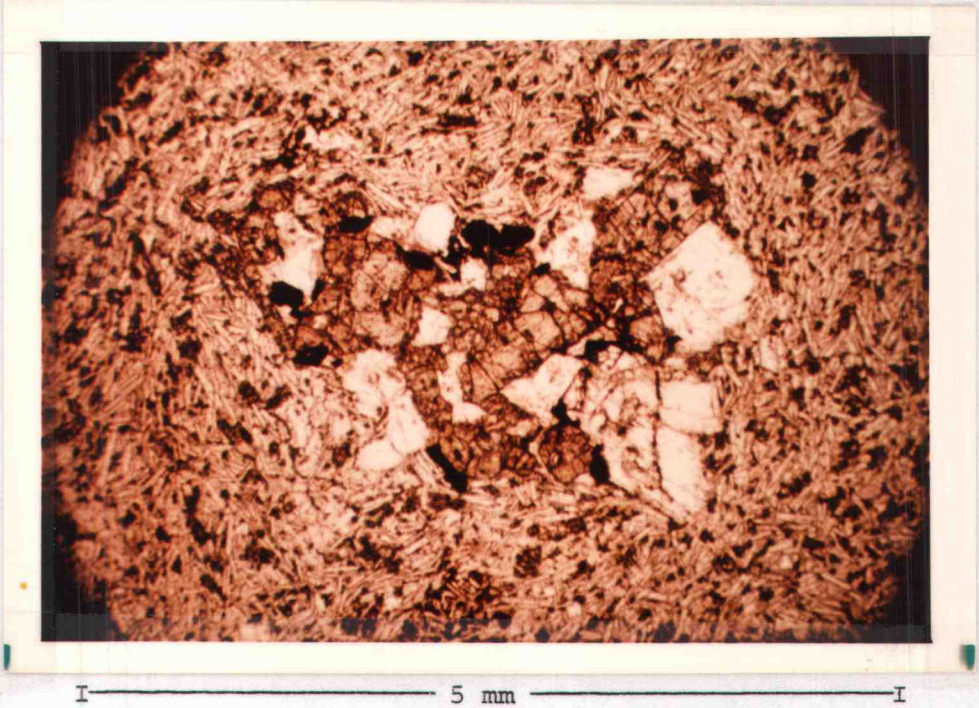

Figure 13. Photomicrograph of glomeroporphyritic texture in andesite. Minerals include labradorite, hypersthene, augite and magnetite. (Sample JWH-102 from NE¼, NW¼, Sec. 16, T. 10 S., R. 20 E.)

The groundmass minerals show some slight differences from the basaltic andesites. The plagioclase is mostly a calcic andesine except in the low silica andesites, where it is a sodic labradorite. The composition range is between An_{43} to An_{54} averaging An_{49}. The plagioclase almost always accounts for over 60 percent of the rock and averages around 63 percent. There is a slight increase in the amount of hypersthene relative to augite in the groundmass which is also true of the phenocryst phases. Both biotite and magnetite are less abundant in the groundmass of the andesites compared to the groundmass of the basaltic andesites.

Except for its rare occurrence as a phenocryst, the iron oxides in the andesites are very similar to those observed in the basaltic andesites.

The most characteristic feature of the andesites in this area is the presence of quartz phenocrysts. About 30 percent of the andesites examined under a microscope contained quartz phenocrysts. The largest concentration of quartz-bearing andesites is in the northwest corner of this thesis area where a sequence of gently dipping flows are found. These quartz-bearing andesites are located along the boundary of Section 3 and Section 4 and extend into the eastern half of Section 9. Samples collected from this sequence, from bottom to top include JWH-86, 72, 73, 74 and 93. As can be seen in Appendix A, the

chemistry in these flows is very similar and for this reason probably represent a series of eruptions from the same vent or at least from the same magma chamber. Other than the presence of the quartz phenocrysts, these andesites have the same features as other andesites in the area. Volumetrically the largest percent of quartz phenocrysts in any flow is 3.6 percent. Although most abundant in the andesites, there are a few flows of basaltic andesite and one flow of dacite which also contain some quartz phenocrysts.

Most of the quartz phenocrysts have similar features to each other. Figures 14 and 15 show a phenocryst in which there is a thick reaction rim of glass and many small clinopyroxene crystals. The clinopyroxene is completely immersed in glass of two different colors. The brown glass is always restricted to these reaction rims while the light gray-colored glass is found scattered throughout the rock, often with no association with quartz phenocrysts. All of the quartz phenocrysts in this flow show this same type of reaction rim although the thickness of the rim varies slightly. Figure 16 shows a similar reaction rim although in this sample there is no associated glass. Also the clinopyroxene has grown to a much larger size, there is minor chalcedony and the quartz is not as smoothly rounded. Not all quartz phenocrysts are surrounded by reaction products. Figure 17 is a phenocryst from a dacite flow

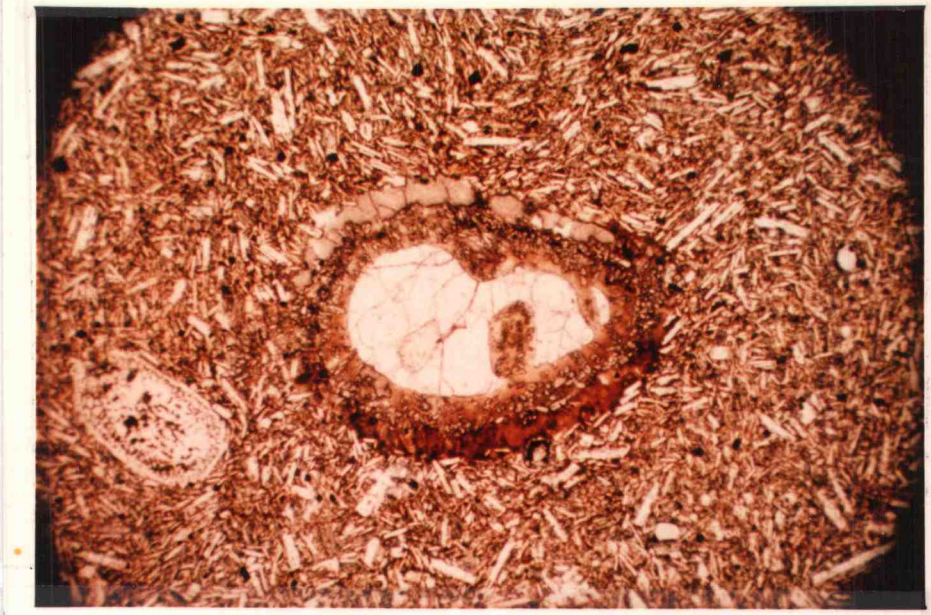

I——————————— 5 mm ———————————I

Figure 14. Photomicrograph of quartz phenocrysts in andesite with reaction rim of glass and clinopyroxene. Note rounding and embayment caused by partial resorption. (Sample JHW-38 from SW¼, NE¼, Sec. 11, T. 10 S., R. 20 E.)

I——————————— 5 mm ———————————I

Figure 15. Same as Figure 14 above but with crossed nicols.

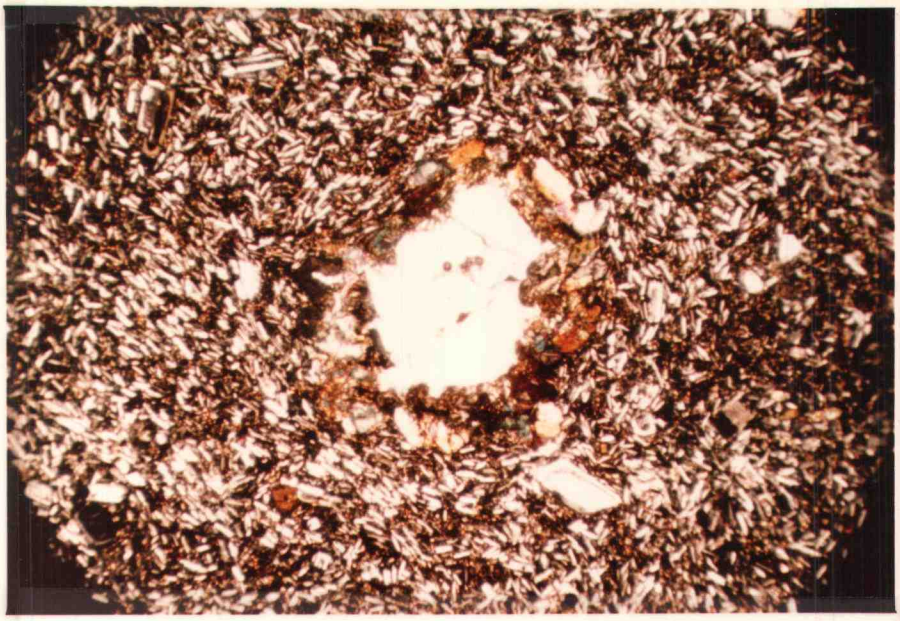

I——————————— 5 mm ———————————I

Figure 16. Photomicrograph of quartz phenocrysts in andesite with thick reaction rim of large clinopyroxene. Crossed nicols. (Sample JWH-93 from SW¼, NE¼, Sec. 9, T. T. 10 S., R. 20 E.)

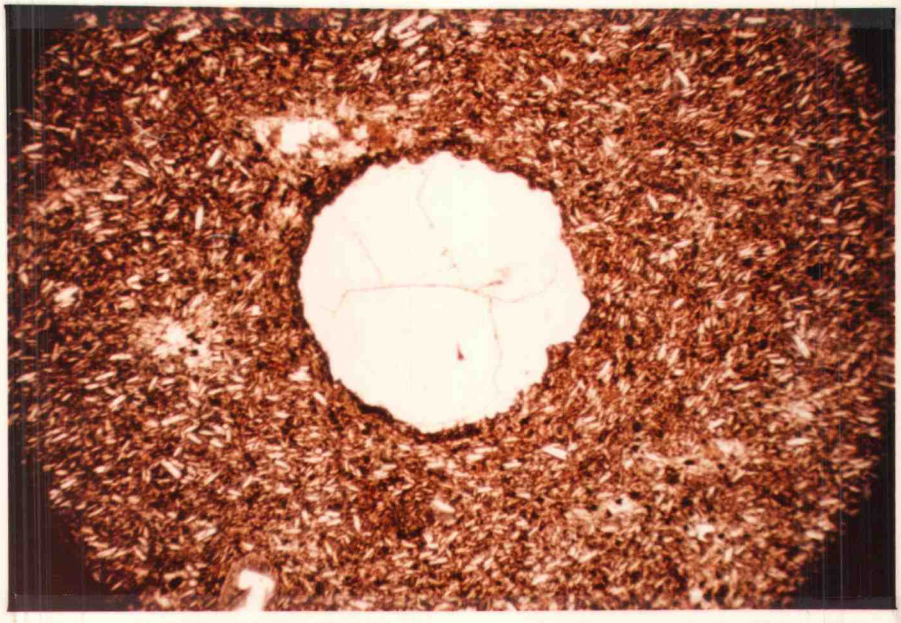

I——————————— 5 mm ———————————I

Figure 17. Photomicrograph of quartz phenocrysts in dacite showing corroded edges but no reaction rim. (Sample JWH-52 from NE¼, SE¼, Sec. 11, T. 10 S., R. 20 E.)

and shows only embayment and rounding due to resorption.

There seems to be a gross relationship between the silica content of the rock and the formation of a reaction rim on quartz. In general, reaction rims form to a lesser degree in rocks of higher silica content. This is to be expected, although there are exceptions in both basic and siliceous samples.

Figures 18 and 19 show two quartz phenocrysts from the same flow. In Figure 18 the first reaction was the formation of hornblende, biotite and larger clinopyroxene. The concentric organization of these reaction products makes it possible to infer the order of formation. The outer rim of clinopyroxenes has largely been altered to chlorite but the hornblende and biotite remain quite fresh. The unusual feature of this phenocryst is that these rings of reaction products are completely immersed in and surrounded by quartz. The quartz on the outside of these reaction products has formed as a mosaic of interlocking crystals while the inner part forms one optically continuous crystal. These relationships may be due to changing magmatic conditions within the magma chamber prior to eruption.

Figure 19 shows a very similar relationship as Figure 18 although there is no formation of hornblende and the biotite is more abundant. As these figures show, almost all of the phenocrysts are cut by irregular fractures. Inclusions are rare although occasionally a zircon, apatite or

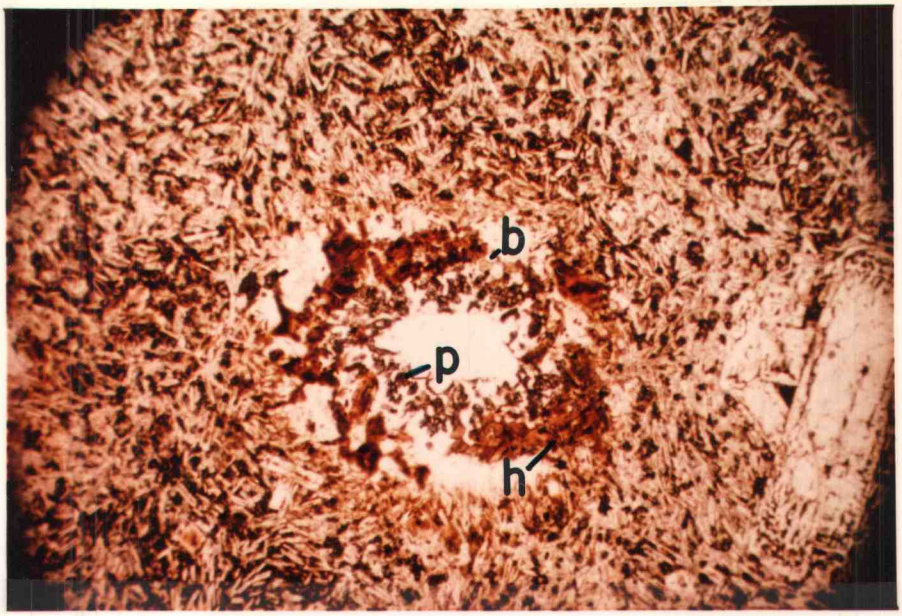

I——————————— 5 mm ———————————I

Figure 18. Photomicrograph of quartz phenocrysts in andesite. Note inclusions in zonal arrangement where p = clinopyroxene, b = biotite, h = hornblende. Crossed nicols. (Sample JWH-74 from NE¼, NE¼, Sec. 9, T. 10 S., R. 20 E.)

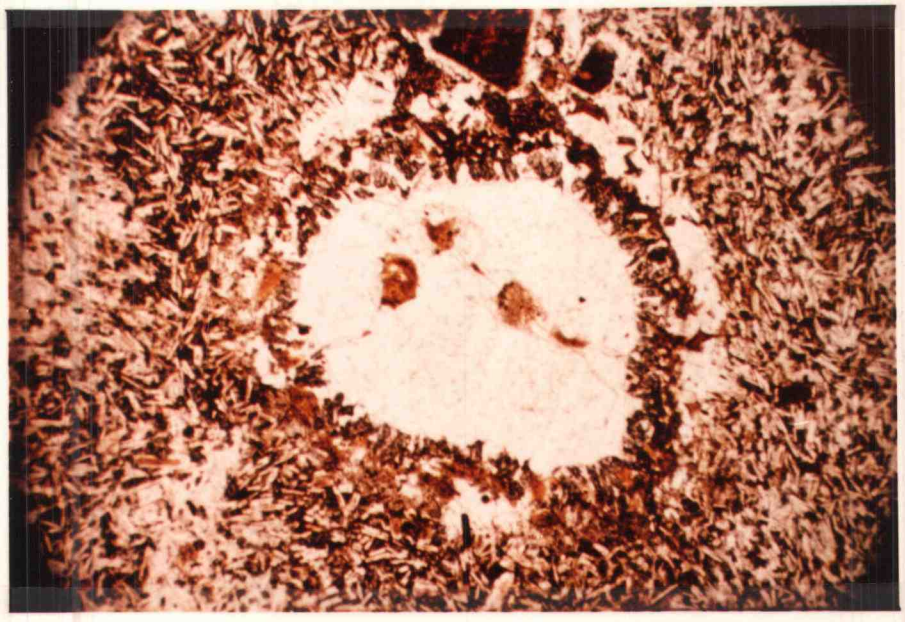

I——————————— 5 mm ———————————I

Figure 19. Photomicrograph of quartz phenocryst in andesite with zoned inclusions of clinopyroxene and biotite. (Sample JWH-74 from NE¼, NE¼, Sec. 9, T. 10 S., R. 20 E.)

pyroxene crystal can be identified. There is also commonly a fine dust size material included and may be an iron oxide although accurate identification was not possible.

There are numerous references to quartz phenocrysts or quartz "xenocrysts" from calc-alkaline rocks in many parts of the world. Many of the unpublished masters theses done in the 1950's and 1960's in areas containing Clarno flows have reported the occurrence of quartz phenocrysts. Despite the relatively common occurrence of this porphyritic quartz phase, its origin is imperfectly understood. Experimental work indicates that in a granitic melt ($NaAlSi_3O_8$ - $KAlSi_3O_8$ - SiO_2 - H_2O system) quartz may appear on the liquidus under condition of high water vapor pressure (Tuttle and Bowen 1958). This changes the position of the quartz-feldspar minimum in the simple binary eutectic. Ewart (1965) has used these results to explain the resorption of quartz phenocrysts found in several ignimbrite sheets in New Zealand. He believed the resorption was due to fluctuations in water vapor pressure which would cause feldspar to appear on the liquidus and the quartz would no longer be in equilibrium with the melt. However Green and Ringwood (1968) point out:

> ... in such a mechanism the release of water vapor pressure would result in a rise in liquidus temperature and consequently an increase in crystallization. This would be the major effect-any shift in the eutectic causing feldspar instead of quartz to crystallize (and hence causing resorption of quartz) would be a second order feature.

They found from their experimental work that the change in

load pressure and not water vapor pressure, where $P_{H_2O} < P$ load, may cause the resorption of quartz. Their results showed that at high pressure and under dry conditions, quartz is the crystalline phase in equilibrium with the melt while at low pressure feldspar becomes the crystalline phase. When quartz is no longer on the liquidus, it will be resorbed because of disequilibrium with the melt. Therefore, a magma containing quartz phenocrysts ascending from depth will change the equilibrium relative to quartz causing the resorption process. Using calculated values of silica activity, Nicholls and others (1971) calculated the pressure at which magmas of basaltic andesite composition would be saturated with quartz. Pressures of about 25 kilobars were found assuming an equilibration temperature of 1100° C. The presence of garnet phenocrysts rich in pyrope in some calc-alkaline rocks (Green and Ringwood 1968b) adds support to this depth of origin. Although no garnet was observed in the rocks of this area, Taylor (1977, personal communication) found Clarno andesites in the area of Tony Butte, 16 km to the east which contain euhedral pink garnet.

Taylor (1960) in studying Clarno lavas, northwest of this area, recognized a close association between the embayed quartz phenocrysts and the zeolite heulandite. Because heulandite is only stable at relatively low temperatures, he felt the resorption process may have taken

place at or near the surface during the "final stages of cooling." In the lavas studied by the author no association was noticed between the quartz phenocrysts and heulandite.

An unusual flow located in NW¼, NW¼, Sec. 11, T. 10 S., R. 20 E. is of andesitic composition and contains epidote phenocrysts. The author identified these phenocrysts as epidote because of their yellow-green color (faint pleochroism), high relief and strong birefringence. No optic sign was obtained. The textures are very similar to other andesite flows seen in the area and the rock fractures in an irregular platy fashion. In addition to the epidote phenocrysts, which make up 1.0 volumetric percent of the rock, there is 3.7 percent of highly altered plagioclase. No pyroxene was seen as a phenocrystic phase. The alteration of the phagioclase is severe enough that no composition could be measured. Occasionally the epidote is found as inclusions within the plagioclase along with apatite and magnetite. The epidote is granular in appearance and is generally subhedral while reaching 0.6 mm in diameter. The groundmass is also very altered and appears to contain minerals similar to other andesites in the area.

III. Dacites

General Statement

The dacites of this area appear to be concentrated in

the northeast between Bridge Creek and the John Day River and at the southern end close to Painted Hills State Park (Plate I). Except for a few locations, the dacite represents the last phase of volcanism in this area and is located stratigraphically above the andesites and basaltic andesites.

The flows are relatively thin, up to 20 m, and do not seem to fill small valleys like many of the andesites. The flow tops are very vesicular in many areas and these zones of vesicles are up to 5 m thick. The fracture patterns are similar to those previously described although commonly the platy fracture is extremely well developed, almost resembling slate (Figure 20). In addition the best columns seen in this area were found in dacite flows (Figure 21).

The dacites show the widest variation in color of the flows in this area. Some are as dark as grayish black (N2) but most are much lighter in color. Light brownish gray (5 YR 6/1) was found in one flow.

Petrography

The dacites show a great deal of similarity to the other flows in this area in terms of mineralogy. There are some minor differences, however, and only these will be discussed here. Except for the less common occurrence of glomeroporphyritic clumps, the textures are the same as seen throughout the area including pilotaxitic and intergranular.

Figure 20. Platy fracture in a dacite flow. Location is in the SW¼, SE¼, Sec. 12, T. 10 S., R. 20 E. along the road to Twickenham.

Figure 21. Top view of a five-sided column formed in dacite flow located at SW¼, SW¼, Sec. 33, T. 10 S., R. 20 E. Column approximately one half meter in diameter.

The plagioclase phenocrysts show a compositional range of An_{53} to An_{64} and average An_{54}, a mid-labrodorite. In abundance they range from 0.6 to 26.4 volume percent while averaging 10 percent. They form up to 5.5 mm in length but average 3.0 mm.

The pyroxene phenocrysts include augite and hypersthene. Augite, although commonly missing, comprises an average of 1.4 percent of the rocks when present and ranges from a trace to 5.5 percent. The crystals have formed up to 3.0 mm in diameter, averaging 1.0 mm and always shown a 2V of 60 degrees. The hypersthene also is occasionally missing but when found it makes up an average 1.2 percent of the rock and ranges from a trace to 2.3 percent. The hypersthene is generally larger than the augite. It averages 1.6 mm and reaches a maximum of 3.0 mm. The 2V of these crystals is usually about 75 degrees. Together the pyroxenes average about 2.3 volumetric percent ranging from a trace to 5.5 percent.

A distinctive feature of the dacites is the appearence of magnetite phenocrysts from 0.2 mm to 0.5 mm in size. They are euhedral to subhedral and are found forming up to 1.0 percent and averaging 0.5 percent of the rock. Only two flows contain quartz phenocrysts.

The groundmass mineralogy is different from the basaltic andesites and andesites (Table 3). The plagioclase is more sodic with an average composition of An_{48},

Table 3. Volumetric modes of selected Clarno dacites.

Sample*	JWH-7	JWH-50	JWH-49	JWH-15B
Phenocryst Phases:				
Labradorite	15.6	14.7	11.6	4.6
Augite	1.2	0.8	0.7	0.4
Hypersthene	0.4	0.8	2.0	0.2
Groundmass Phases:				
Andesite	43.1	41.1	48.0	58.7
Augite	19.0	13.1	12.0	20.1
Hypersthene	2.1	1.5	-	3.0
Magnetite	4.4	4.4	4.9	3.8
Biotite	-	-	T	-
Apatite	T	T	-	-
Glass	31.4	39.3	25.5	12.9
Clay	T	T	3.4	1.0
Zeolite	-	-	6.2	0.5
Carbonate	-	0.6	-	-
Hematite	-	-	-	T

(T = less than 0.2%)

* See Appendix A for sample location and chemical analysis.

showing a wide range of between An_{59} and An_{36}. The percentage of plagioclase in the groundmass is much lower with an average of 47 percent. This decrease in percentage is true for the pyroxenes and biotite as well. The most distinctive feature of the dacite flows is the very common occurrence of glass in the groundmass. Many times the glass accounts for a substantial percentage of the total rock. In sample JWH-50 (Table 3) the glass, which is light brown, is so abundant, that the minerals appear to be floating in it. The texture of this and several other examples could be called hyalo-ophitic.

IV. Painted Hills Dacite

General Statement

This dacite flow forms a distinctive unit located within Painted Hills State Park in parts of Sections 25, 35 and 36 which crops out over a total of about one square kilometer (Plate I). Although it was very difficult to determine how many flows make up this unit, there are at least two. These flows form the "pre-John Day Hills" described by Hay (1962). He referred to these flows as "highly porphyritic andesites" although chemical analyses by the author show these clearly to be dacites (Appendix A, samples JWH 186 and 187). From these outcrops, Hay determined that the relief in this vicinity reached 91 m prior

to the eruption of the overlying John Day tuffs. The contact between these dacite flows and the John Day Formation is shown in Figure 22. Both of these flows are approximately 35 m thick. The lower flow forms cliffs and hoodoos (Figure 23) along Bear Creek with east facing outcrops. This flow has thick platy to blocky fracture and in places forms very large, poorly developed columns. On fresh surfaces the color is either medium dark gray (N5) or medium light gray (N6) and on weathered surfaces is varying shades of red and brown. The upper flow caps the largest of the "pre-John Day Hills" and is found in the NW¼, SW¼, Sec. 36, T. 10 S., R. 20 E. It fractures into very thick plates or large irregular blocks. Pale red (5 R 6/2) is seen on the freshest surface and grayish red (5 R 4/2) on weathered surfaces. All samples show some pilotaxitic and glomeroporphyritic textures. These two dacite flows represents the last phase of volcanism of the Clarno Formation in this area.

Petrography

Two features make these two dacite flows different than others in this thesis area. These features are the large percentage of plagioclase phenocrysts and the high degree of alteration. Mineralogically, these two flows are very similar and, therefore, will be described togther.

The plagioclase phenocrysts compose from 18.0 percent

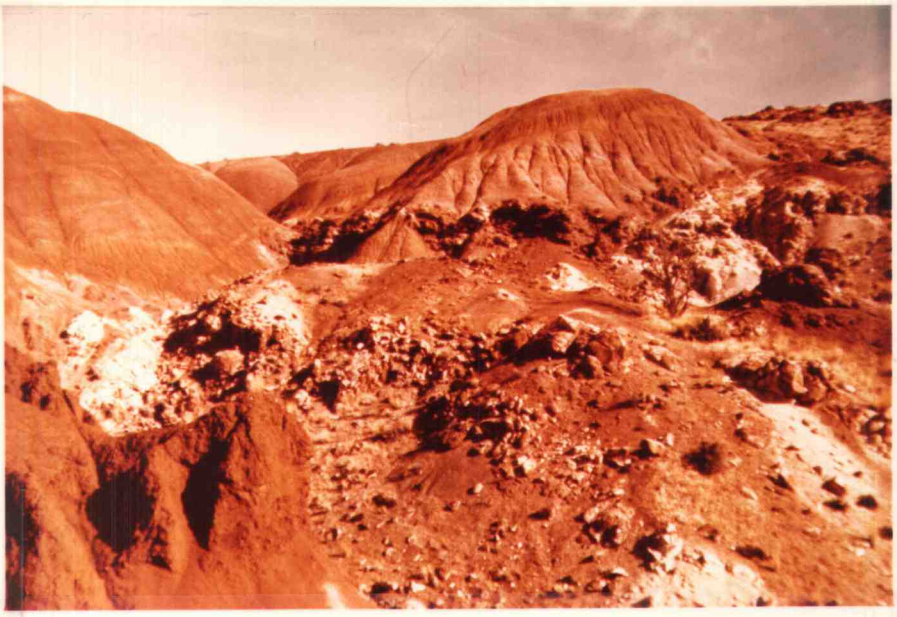

Figure 22. Contact between the Painted Hills Dacite and overlying John Day Formation. Note extreme weathering in dacites and deep red soil (left foreground) regolith forming the top of the Clarno Formation in this area. (Location is SE¼, SE¼, Sec. 35, T. 10 S., R. 20 E.)

Figure 23. Hoodoo-forming outcrop of Painted Hills Dacite along Bear Creek. The largest hoodoo in the center of the picture is about three meters high. (Location is SW¼, SW¼, Sec. 25, T. 10 S., R. 20 E.)

to 26.4 percent of the rock by volume. They are sodic labradorite measured to be approximately An_{55}. The crystals are usually subhedral but euhedral forms are found and where resorption has occurred, annhedral crystals remain. Many are very large forming up to 5.5 mm in length. The plagioclase in these flows is always very altered and the cores are often altered completely. The products of alteration include carbonate, clay minerals and zeolites including heulandite and chabazite. A greenish mineral resembling chlorite is also found which is replacing some of the plagioclase.

The only other phenocrystic phase forms about 3.0 percent of the volume of the rock and was probably a pyroxene now completely altered to magnetite and chlorite. This mineral is subhedral to annhedral in form. It forms as large as 2.1 mm in diameter but most are much smaller, usually about 0.7 mm. In addition to pyroxene, magnetite has formed as phenocrysts in one of these flows.

The groundmass minerals are very difficult to identify. The only original minerals identifiable are plagioclase microlites and magnetite. In addition to these, a few thin sections revealed very abundant lath shaped iron oxides which may represent psuedomorphs after original hornblende. One section also shows the same spherical bodies which are seen and described for the Pass Gulch Rhyodacite and presumably also represent glass

devitrification to alkali-rich feldspar and cristobalite. The alteration products referred to above are also seen in the groundmass and in addition hematite has formed after magnetite. Every thin section made show void spaces, commonly filled with zeolites, which account for approximately 2.0 percent of the rocks by volume.

V. Pass Gulch Rhyodacite

General Statement

A rhyodacite flow which can be reliably mapped using characteristics observable in the field is found in the southwestern most corner of this area in the SW¼, SW¼, Sec. 33, T. 10 S., R. 20 E. This flow is 46 m thick and crops out over only a few hundred meters. It fractures in large irregular blocks although in many places flow texture is extremely well developed and banding can be seen. There are abundant inclusions of andesitic rock fragments and what appears to be pumice. The color on fresh surfaces is grayish red purple (5 RP 4/2) and on weathered surfaces is pale red (5 R 6/2). The reddish coloration is due to hematite or limonite staining which is disseminated through the rock.

This flow was called a rhyodacite on the basis of its chemistry (Appendix A, sample JWH 167). The amount of silica present is a slightly inflated value because of minor secondary quartz although it did not appear to be enough to change the naming of the flow. The closest named

geographical feature to this flow is Pass Gulch which is one kilometer to the south of this thesis area and this name was chosen for convenience of description.

Petrography

The only phenocryst phase present is a plagioclase of undetermined composition. The An content was not determined because of the scarcity of phenocrysts (2.2 volume percent) and degree of alteration. These plagioclase cyrstals occur up to 1.5 mm in length and are subhedral in form. There are abundant grains and dust of iron oxide as well as small crystals of apatite included in many of the plagioclase phenocrysts.

In addition to the plagioclase phenocrysts there are microphenocrysts of plagioclase and what appears to have been hornblende. These hornblende crystals are now completely altered to chlorite and magnetite and form up to 0.5 mm in length and subhedral to annhedral in form.

The groundmass is composed of tiny needles of plagioclase, hornblende (?), small grains and dust of magnetite and abundant clear glass. In addition there are rare apatite crystals which have been stained brown and show a faint pleochroism. An unusual feature of the groundmass is numerous small spherical splotches which are colorless and show low relief and birefringence. These may be areas where the glass has devitrified to an alkali-rich feldspar and possibly cristobalite.

As mentioned earlier, there is some minor secondary quartz which has filled small fractures and occasional voids. In addition to this some zeolite of undetermined type has also filled voids.

VI. Intrusive Rocks

General Statement

This thesis area is unusual relative to the Clarno rocks in adjacent areas because of the scarcity of intrusive rocks. Only one example was found that could be called intrusive with any degree of confidence. This was an east-west trending dike of basaltic andesite located in the NW¼, SW¼, Sec. 3, T. 10 S., R. 20 E. The dike crops out for approximately 50 m and is only a few meters wide. Although this is the only intrusive rock within this thesis area, there are abundant intrusions of andesite across the John Day River to the north and a small silicic plug and mafic vent a kilometer to the east (Swanson 1969, Robinson 1975). There are also numerous intrusive rocks of different types and a variety of compositions to the south (Owen 1977, Barnes, 1977 personal communication).

Petrography

The dike is two-pyroxene basaltic andesite with rare quartz phenocrysts. Aside from the quartz, there are no distinctive phenocrystic phases present. The rock is

relatively equigranular and more coarsely crystalline than the groundmass in most flows. On fresh surfaces, the color is medium dark gray (N4) and this weathers to pale brown (5 YR 5/2). Pilotaxitic as well as intergranular texture are well developed.

Plagioclase accounts for 64.7 percent of the rock and is a very calcic labradorite (An_{69}). The pyroxene phases make up 26.4 percent with augite forming 18.0 percent and hypersthene forming 8.4 percent. Magnetite is dispersed throughout the rock as small euhedral grains and large late-forming interstitial masses. The magnetite accounts for 5.3 percent by volume while brown glass forms 1.7 percent. The remaining percentage is composed of alteration products including zeolite, clay minerals, hematite and abundant calcite. Although calcite forms in some flows, mainly associated with plagioclase phenocrysts, it is far more abundant in the dike where it is found as interstitial material between clear, fresh plagioclase laths.

The quartz phenocrysts in this rock are surrounded by the thickest reaction rims observed in any rock of this area (Figure 24). In addition this rock has the lowest silica content (55.1 percent) of any sample containing quartz pheoncrysts. The rims are composed of radiating slender clinopyroxene crystals with minor clear and green glass. On the outside is abundant magnetite which is slightly oxidized to hematite.

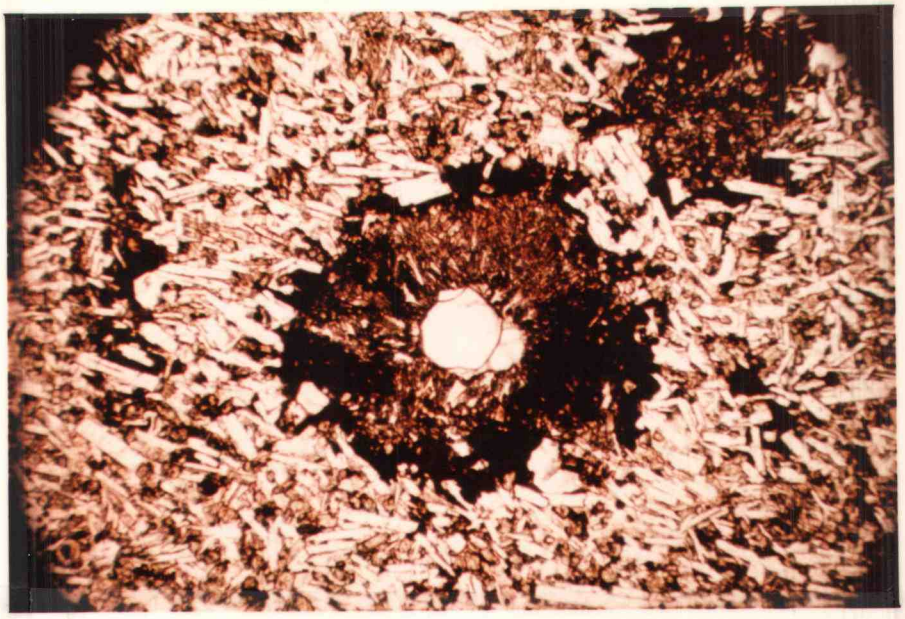

Figure 24. Photomicrograph of thick reaction rim surrounding small quartz phenocrysts in basaltic andesite dike. Note well developed pilotaxitic and intergranular texture. (Sample JWH-76 from NW¼, SE¼, Sec. 3, T. 10 S., R. 20 E.)

VII. Mudflows

General Statement

Mudflow deposits are found in two locations in this thesis area. Most of the NW¼ of Sec. 4, T. 10 S., R. 20 E. is composed of mudflows and another small outcrop is found in the SE¼, NW¼ of Sec. 11. These deposits are very poorly sorted with andesite clasts up to about one meter in diameter which are rounded to subrounded and are in matrix support. The outcrop in Section 4 has some crude bedding which is seen more clearly across the John Day River in a continuation of the same deposit.

Petrography

Only one thin section was made of these mudflow deposits because of their minor importance. The clasts are all mineralogically similar to those rocks described in previous sections. The matrix is composed of abundant, broken crystals of labradorite, rock particles (mostly andesite) and altered pyroxene. There is also some magnetite, hematite, apatite and, unlike the lavas in this thesis area, some large unaltered biotite. X-ray analyses indicate large amounts of smectite clay.

VIII. Tuffs

General Statement

The tuff beds of the Clarno formation in this area occur sporadically between flows and in minor amounts. All appear to have been reworked ash falls and deposited locally as interbeds within the much more extensive lavas. These tuffs, except for only a few localities, are now composed almost entirely of mudstone with only minor amounts of sand size crystals, predominately feldspars. Some magnetite, hematite and possibly pyroxene is seen with the aid of a binocular microscope. Thin sections could not be made of these mudstones because they are poorly indurated, breaking into thousands of small pieces very easily. A good example of these tuff beds is in the NW¼, NW¼, Sec. 12, T. 10 S., R. 20 E. along the border with Section 11. Several layers of mudstone of different color are found. Associated with these are areas of small nonindurated pebble beds indicating the fluvial nature of the tuffs at this locality. The rounded pebbles are predominately basaltic andesite and andesites with occasional dacite. The colors of the tuff beds at this location are dominantly a grayish red (5 R 4/2) or pale yellowish brown (10 YR 6/2) although some show a yellow tint. The thickness of several of the beds at this locality is about 1.5 m but a few are up to 8.0 m. Most tuff beds in this thesis area are deep shades of red and very difficult to distinguish from weathered

flow tops.

Procedures

Since petrographic examination was not possible for all but one of the tuff beds in this area, the author used x-ray diffraction analysis to determine the clay mineralogy of four of these beds. Procedures followed are modified after those used by Dr. M. Harward of the Department of Soils Science, Oregon State University. These procedures will be briefly summarized here.

A clay concentrate is first obtained by disaggregating the sample and passing it through a 4Ø-size wet sieve. This 4Ø-size fraction is then dispersed in distilled water and centrifuged for a few minutes at 750 rpm which leaves only the clay (less than 2μ) size material in suspension. This suspension is poured off and centrifuged for 10 minutes at 6,000 rpm which pulls the clay fraction out of suspension. Each of the clay residues is then split into two parts. One half is saturated with magnesium by repeated washing and centrifuging with 1N $MgCl_2$ solution and the second half is saturated with potassium by repeated washing with 1N KCl. One slide of each, or two slides per sample is then prepared by smearing the clay residue. The magnesium-saturated samples are allowed to air dry while the potassium-saturated samples are dried at 105° C.

The magnesium-saturated slides were allowed to

equilibrate in a 54 percent relative humidity dessicator and then analyzed with x-rays keeping the humidity close to 54 percent throughout the run. Following this, these slides were placed in a dessicator with ethylene glycol, a vacuum was drawn and they were heated at 65°C for three hours. After cooling for 12 hours the slides were again analyzed. In this run the humidity was also controlled at 54 percent.

The potassium-saturated slides were first analyzed under a controlled humidity of about zero percent. They were then placed in the 54 percent dessicator, allowed to equilibrate and again analyzed but with the humidity controlled at 54 percent. The last x-ray on these slides was run after heating the slide at 550°C for three hours and with a humidity of close to zero percent.

These samples are, therefore, analyzed five times following different treatments and under varying conditions. This is necessary to obtain a reliable analysis of clays in the sample.

Discussion

Three of the four samples analyzed for clay minerals are composed predominately of the smectite montmorillonite. The diffraction peaks formed on the x-ray chart in two of these samples are narrow and well defined indicating the montmorillonite is fairly well crystallized. The third sample has a much broader peak and is probably poorly

crystallized. Two of the samples also have peaks indicating very minor, poorly crystallized kaolinite. In all three of these samples the possibility of the presence of a chlorite intergrade could not be ruled out. The last sample has only kaolinite as its clay mineral component. This sample is dark reddish brown (10 R 3/4) in color. As noted in a following section on rock alteration, the predominant clay mineral found in paleosoils on weathered flow tops is kaolinite and this sample may represent material from an altered flow. However, in the field it greatly resembled interbedded tuff. Further detailed study between proven altered flow tops and tuff beds may show that the presence of large amounts of kaolinite could serve to distinguish paleosoils and tuff beds.

An interbedded tuff located in the SW¼, NW¼, Sec. 33, T. 10 S. , R. 20 E. was indurated enough for a thin section to be made. In addition, x-ray analysis was performed following the procedures outlined in the section on rock alteration. From the petrographic and x-ray examination of the sample, it was found to be altered to smectite and the zeolite clinoptilolite (Figure 25). Presumably the original tuff was composed predominately of vitric material since only very minor original minerals can be identified in thin section. These are zircon, apatite, magnetite and possibly some pyroxene.

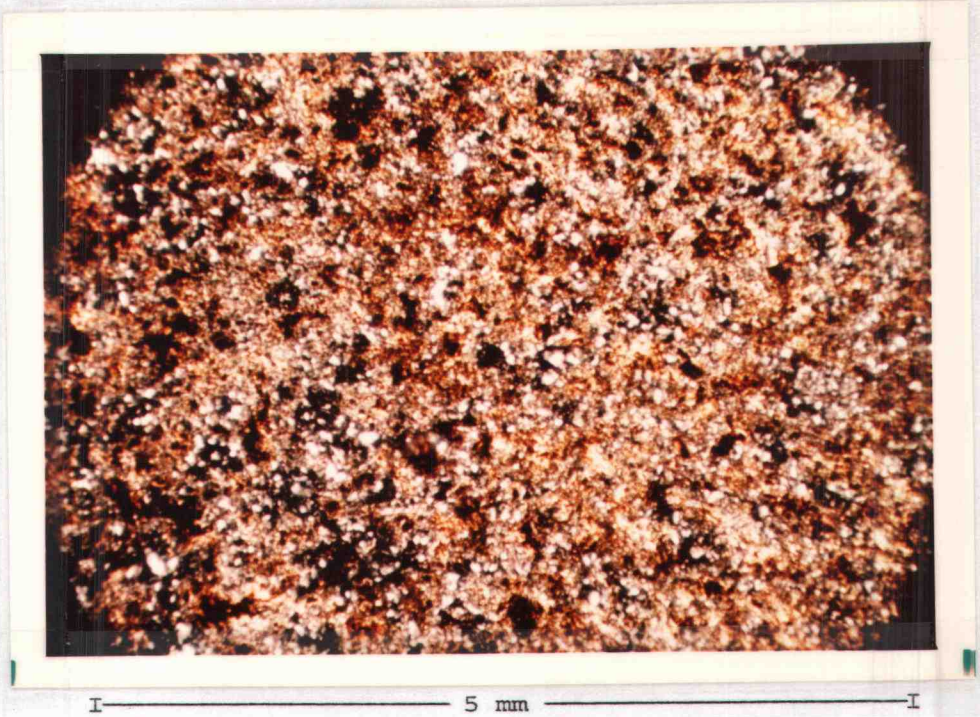

Figure 25. Photomicrograph of tuff altered to smectite and clinoptilolite. Crossed nicols. (Sample JWH-160 from SW¼, NW¼, Sec. 33, T. 10 S., R. 20 E.)

IX. Alteration of Clarno Lavas

General Statement

The rocks of this area all show some degree of alteration. The phenocryst phases which show alteration are thought by the author to be deuteric in origin with further change caused by exposure after extrusion and surficial weathering. Most of the groundmass minerals are thought to have altered because of surficial weathering and groundwater activity. During the field work for this study, an attempt was made by the author to collect rocks with varying degrees of alteration with the intention of performing a detailed petrographic examination. For this purpose, 20 samples were collected and thin sections made. Although many alteration minerals were identified with the aid of the microscope, there were several in which identification with confidence was not possible. Following the suggestion of Dr. Harold Enlows of the Geology Department at Oregon State University, several of the samples were analyzed with x-ray diffraction to help with the identification of the clay alteration products. The procedure followed is not the same as that described for the analysis of the tuff beds and is much less reliable. However, these analyses give a general idea of what clays are present and helped to support the petrographic interpretations. In this respect, the diffraction patterns are a real assistance.

Thirteen samples were analyzed using x-ray diffraction. These samples were prepared by first gently crushing a small amount of the rock in a mortar and pestal. The crushed sample was then mixed with distilled water and stirred, dispersing as much of the clay fraction as possible. After allowing the coarser grained material to settle, some of the water with the clays in suspension was poured onto a glass slide. After about twelve hours the water evaporated and an x-ray diffraction pattern was obtained. Several samples had strong, well defined peaks with a d-spacing of between 15.0 and 15.3 angstroms. The samples with these spacings were glycolated following the procedures for glycolation described in the section dealing with tuff. Again diffraction patterns were obtained to see if any expansion of the clay structure had occurred. Expansion did occur in several samples indicating the presence of smectite clays or possibly smectite interlayered with other clay minerals such as vermiculite or mica.

Discussion

The plagioclase phenocrysts altered to a wider variety of products than any other mineral in this area. Many of these plagioclase crystals were not in equilibrium with the melt when it was extruded. The effect of this desequilibrium was discussed earlier when describing patchy zoning. The changes caused by these conditions increased the deuteric and possibly the surficial weathering effects

on the plagioclase phenocrysts. Figure 26 shows a plagioclase phenocryst composed of several crystals in a synneusis relationship which has been resorbed and later partially altered to a greenish-yellow to brown, highly birefringent material. This material appears to be a smectite clay based on evidence seen in diffraction patterns. The optical properties suggest that it may be nontronite. It is faintly pleochroic. The plagioclase phenocryst in Figure 27 shows almost complete alteration to smectite and some zeolite. Only a narrow rim of late crystallizing plagioclase remains unaltered which is true of most of the groundmass microlites. Other alteration products of plagioclase not already mentioned include carbonate (probably calcite), the zeolites heulandite and possible analcite or chabazite, minor chlorite and very minor sericite. One x-ray pattern showed a sharp peak at 7 angstroms indicating kaolinite. In thin section, this material appears as a brownish milky mass usually associated with plagioclase although sometimes it appears to be filling vesicles.

The pyroxene phenocrysts are generally altered to only two principle minerals. Figures 28 and 29 show a hypersthene phenocryst which is almost completely altered to chlorite and minor magnetite. At times magnetite will form pseudomorphs after pyroxene. Augite is also observed to alter to chlorite and magnetite. These are not the only

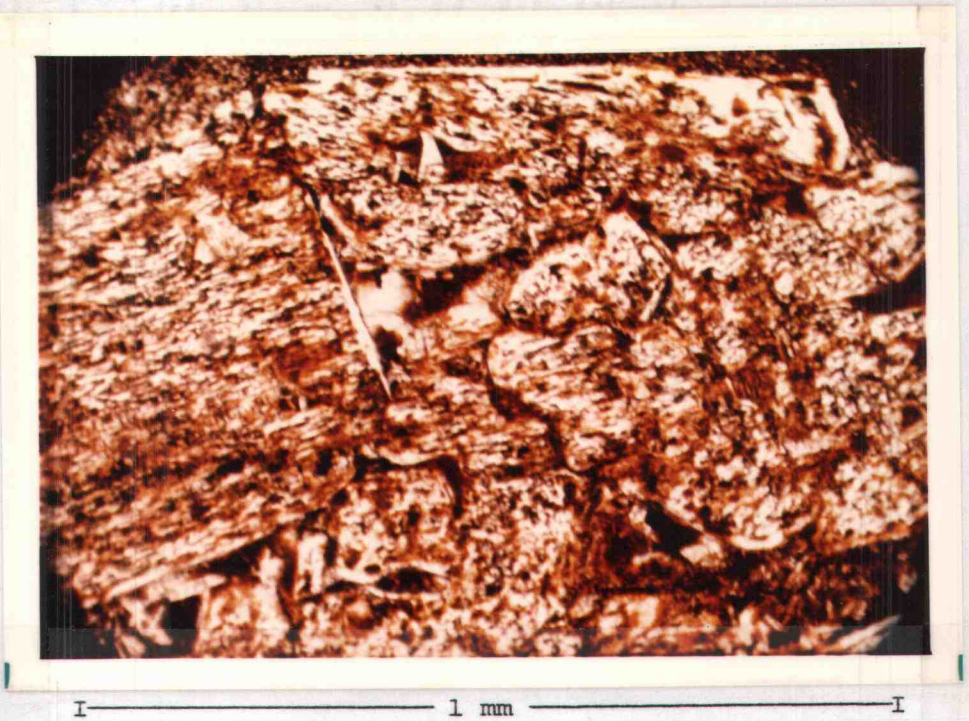

Figure 26. Photomicrograph of plagioclase altering to smectite in a dacite flow. (Sample JWH-99 from NE¼, SW¼, Sec. 10, T. 10 S., R. 20 E.)

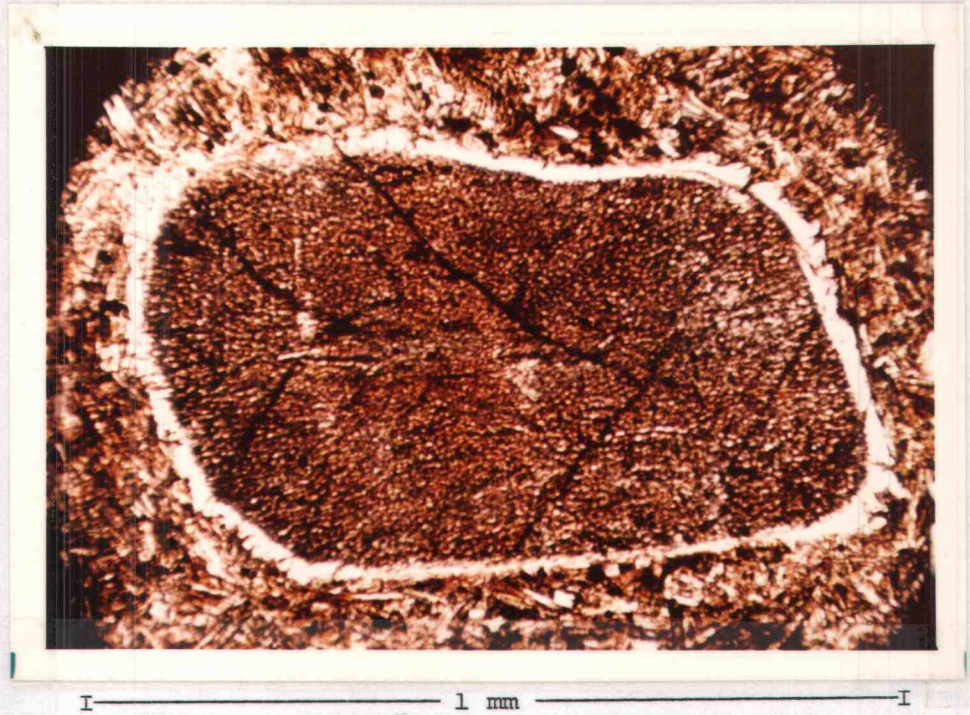

Figure 27. Photomicrograph of plagioclase phenocryst in an andesite showing almost complete alteration. (Sample JWH-72 from NW¼, SW¼, Sec. 3, T. 10 S., R. 20 E.)

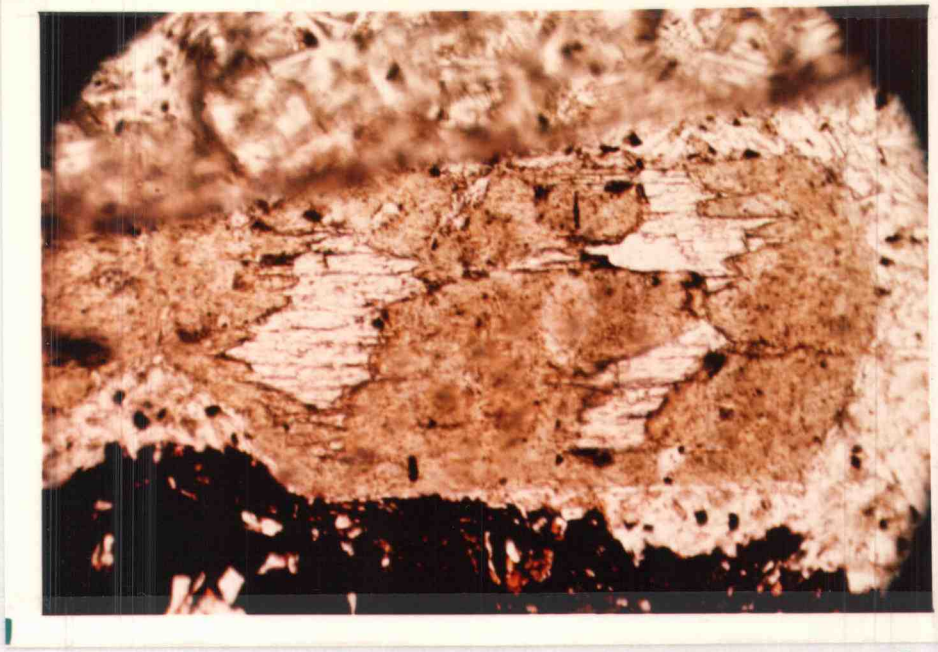

I——————————— 1 mm ———————————I

Figure 28. Photomicrograph of hypersthene phenocryst in a basaltic andesite altering to chlorite. (Sample JWH-113 from NE¼, NE¼, Sec. 15, T. 10 S., R. 20 E.)

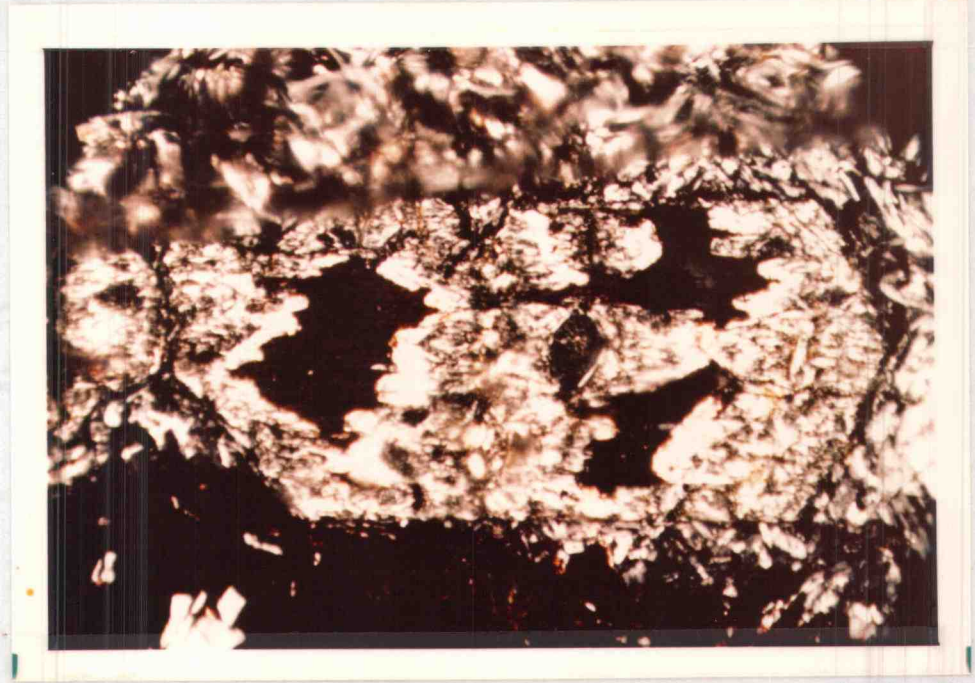

Figure 29. Same as Figure 28 above but with crossed nicols.

products of pyroxene alteration. Figure 30 shows a pyroxene phenocryst altered to a variety of different products. These include a light bluish green material believed by the author to be celadonite, small amounts of magnetite and minor carbonate. In addition to these is a brownish material which could not be identified although it is probably a smectite clay. Figure 31 shows a pyroxene phenocryst which is completely altered to chlorite, calcite and the smectite nontronite.

Many of the flows in this area are covered by a flow-top breccia which is usually extremely altered and distinctive in the field. A few of these breccias greatly resemble thin mudflow deposits although they can usually be observed grading downward into an unbrecciated flow. These breccias often contain abundant void spaces which were found to be partially or completely filled with secondary material. Figure 32 shows one of these breccias in which the void spaces have been partially filled with zeolites and chlorite. Flows in this thesis area are also commonly vesicular and these voids also are filled occasionally with secondary products, including a variety of zeolites. X-ray diffraction indicates the possibility of heulandite and natrolite and petrographic evidence further indicates the possibility of chabazite or analcite. Many vesicles are also filled with chlorite as shown by Figure 33.

The upper flow in the Painted Hills Dacite is the

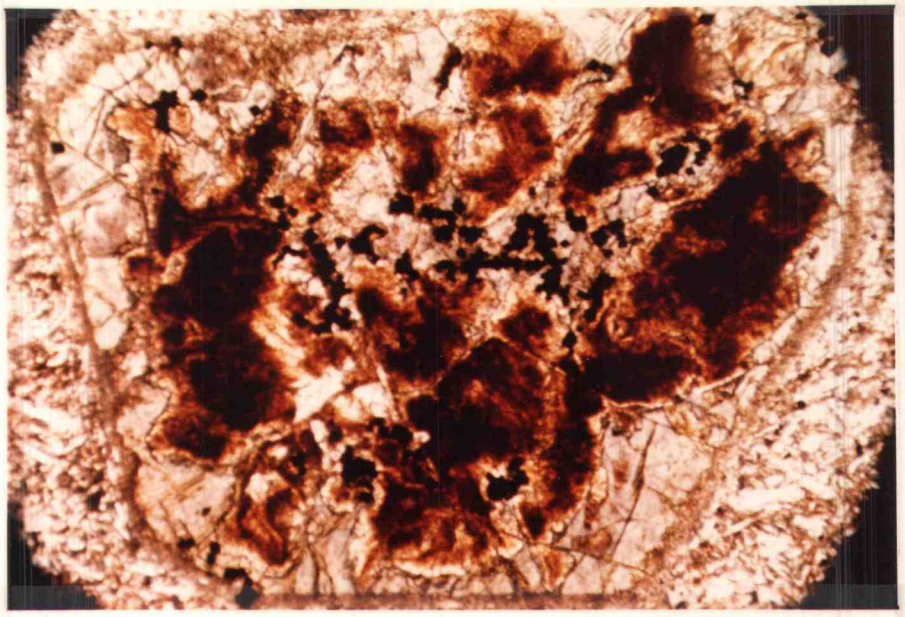

Figure 30. Photomicrograph of completely altered pyroxene phenocryst in an andesite. (Sample JWH-77 from SW¼, SE¼, Sec. 3, T. 10 S., R. 20 E.)

Figure 31. Photomicrograph of completely altered pyroxene in a dacite. Crossed nicols. (Sample JWH-155A from SE¼, NW¼, Sec. 27, T. 10 S., R. 20 E.)

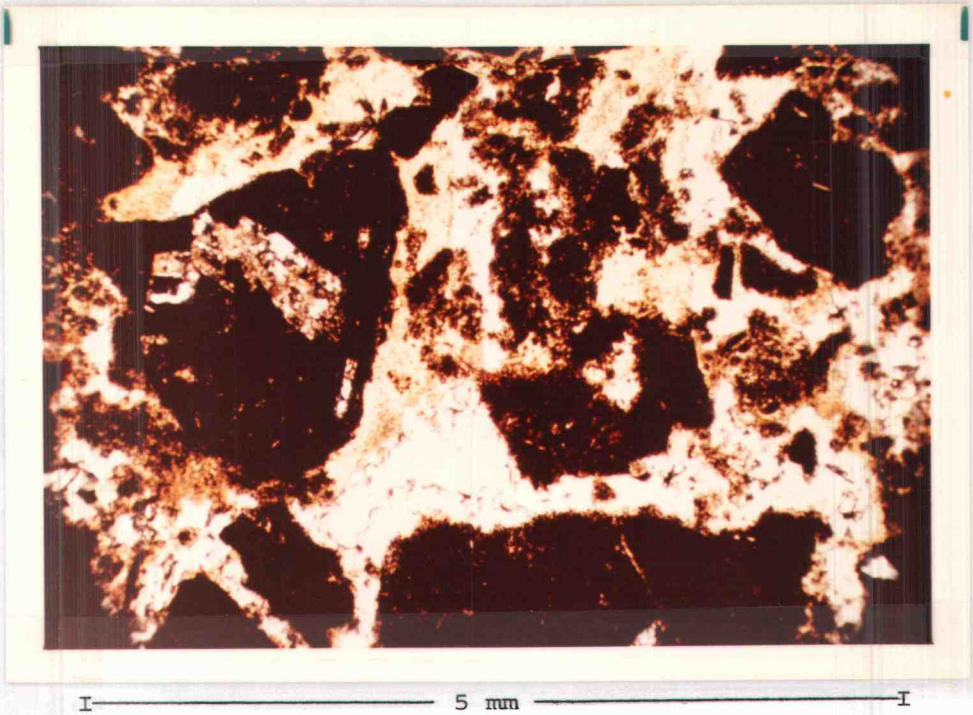

Figure 32. Photomicrograph of zeolite and chlorite forming in void spaces of a flow top breccia. (Sample JWH-169 from NE¼, SW¼, Sec. 33, T. 10 S., R. 20 E.)

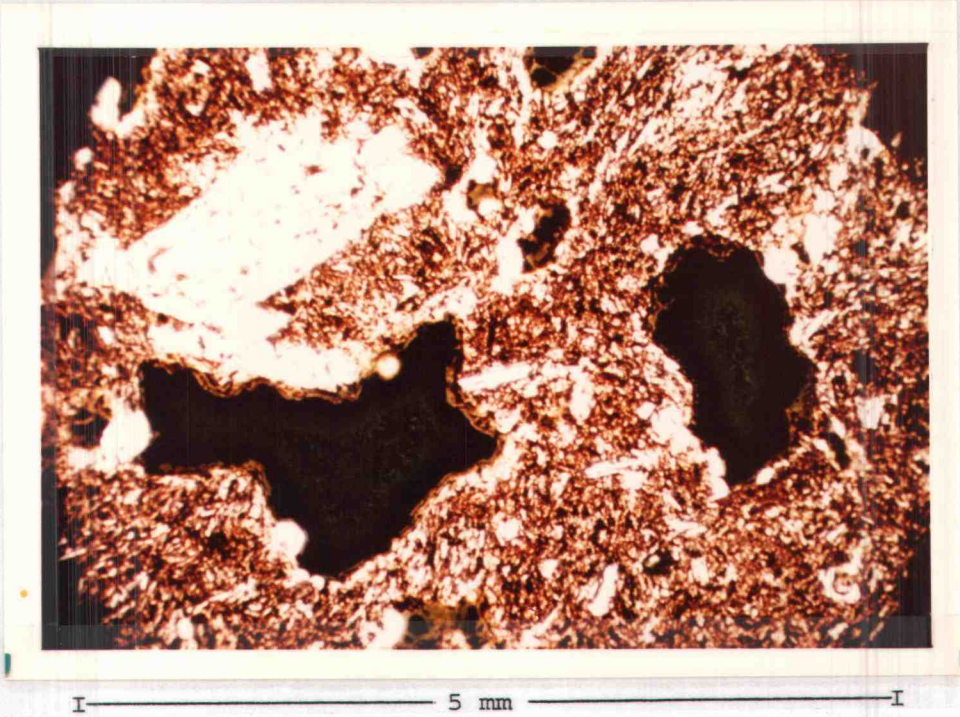

Figure 33. Photomicrograph of chlorite filling vesicles. (Sample JWH-124 from NE¼, NW¼, Sec. 21, T. 10 S., R. 20 E.)

youngest flow in the Clarno rocks of this area and its weathered surface forms the contact between the Clarno and John Day formations. Because of the unconformable relation of the contact this flow may have been exposed at the surface for a greater length of time than any in the area. Five samples, which encompass the least altered to the most altered, were collected from this flow and all were examined for clay minerals using x-ray diffraction. It was found that the freshest sample showed no evidence for kaolinite while each of the other samples of increasing alteration showed a kaolinite peak of consistently greater intensity and definition. This may indicate a gradual increase in abundance of kaolinite and its degree of crystallinity with increasing alteration. In addition to the kaolinite peak each sample showed a small, poorly defined peak which may be minor poorly crystallized smectite or chlorite-intergrades.

X. Geochemistry of the Clarno Lavas

The lavas of the Clarno Formation in this thesis area range in composition from basaltic andesite, with 55 weight percent SiO_2, to rhyodacite with approximately 70 weight percent SiO_2. The chemical analyses for these rocks can be found in Appendix A. The rhyodacites are rare while the basaltic andesites, andesites and dacites occur in about the same abundances.

When plotted on variation diagrams (see Appendix B), patterned after those of Harker, the major element oxides all show typical changes with increasing silica weight percent. With increasing silica content, the alkali concentrations increase while the concentrations of Al_2O_3, FeO, MgO, CaO and TiO_2 all decrease in varying degrees. The sodium and aluminum plots both show a great deal of scatter although a general trend can be identified. In the iron diagram the low point at 58 percent SiO_2 is believed to be caused by an analytical error and is probably about two weight percent greater. The other three abnormally low points are believed to be accurate and represent low iron lavas. The calcium variation shows the lowest degree of scatter giving a well defined variation which is characteristic of Clarno lavas (Taylor, 1977 personal communication).

The volcanic rocks of this area are calcic when plotted on a Peacock (1931) alkali-lime index giving an index value of 62 (Fig. 34). This calcic character is found in other areas with Clarno rocks as well (Owen 1977, Taylor, 1977 personal communication, Barnes, 1977 personal communication) but may be due to alteration effects. These rocks have been described as true calc-alkaline by others (Wilson 1973, Novitsky and Rogers 1973, Novitsky-Evans 1974, Rogers and others 1975).

Most of the flows in this area have relatively high alumina values. All but two, which have 14 weight percent, contain between 15 and 18 weight percent alumina. Figure 34 shows the high alumina field of Kuno (1968) and it can be seen that most of the rocks in this area plot within this field or on the boundary between the tholeiitic and high alumina fields. This was also found to be true by Wilson (1973), Novitsky-Evans (1974), and Owen (1977).

The volcanics of this area may be calcic but when plotted on AFM and KCN diagrams (Figs. 35 and 36) of Nockolds and Allen (1953) they show distinctive calc-alkaline trends and compare closely to other recognized calc-alkaline series (Best 1969, Carmichael and others 1974). Figure 35 also shows the area of Kuno's (1968) hypersthenic series and it can be seen that the rocks of this area fall mostly within this series. These diagrams agree closely with data by Wilson (1973), Novitsky-Evans (1974) and Owen (1977).

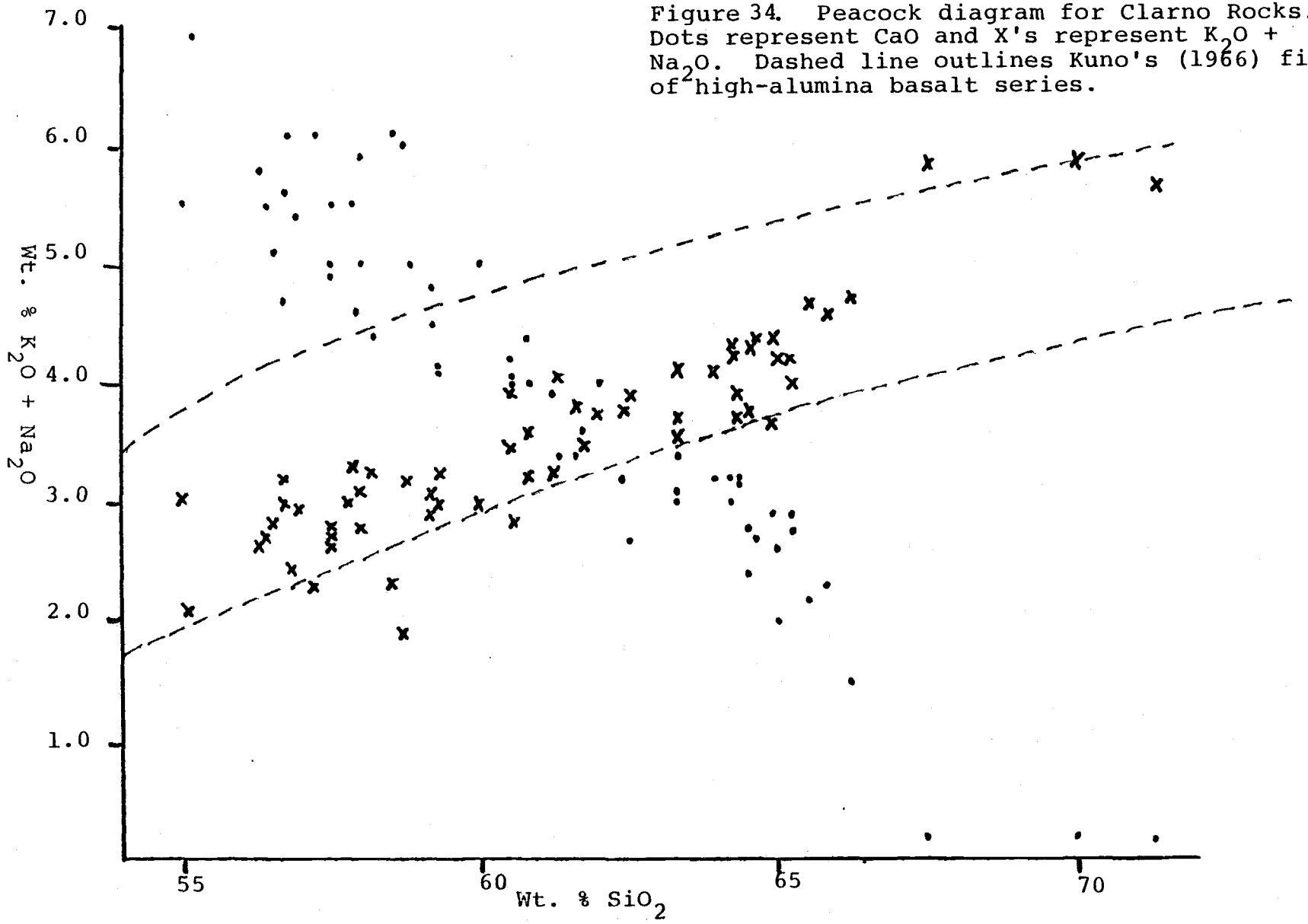

Figure 34. Peacock diagram for Clarno Rocks. Dots represent CaO and X's represent K_2O + Na_2O. Dashed line outlines Kuno's (1966) field of high-alumina basalt series.

Figure 35. AFM diagram after Nockolds and Allen (1953) for Clarno Rocks. Dashed lines show Kuno's hyperthenic series (1968).

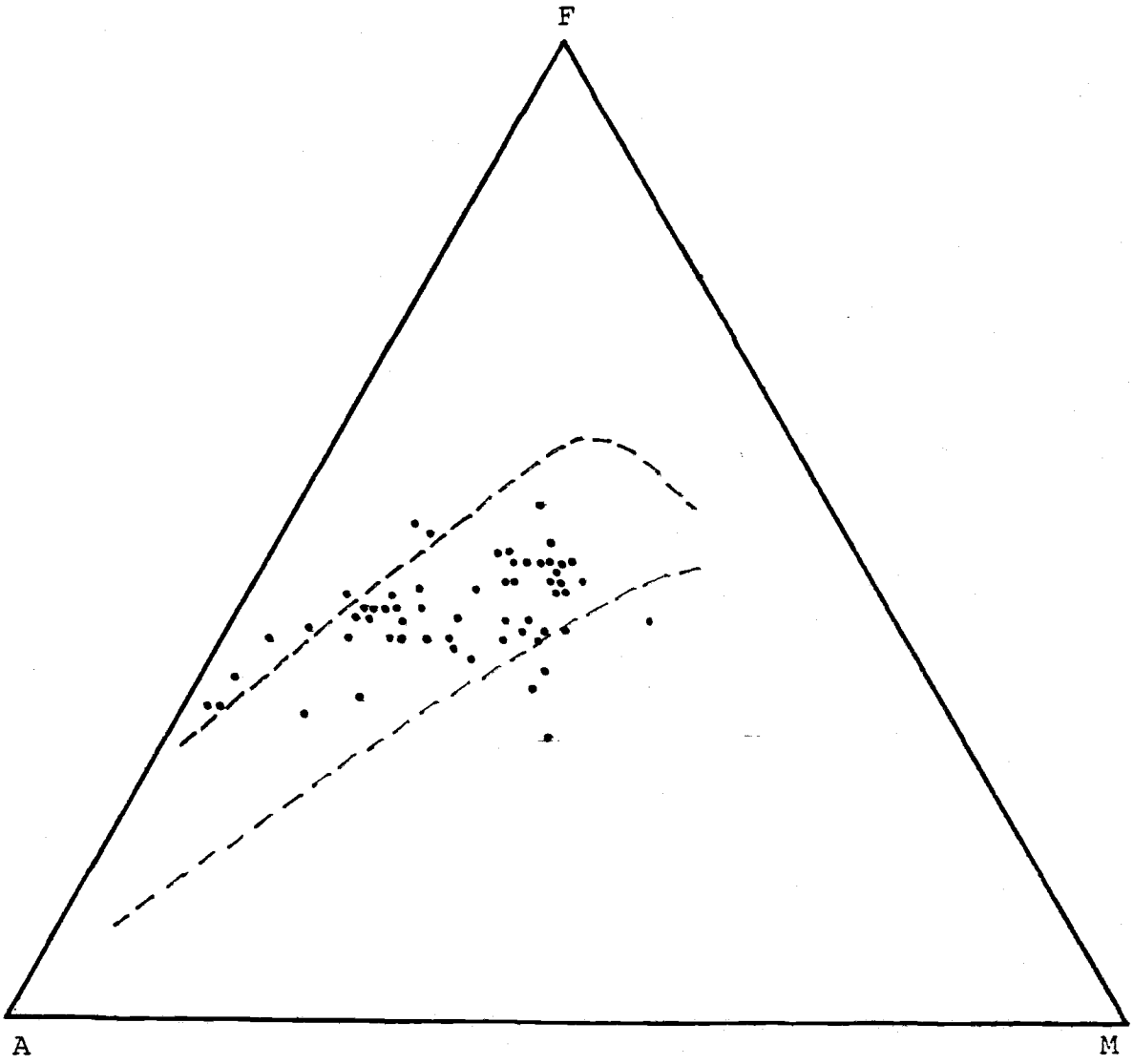

Figure 36. KCN diagram, after Nockolds and Allen (1953), for Clarno Rocks.

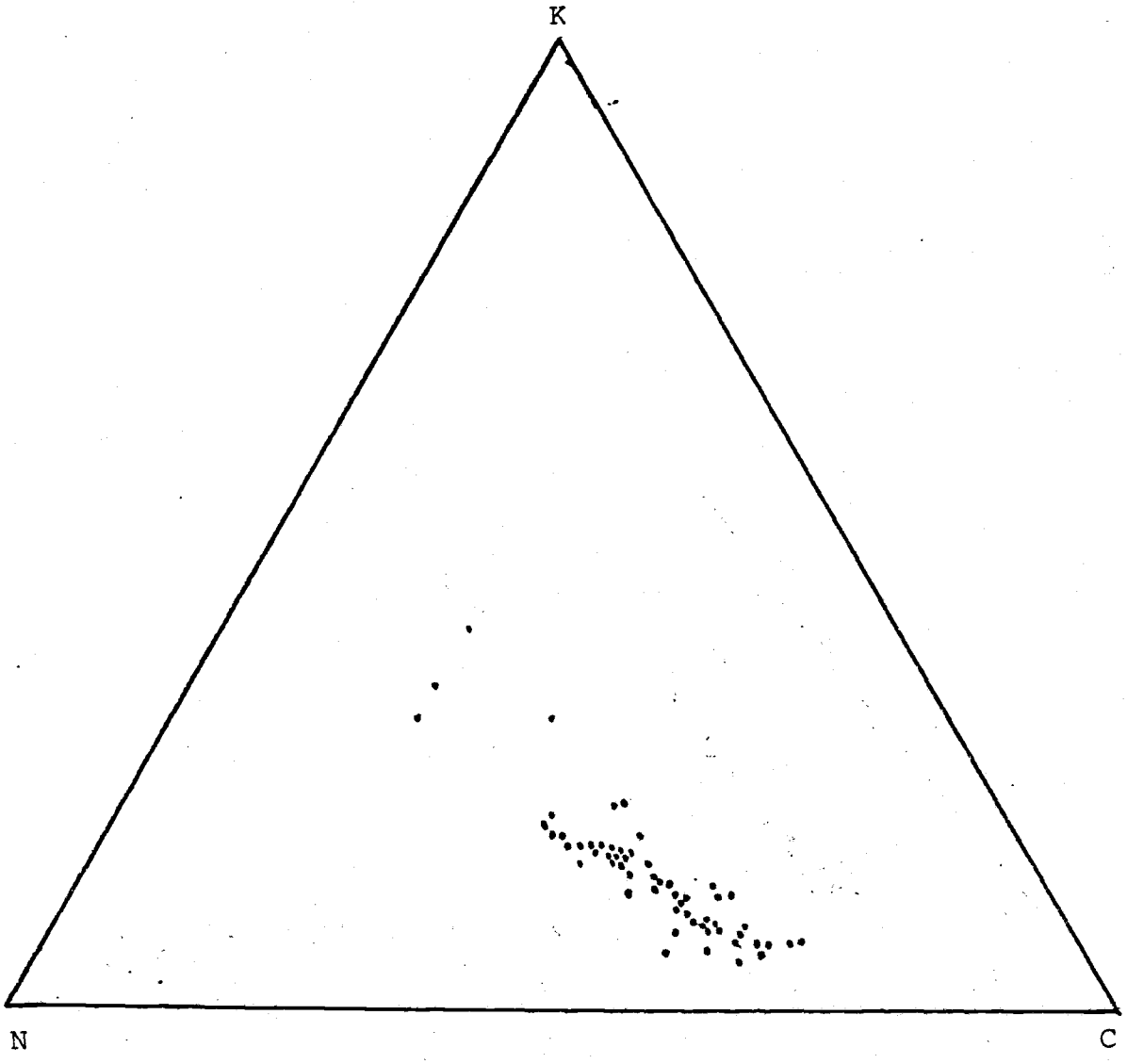

John Day Formation

Introduction

The John Day Formation comprises approximately 11 km^2 in this thesis area. The entire sequence lies within the eastern facies of the formation (Robinson 1968, 1973). Figures 37 and 38 illustrate how the John Day Formation crops out in this thesis area.

The author has completed only field mapping of the John Day Formation. Because the Clarno Formation was the area of primary study for this project, the following represents a summary of previous work on the John Day rocks of this area. This summary incorporates the work of Hay (1962b, 1963) and Fisher (1966b). The subdivisions of Hay (1962b) will be used. He divides these rocks into a lower, middle and upper member.

I. Lower Member

General Statement

The lower member is slightly over 335 m thick and is composed predominately of tuffaceous mudstone with minor thin layers of vitric tuff. The lower 100 m of this member is red while the remaining is mostly yellow to cream in color with small areas of light green and brown. Many of these beds contain abundant, well preserved leaf fossils (Chaney 1924, 1948).

Figure 37. Painted Hills State Park. Light colored units of the lower member capped by the cuesta forming ignimbrite middle member of the John Day Formation.

Figure 38. Standing on top of cuesta shown in Figure 37 above looking north. All three members shown dipping below Picture Gorge Basalts of Sutton Mountain at right.

Lithology

The mudstone beds are usually massive in character and have a vitroclastic texture. Pumice fragments and shards are ubiquitous throughout the entire lower member except in a few of the red mudstones. In addition to the glassy materials, now mostly altered, many beds contain minor amounts of plagioclase crystals with some sanidine and rare quartz. Andesine is the dominant feldspar; however, oligoclase and labradorite are common and in some layers predominate. Occasionally, lithic fragments of volcanic rock ranging in composition from basaltic to rhyolitic are found. Alteration products include montmorillonite and orthoclase after plagioclase, montmorillonite after glass and vermiculite after biotite. The yellow mudstones contain only montmorillonite as their clay alteration product. The red mudstones, which get their color from large amounts of hematite and limonite relative to other layers, have montmorillonite as well as varying amounts of kaolinite. Celadonite is restricted to the green mudstones.

The vitric tuffs range in thickness from several centimeters to a few meters but in some places fluvial processes have formed thicknesses of up to 25 m. These tuffs are usually white except on fresh surfaces where they are light shades of gray. Montmorillonite and clinoptilolite form the matrix of these tuffs although

montmorillonite is much more common. Pumice fragments and glass shards were the dominant constituents of the original unaltered tuffs and although fresh glass is still present, most has been altered. Mineral components include sanidine, oligoclase and sodic andesine with minor quartz and rare pyroxene. The percentages of these minerals in the different beds vary but together they rarely account for more than 10 percent of any given unit.

One sanidine-rich layer found in the lower member is important because it is believed to correlate to the lower ignimbrite of Peck's (1964) member H found in the western facies (Hay 1963 and Robinson 1968, 1973). This layer is from zero to one meter in thickness and is found from 150 m to 250 m above the base of the formation. Sanidine crystals are characterized by mantles of myrmekitic intergrowths of quartz and are from one to four mm in diameter with a composition of $Or_{43}Ab_{54}An_3$.

Deposition

The lower member at Painted Hills appears to have been deposited predominantly by pyroclastic air-fall with minor reworking by sheet-wash and fluvial processes. Hay (1962b) states:

> Size distribution of the crystals and rock fragments indicates that the ash fell directly from eruptive clouds, rather than being eroded from the surface elsewhere and transported by wind before finally being deposited as suggested by Fisher and Wilcox (1960) for the bulk of the John Day near Monument, 40 miles east-northeast.

> The wind-transported mineral grains of dunes and blanketlike deposits such as loess are well sorted, whereas the crystals and rock fragments of most samples from the John Day Formation are graded rather evenly throughout a considerable range in size - commonly from coarse silt to medium sand.

In a later paper, Fisher (1966d) confirmed an air-fall origin with a study of the textural characteristics of John Day siltstone in the Monument and Kimberly quadrangles. In this study, he determined and plotted median diameters and sorting coefficients of the siltstone. These were similar to both volcanic ash and loess but plots using the ratio of these two parameters show that these rocks most likely have an air-fall origin. The lack of structures, such as finely stratified beds, which are expected in air-fall tuffs is explained as follows by Hay (1962):

> The massive poorly defined bedding of most claystones is attributed to reworking and weathering of the surface layers of ash. Reworking of the surficial ash by roots, burrowing organisms (particularly earthworms), and sheet wash probably eliminated the initial stratification and mixed the pyroclastic detritus, thus explaining the wide range of feldspar composition commonly observed in single samples.

Desiccation cracks, mudstone breccias and possible clay-filled root markings in the lower 100 m of the member all indicate a rather slow deposition rate for the lower member tuffs. Hay (1962) believes that accumulation was slow enough to convert most vitric material to montmorillonite prior to burial. Potassium-argon dates in the upper 300 m of the lower member indicate a period of deposition

lasting approximately 7 million years which gives an accumulation rate of 5 cm/100 yrs.

The climate during deposition was warm-temperate to sub-tropical with abundant rain fall (Chaney 1927, 1952; Wolf and Hopkins 1967). Therefore, there would have been plenty of time for weathering to have take place at or near the surface (Hay 1960).

The reddish coloration of the tuffs is confined to the lower third of this member. This coloration may be caused by the contamination of underlying deeply weathered Clarno rocks which are a deep red where exposed in this area. Clay analysis by Hay (1963) shows that kaolinite is the dominant mineral in the weathered profile and x-ray analysis performed by the present author confirm this. The red tuffs in the overlying John Day are the only ones to contain kaolinite and it is most probable that their red coloration is due to contamination from Clarno soil. Hay states:

> The red claystones can be explained best as deposits of sheet wash, small streams, and possible thin, soupy mudflows, most of which originated on the upper slopes of the larger hills, where sheet erosion slowly removed and mixed the juvenile ash with the older, kaolinitic soils.

These hills of Clarno rock would slowly be covered and this may account for the gradual decrease in red colored beds from the base of the lower member upward (Hay 1962; Fisher and Wilcox 1960).

Fisher (1968), however, compares the tuffs in the

lower member to laterites found developing on tholeiitic rocks in Hawaii. Chemically the tuffs and laterites show similar trends and Fisher suggests that the red color is due to conditions (Eh and pH) present during alteration of the tuffs in situ.

II. Middle Member

General Statement

Fisher (1966b, c) has completed a comprehensive regional study on the ash-flow tuff middle member in which he named it the Picture Gorge Ignimbrite from exposures to the east. This ignimbrite sequence is composed of two separate cooling units which are divided into six zones following the terminology described by Smith (1960b) (Figure 39). The lower cooling unit is divided into four zones. From the base upward they are: the lower zone of no welding, the zone of dense welding, the vapor-phase zone and the upper zone of no welding. The upper cooling unit is divided into a zone of partial welding at the base and a zone of no welding above. Immediately above and below the ignimbrite sequence are thin layers of finely laminated air-fall tuff. Lithologic descriptions of the two cooling units are summaries from Fisher (1966) and Hay (1963). Chemical analyses performed by several different authors indicate this ash-flow tuff to be rhyolitic in composition (Table 4). In

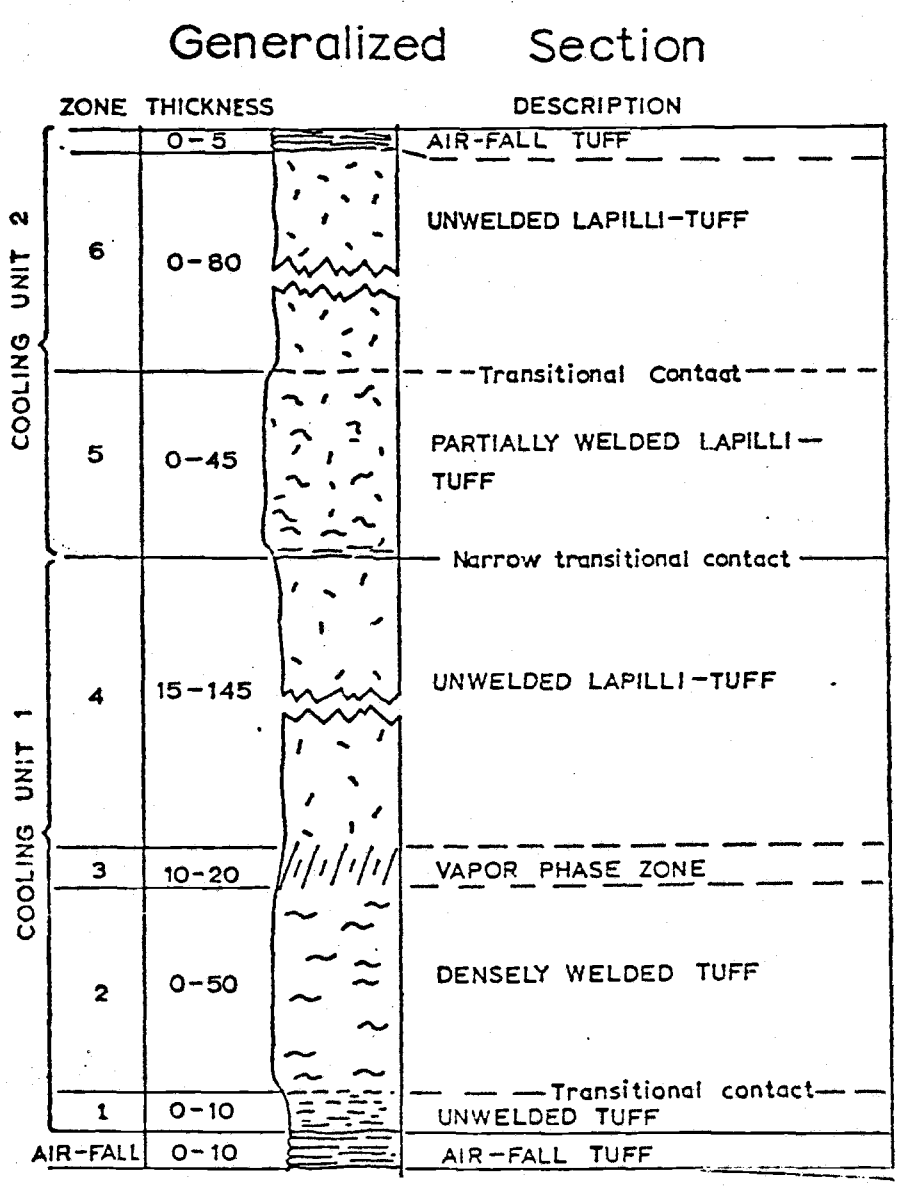

Figure 39. Generalized columnar section of middle member ignimbrite after Fisher (1966b).

Table 4. Chemical analyses of John Day Ash-Flow Tuff.

Sample	1 Hay 1962	2 Hay 1963	3 Hay 1963	4 Hay 1963	5 Fisher 1966	6 Fisher 1966	7 Peck 1964
SiO_2	73.56	71.36	70.85	75.20	70.40	70.68	72.2
Al_2O_3	12.78	11.57	11.90	12.49	13.65	12.49	11.40
Fe_2O_3	2.07	1.06	1.12	0.33	1.18	1.58	1.40
FeO	0.09	1.74	1.69	nil	1.81	1.36	0.66
MnO	tr	0.05	0.05	tr	0.04	0.04	0.08
MgO	0.24	0.17	0.27	0.06	0.07	0.09	0.33
CaO	0.66	0.71	0.91	0.66	1.58	1.46	0.61
Na_2O	3.89	3.09	3.61	2.73	3.76	3.85	2.90
K_2O	3.86	4.85	3.99	5.93	3.90	3.44	3.40
TiO_2	0.38	0.30	0.30	0.44	0.21	0.20	0.16
P_2O_5	0.10	0.07	0.10	0.14	0.06	0.16	0.01
$H_2O \pm$	1.97	4.52	4.71	1.52	4.03	5.06	6.00
CO_2	0.05	-	-	0.03	-	-	0.07
Total	99.65	99.49	99.50	99.53	100.69	100.41	99.22

1 Densely welded tuff near base of ignimbrite, NW¼, SW¼, Sec. 31, T. 10 S., R. 21 E. (Whole rock analysis).

2 Black densely welded vitric tuff from lower part of ignimbrite, center N½, SW¼, Sec. 31, T. 10 S., R. 21 E. (Glass analysis).

3 Pale gray densely welded vitric tuff near base of ignimbrite, SW corner, Sec. 1, T. 10 S., R. 22 E. (Whole rock analysis).

4 Semiwelded devitrified tuff near base of ignimbrite, NW¼, NE¼, Sec. 36, T. 10 S., R. 20 E. (Whole rock analysis).

5 Vitrophyre from zone of dense welding - zone 2. (Whole rock analysis).

6 Vitrophyre from zone of dense welding - zone 2. (Whole rock analysis).

7 Welded ash flow, member H, Sec. 20, T. 9 S., R. 15 E. (Whole rock analysis).

this thesis area, the sequence forms a gently dipping hog-back ridge and is approximately 30 m thick. A potassium-argon age of 25.3 m.y. was determined for the ignimbrite (Evernden and others 1964).

Lithology

Cooling Unit 1:

The lower zone of no welding is a light-colored tuff which grades upward into the zone of dense welding. This tuff is composed dominantly of glass shards and pumice fragments mostly devitrified to alkali feldspar and cristobalite or altered to clinoptilolite and minor montmorillonite. This zone shows a slight fissility due to the partial flattening of the glass shards. Crystals, which together account for less than ten percent of the rock, include oligoclase, albite and ferroaugite with accessory amount of augite, hypersthene, quartz, oxyhornblende, zircon, magnetite and apatite. Lithic fragments in minor amounts also occur.

The zone of dense welding and the vapor-phase zone are composed essentially of the same minerals and lithic fragments as the lower zone of no welding, although quantities of the various phases differ slightly. Welded glass shards and collapsed pumice fragments are the dominant materials and give the more densely welded zones a poorly developed eutaxitic texture. Devitrification and vapor phase

crystallization to alkali feldspar and cristobalite with minor tridymite has occurred.

The upper zone of no welding, which grades downward into the vapor-phase zone, is the thickest zone of cooling unit 1. Again the same minerals and lithic fragments are present but the proportions of several are markedly different from the nonwelded zone at the base of the unit. Crystals of zoned feldspar, andesine in particular, are much more abundant and much larger than the feldspars in the lower nonwelded zone. Rounded and embayed quartz is more common and augite increases in abundance relative to ferroaugite. In addition there is a higher percentage of oxyhornblende in the upper zone. The greatest contrast is shown by the magnetite content which is 10 times that of the lower zone. In some areas the sizes of pumice fragments in the upper zone show grading with the largest fragments at the base. Overall they are much larger than in the lower zone. The alteration products found in the upper zone of no welding consist of celadonite, nontronite and clinoptilolite which are slightly different from those of the lower zone.

Cooling Unit 2:

The contact between cooling unit 1 and cooling unit 2 is transitional over a short distance with no observable break. The two zones, the zone of partial welding and

overlying zone of no welding, forming this unit also show a transitional contact.

The minerals of unit 2 are different in many respects to those of cooling unit 1. Zoned andesine is more abundant than oligoclase and the amounts of oxyhornblende, apatite and augite are greater in unit 2. Mafic minerals such as iddingsite (after olivine?), enstatite, epidote and clinozoisite are found in trace amounts while in unit 1 they are not found.

The pumice and lithic fragments in cooling unit 2 are in general smaller than in unit 1. Alteration of the shards and pumice is similar to that described for the upper zone of no welding in cooling unit 1 although fresh glass is common.

Deposition

These tuff units show many of the characteristics now recognized and described for tuffs of ash-flow origin (Smith 1960a, b; Ross and Smith 1961; Peterson 1970; Fisher 1966c; Walker 1972; Sparks and others 1973). Fisher (1966c) described a possible mechanism for the deposition of the Picture Gorge Ignimbrite. He uses the boundary layer concept of fluid mechanics to explain the changes in mineral size and abundance and the lack of sorting in pumice and lithic fragments away from the source.

With the use of isopach maps Fisher found a decrease

in thickness in the two cooling units from west to east. He also found decreases in the sizes of pumice, lithic fragments and in the weight percent of heavy minerals (magnetite and clinopyroxene) from west to east. Finally, the abundance of magnetite decreased faster than feldspar in the same direction. All of this evidence indicates a source for these ash-flow tuffs somewhere to the west. Noted, however, is the fact that the sizes of the feldspar crystals remain fairly constant throughout the extent of the ignimbrite. Fisher states, "these relationships require a transporting system where coarse and fine-grained fragments may be simultaneously deposited without a marked decrease in forward velocity of the main flow." The mechanism envisaged relates to the boundary layer in which there is a lack of turbulent motion. Fisher further states:

> Turbulent motion in a flow results in nearly random movement for a given suspended particle depending upon (1) the velocity, energy and directions of current eddies, (2) the settling velocity of the particles, (3) the energy of possible gasses escaping from the particles, and (4) the interference of other particles. Thus, it is probable that particles enter the boundary zone at random irrespective of the forward velocity of the main flow. Particles of highest settling velocities tend to enter the boundary zone more often than particles of low settling velocities, but both may be deposited simultaneously.

and:

> The chance for deposition of a small lightweight particle is nearly as great as for a large and relatively heavy particle; therefore, development of layering is inhibited, and deposits tend to be poorly sorted at any particular locality.

Because of this type of deposition, the ignimbrite layer will gradually increase in thickness at any point as the flow is moving by. These depositional processes lead to interesting vertical and lateral relationships as described by Fisher:

> At any one vertical section, the stratigraphically higher portions of the ignimbrite are the youngest, but vertical sections far away from the ignimbrite source are younger than vertical sections near the source because laterally equivalent lithologic zones are not time equivalent.

Fisher (1966b) suggests that the two cooling units, representing two distinct ash-flow events, are formed from the same eruptive episode. These flows were preceeded by a small volume of air-fall material which was also comagmatic. From the study of mineral relationships in the different zones of the two cooling units, particularly the upper and lower zones of no welding of unit 1, Fisher concluded that the zones represented varying levels within the magma chamber. The basal air-fall zone is representative of the upper parts of the chamber and each zone above this represents successively deeper levels within the magma chamber. Evidence for this is the increase in An content of the feldspars and the increased percentage of magnesium-rich clinopyroxene in the upper zones, both of which indicate higher temperatures of formation. Additional evidence is found in the two zones of cooling unit 2 in which minor amounts of euhedral olivine, enstatite and labradorite and

some anhedral clinozoisite and epidote occur. These two zones while stratigraphically the highest should represent the lowest levels to be erupted from the magma chamber. The mineral proportions tend to support this conclusion. The higher percentage of magnetite, the increase of augite relative to ferroaugite and the greater percentage of oxyhornblende in the upper stratigraphic levels of the ignimbrite indicate an increase in the partial pressure of oxygen with depth in the magma chamber.

III. Upper Member

General Statement

The upper member forms only a thin unit in this thesis area although immediately to the east it reaches a thickness of about 300 m. It is composed of light-colored massive tuffaceous mudstone and tuff, some of which have been reworked by fluvial processes. In appearance these tuffs greatly resemble those in the upper part of the lower member.

Lithology

The bulk of these beds is composed of glass pumice shards and pumice with from 5-10 percent of feldspar crystals (primarily andesine) and fragments of silicic lava. Some clinopyroxene and magnetite with minor ilmenite, hornblende and biotite is also found. Refractive index measurements on

the glass indicate a silicic composition (Hay 1963). Unlike many of the tuffs of the lower member there is a complete lack of sanidine. In addition, the upper member contains abundant fresh glass while the glass in the lower member is mostly altered to zeolites and clay.

Deposition

The tuffs and tuffaceous mudstone of the upper member were initially deposited by air-fall processes. Upon deposition many were reworked by fluvial action or disturbed by organisms and plants as was the lower member.

IV. Age and Source

Potassium-argon ages for the John Day Formation have been published by many authors from different areas and range from 23.3 to 36.1 m.y. Following the divisions of Harland and others (1964) this would fall between the lower Oligocene and the lower Miocene. Paleontological evidence based on leaf and mammal fossils give ages which range from middle Oligocene to lower Miocene (Chaney 1927, 1948, 1952; Rensberger 1965).

Several writers feel that the John Day rocks represent deposition from two different source areas (Hay 1963; Peck 1964). The ash-flow tuffs are predominatly rhyolitic in composition and are believed to have come from a local source. Although no detailed chemical comparisons have been

made, these ash-flow tuffs may have originated from the numerous small silicic intrusives and domes found throughout this region and a short distance to the west. Hay (1962b) suggests the air-fall tuffs are commonly andesitic and dacitic as well as rhyolitic in composition. He bases these conclusions on mineralogical evidence. These air-fall tuffs may be correlative to volcanic material of similar composition found in the western Cascades 150 km to the west, and described by Peck (1960). A similar time span is represented by John Day and Western Cascade rocks. This possibility was first suggested by Hodge (1932) and later supported by Hay (1962b, 1963) and Peck (1964).

Quaternary Deposits

Quaternary deposits in the area are of three types. The most extensive are landslide deposits. There are three mappable landslides, two of which are very large and together cover approximately 3 km^2. The largest of these covers most of Section 4 and part of Section 9, T. 10 S., R. 20 E. Clarno tuff beds are usually associated with these landslides and are probably responsible in large part for them. As described earlier, most of the tuff beds are composed predominately of expanding smectite clays and these would make the ground very unstable.

The second most extensive deposit is stream alluvium. This is found in varying thicknesses in all of the canyon bottoms but is most abundant along Bridge and Bear Creek. These deposits are unconsolidated, poorly sorted deposits usually dumped rather rapidly in association with rainfall during summer thunderstorms.

The last type of deposit is the result of small localized slumps. These slumps are usually small blocks of flow rock which has slipped downslope without breaking into a jumbled mass of rock as seen in the landslide. These are also associated with tuff beds and weathering profiles from underlying flows.

In some areas a white lense-shaped ash deposit is found which accumulated in the canyons and valleys. The

thickest accumulation of this material is found in the NW¼ of Section 1 and is about two meters thick. These deposits are only identified in the northern half of the thesis area. This is believed by the author to be Mazama ash which has been reworked.

STRUCTURE

General Statement

The structural relations in this thesis area are difficult to define because of the nature of the rocks in the Clarno Formation. The flows are rarely widespread or sheet-like and although faulting and erosion can be demonstrated to be the cause of some of this, most is probably due to conditions of deposition. Many flows originally were short and stubby or long and narrow. In addition to this, recent slumping and sliding has created a great deal of confusion in the attitudes of the flows. In contrast, reliable attitudes are obtained for the John Day Formation because the middle ignimbrite layer and its structures are clearly visible.

Folds

As mentioned above, the attitudes of the Clarno rocks are difficult to determine but it appears most of this thesis area lies on the northwest limb of the Sutton Mountain syncline (Plate I). The axis of this fold runs through the southeast corner of the area trending northeast-southwest and plunging gently to the northeast. This structure can be seen in the Picture Gorge Basalts of Sutton Mountain and is easily recognizable. This fold was mapped by Hay (1962) and later shown by Rodgers (1966), Fisher (1967), Swanson (1969), Enlows and Oles (1971) and Robinson (1975).

It forms one of a series of northeasterly trending fold structures in this part of Oregon. The largest of these is the Blue Mountain anticlinorium lying a few kilometers to the northwest of this thesis area. Fisher (1967) believes this trend has been dominant for a long period of time, possibly originating before deposition of the Clarno Formation.

Faults

All of the faults which have been recognized in this area are small and have a simple normal component. Offsets vary from a few meters up to 20 m. In two localities hinge faults are recognized. In the SE¼, Sec. 2, T. 10 S., R. 20 E., a hinge fault with maximum displacment of 20 m is found. Displacement was difficult to determine on another hinge fault in the NW¼, Sec. 34, T. 10 S., R. 20 E.

The faults in the northeast part of the thesis area trend mostly east-west while those in the southwest trend dominately north-south.

GEOLOGIC HISTORY

The rocks of this area represent two major episodes of volcanic activity. The Clarno Formation was deposited between middle-late Eocene to early Oligocene time. The eruptions of these lavas, mudflows and pyroclastics were probably separated by relatively long periods of quiesence since many flows show extensive weathering at their surfaces, many canyons were carved which were later filled with lava and all the pyroclastics have been reworked by fluvial processes. In this area the eruptions seem to have gradually increased in silica content through time since most of the basaltic andesites are found at or close to the base of the section and these change to andesite and then to dacite in the upper part of the section. Following the Clarno volcanism was a long period of inactivity during which erosion and weathering created mild local relief and extensive soil formation. During this time mild structural deformation occurred which slightly tilted many of these flows.

The John Day Formation was deposited unconformably upon the Clarno Formation during Late Oligocene time. The John Day eruptions extruded distinctly different material from the Clarno including more abundant air-fall tuffs and areally extensive ash-flow tuffs. These deposits probably represent two different source areas with the ash-flow tuffs coming from local vents and the air-fall material

being blown in from the west (Hodge 1932, Hay 1962, 1963, Peck 1964). Following John Day time the area was again subjected to stresses which gently folded and tilted the rocks into a broad syncline.

During recent times the area has been subjected to extensive stream erosion and mass wasting. All of the faults in this area are believed to have formed during the Quaternary period.

The Clarno rocks of this area are probably surface manifestations of subduction tectonics. The geochemistry of these rocks compares closely with rocks in areas where subduction processes are believed to have occurrred. In particular the trend of K_2O versus SiO_2 (see Appendix B) agrees with trends found by other writers in areas where subduction is occurring (Hatherton and Dickinson 1969, Lipman and others 1972, Dickinson 1975).

Wilson (1973) suggests the value found for K_2O weight percent of Clarno rocks is too low for these rocks to be associated with a north-south trending subduction zone several hundred kilometers to the west. The present author finds the K_2O content to be higher than that suggested by Wilson agreeing exactly with the value given by Lipman and others (1972). This value is still low when compared to contemporaneous rocks of the Cascade range (Peck 1964). As Wilson (1973) has pointed out, this may be caused by an east-northeast trending subduction zone during Clarno time

instead of a north-south trend as suggested by Lipman and others (1972), Novitsky and Rogers (1973), Novitsky-Evans (1974), and Rogers and Novitsky-Evans (1977). Although much more work is needed, there is evidence which suggests there may indeed have been an easterly trending subduction zone during Eocene-Oligocene time in Oregon (Moore 1959, Lovell 1969, Atwater 1970, McWilliams 1972).

The fact that this area is composed completely of calc-alkaline type volcanism indicates these rocks developed on a continental type crust (Miyashiro 1974). Novitsky-Evans (1974) suggests the Clarno Formation formed on poorly developed continental crust such as that found in the Aluetian Island volcanic chain today. As pointed out by Rogers and Novitsky-Evans (1977), the Clarno Formation is unlike island arc assemblages because it is entirely subaerial. However, the petrography and chemistry is so similar to island arc volcanics they concluded that the Clarno rocks represent an intermediate association between intraoceanic and continental volcanism. The present author agrees with this conclusion.

BIBLIOGRAPHY

American Commission of Stratigraphic Nomenclature, 1961, Code of Stratigraphic Nomenclature: Amer. Assoc. Pet. Geo. Bull., V. 45, p. 645-665.

Armstrong, R.L., Taylor, E.M., Hales, P.O. and Parker D.J., 1975, K-Ar dated for volcanic rocks central Cascade Range of Oregon: Isochron/West, No. 13, p. 5-10.

Arnold, Chester and Daugherty, Lyman, 1964, A fossil Dennstaedtioid fern from the Eocene Clarno Formation of Oregon: Mich. Univ. Mus. Paleon. Contr., V. 19, No. 6, p. 65-88.

Atwater, T., 1970, Implications of plate tectonics for the Cenozoic tectonic evolution of western North America: G.S.A. Bull., V. 81, p. 3513-3536.

Baksi, A.K., 1972, The age of the Picture Gorge Basalts, Central Oregon: G.S.A. abs. with programs, V. 4, No. 7, p. 441.

Baldwin, E.M., 1964, Geology of Oregon: Ann Arbor, Mich., Edward Brothers, Inc., 161p.

Beaulieu, John D., 1972, Geologic formation of eastern Oregon: Ore. Dept. Geo. Min. Ind. Bull. 73, 80p.

_____, 1972, Plate Tectonics in Oregon: The Ore Bin, V. 34, No. 8, p. 129-142.

Bedford, J.W., 1954, Geology of the Horse Mountain area, Mitchell quadrangle, Oregon: Unpublished M.S. Thesis, Oregon State College, 90p.

Best, Myron, G., 1969, Differentiation of calc-alkaline magmas: Ore. Dept. Geo. Min. Ind. Bull. 65, p.65-74.

Bowers, H.E., 1953, Geology of the Tony Butte area and vicinity, Mitchell Quadrangle, Oregon: Unpublished M.S. Thesis, Oregon State College, 152p.

Brogan, Phil F., 1960, Camp Hancock and "Beasts of the Badlands": Geo. Soc. of the Oregon Country, V. 26, No. 9, p. 63-64.

Burvalda, J.P., 1928, Geological features of the John Day region, eastern Oregon: G.S.A. Bull., V. 38, p. 155.

Deer, W.A., Howie, R.S. and Zussman, J., 1966, An introduction to the rock forming mineral: Longman, London, England, 528p.

Dickinson, W.R., 1975, Potash-depth (K-h) relations in continental margin and intra-oceanic magmatic arcs: Geology, V. 3, p. 53-56.

Dobell, Joseph P., 1948, Geology of the Antone district, Wheeler County, Oregon: Unpublished M.S. Thesis, Oregon State College, Corvallis, 102p.

Enlows, H.E. and Oles, K.F., 1973, Cretaceous and Cenozoic stratigraphy of north-central Oregon: Clarno group in "Geologic field trips in northern Oregon and southern Washiington": Ore. Dept. Geo. Min. Ind. Bull. 77, p. 15-19.

_____, and Parker, D.J., 1972, Geochronology of the Clarno igneous activity in the Mitchell Quadrangle, Wheeler County, Oregon: Ore Bin, V. 34, p. 104-110.

Evernden, J.F., Savage, D.E., Curtis, G.H. and James, G.T., 1964, Potassium-argon dates and the Cenozoic mammalian chronology of North America: American Journal of Science, V. 262, p. 145-198.

_____, and James, G.T., 1964, Potassium-argon dates and the Tertiary floras of North America: Amer. Jour. of Science, V. 262, p. 945-974.

Ewart, Anthony, 1965, Mineralogy and petrogenesis of the Whakamaru ignimbrite in the Maraetai area of the Taupo volcanic zone, New Zealand: New Zealand Journal of Geol. and Geophys., V. 8, No. 4, p. 611-677.

Fisher, R.V., 1961, Proposed classification of volcaniclastic sediments and rocks: G.S.A. Bull., V. 72, p. 1409-1414.

_____, 1964, Resurrected Oligocene Hills, eastern Oregon: Amer. Jour Sci., V. 262, p. 713-725.

_____, 1966a, Rocks composed of volcanic fragments and their classification: Earth Science Reviews, V. 1, p. 287-298.

_____, 1966b, Geology of the Miocene Ignimbrite layer, John Day Formation, eastern Oregon: Calif. Univ. Pub., Dept. of Geo. Bull., V. 67, 59p.

Fisher, R.V., 1966c, Mechanism of deposition from pyroclastic flows: Amer. Jour. of Sci., V. 264, p. 350-363.

_____, 1966d, Textural comparison of John Day volcanic siltstone with loess and volcanic ash: Jour. Sed. Pet., V. 36, No. 3, p. 706-718.

_____, 1967, Early Tertiary deformation in north-central Oregon: A.A.P.G. Bull., V. 51, No. 1, p. 111-123.

_____, 1968, Pyrogenic mineral stability, lower member of the John Day Formation, eastern Oregon: Univ. of Calif. Publications in Geol. Sci., V. 75, p. 1-34.

Gamer, Robert L., 1969, The book of ten thousand pages: Geol. Society of Oregon Country Geol. Newsletters, V. 35, No. 9, p. 72-78.

Goddard, E.N., 1970, Rock-Color Chart: The rock-color chart committee, G.S.A.

Green, T.H. and Ringwood, A.E., 1969, Genesis of the calc-alkaline igneous rock suite: Contr. Mineral and Petrol., V. 18, p. 105-162.

Gregory, Irene, 1970, An ancient acacia wood from Oregon: Ore Bin, V. 32, No. 11, p. 205-210.

Hanson, Bruce C., 1973, Geology and vertebrate faunas in the type area of the Clarno formation, Oregon: Cord. Sect. Abs. 69th Meeting G.S.A., V. 5, No. 1, p. 87-88.

Harland, W.B., Smith, A. Gilbert and Wilcock, Bruce, 1964, The phanerozoic time-scale. A symposium dedicated to Prof. Author Holmes: Geol. Soc. London Quart. Journ., Supp. V. 1205, 458p.

Harward, M.E., 1976, Class notes; Clay Mineralogy, Dept. of Soils Science, Oregon State University, Corvallis, Oregon.

Hatherton, T. and Dickinson, W.R., 1969, The relationship between andesitic volcanism and seismicity in Indonesia, The Lesser Antilles, and other island arcs: J. Geophs. Res., V. 74, p. 5301-5310.

Hay, R.L., 1960, Rate of clay formation and mineral alteration in a 4000-year-old volcanic ash soil on St. Vincent, B.W.I.: Amer. Jour. Sci., V. 258, p. 354-368.

Hay, R.L., 1962a, Soda-rich sanidine of pyroclastic origin from the John Day Formation of Oregon: The Amer. Mineralogist, V. 47, p. 968-971.

_____, 1962b, Origin and diagenetic alteration of the lower part of the John Day Formation near Mitchell, Oregon: in "Petrologic Studies", Geol. Soc. Amer., Buddington Volume, p. 191-216.

_____, 1963, Stratigraphy and zeolitic diagenesis of the John Day of Oregon: Calif. Univ. Pub., Dept. of Geo. Sci., V. 42, No. 5, p. 199-261.

Hergert, Herbert L., 1961, Plant fossils in the Clarno Formation, Oregon: The Ore Bin, V. 23, No. 6, p. 55-63.

Hodge, E.T., 1932, New evidence of the age of the John Day Formation: G.S.A. Bull., V. 43, p. 695-702.

_____, 1942, Geology of north-central Oregon: Oregon State College Studies in Geo., No. 4, 76p. (Oregon State monographs. Studies in Geo., No. 3).

Howard, C.B., 1955, Geology of the White Butte area and vicinity, Mitchell Quadrangle, Oregon: Unpublished M.S. Thesis, Oregon State College, 113p.

Irish, R.J., 1954, Geology of the Juniper Butte area, Spray Quadrangle, Oregon: Unpublished M.S. Thesis, Oregon State College, 90p.

Kerr, Paul F., 1959, Optical mineralogy: McGraw-Hill Book Co., New York, 442p.

Knowlton, Frank H., 1902, Fossil flora of the John Day Basin, Oregon: U.S.G.S. Bull., 204, 153p.

Kuno, H., 1936, Petrologic notes on some pyroxene andesites from Hakone Volcano with special reference to some types with pyroxene phenocrysts: Jap. Journ. Geol. and Geog., V. 13, p. 107-140.

_____, 1950, Petrology of Hakone Volcano and the adjacent areas, Japan: G.S.A. Bull., V. 61, p. 951-1020.

_____, 1966, Lateral variation of basalt magma type across continental margins and island arcs: Bull. Volcanologique, V. 29, p. 195-222.

_____, 1968, Differentiation of basalt magmas: in "Basalts", V. 2, Interscience, New York, p. 689-736.

Laursen, J.M. and Hammond, Paul E., 1974, Summary of radiometric ages of Oregon and Washington rocks, through June, 1972, Isochron/West, No. 9, 32p.

Lindsley, D.H., 1960, Geology of the Spray Quadrangle, Oregon: Unpublished PhD Thesis, The Johns Hopkins Univ., 236p.

Lipman, P.W., Prostka, H.J. and Christianson, R.L., 1972, Cenozoic volcanism and plate-tectonic evolution of the western United States. I, Early and Middle Cenozoic: Phil. Trans. Royal Soc. London, V. 271, p. 217-248.

Lovell, J.P.B., 1969, Tyee Formation: Undeformed turbidites and their lateral equivalents: Mineralogy and paleogeography: G.S.A. Bull., V. 80, p. 9-22.

Lukanuski, J.N., 1963, Geology of part of the Mitchell Quadrangle, Jefferson and Crook Counties, Oregon: Unpublished M.S. Thesis, Oregon State University, 90p.

MacDonald, G.A., 1967, Forms and structures of extrusive basaltic rocks: in "Basalt", V. 1, Interscience, New York, p. 1-61.

MacKay, Donald, 1938, Geological report on part of the Clarno Basin, Wheeler and Wasco Counties, Oregon: Ore. Dept. Geol. Min. Ind. Bull. 5, 11p.

Marsh, O.C., 1875, Ancient lake basin in the Rocky Mountain regions: Amer. Jour. Science, Ser. 3, V. 9, p. 45-52.

McIntyre, L.B., 1953, Geology of the Marshall Butte area and vicinity, Mitchell Quadrangle, Oregon: Unpublished M.S. Thesis, Oregon State College, 96p.

McKee, Thomas M., 1970, Preliminary report on fossils, fruits and seeds from the Mammal Quarry of the Clarno Formation, Oregon: The Ore Bin, V. 32, No. 7, p. 117-132.

McWilliams, Robert G., 1972, Stratigraphic evidence for rifting in western Oregon and Washington (abstract): Cordilleran Sec. 68th Annual Meeting, G.S.A., Absta, V. V, No. 3, p. 197-198.

Mellet, James S., 1969, A skull of Hemipsalodon (Mammlaia Deltatheridia) from the Clarno Formation of Oregon: Novitates, Am. Mus. Nat. Hist., No. 2387, p. 1-19.

Merriam, J.C., 1901, A contribution to the geology of the John Day Basin: California University Pub., Dept. of Geo. Bull., V. 2, No. 9, p. 269-314.

Miyashuro, Akiho, 1974, Volcanic rock series in island arcs and active continetal margins: American Journal Science, V. 274, p. 321-355.

Moore, J.G., 1959, The quartz diorite boundary line in the western United States: Journal of Geology, V. 67, p. 198-210.

Nockolds, S.R. and Allen, R., 1953, The geochemistry of some igneous rock series: Geochimica et Cosmochimica Acta, V. 4, p. 105-142.

_____, 1954, Average chemical composition of some igneous rocks: G.S.A. Bulletin, V. 65, p. 1007-1032.

Novitsky, Joyce M. and Rogers, John W., 1973, The Clarno Formation: An example of continental margin volcanism: Cordilleran Section. Abstract. 69th Meeting G.S.A., V. 5, No. 1, p. 87-88.

Oles, K.F. and Enlows, H.E., 1971, Bedrock geology of the Mitchell Quadrangle Wheeler County, Oregon: Ore. Dept. Geo. Min. Ind. Bull., 72, 62p.

Owen, P., 1977, An examination of the Clarno Formation in the vicinity of the Mitchell Fault, Lawson Mountain and Stephenson Mountain area, Jefferson and Wheeler Counties: Unpublished M.S. Thesis, Oregon State University, 166p.

Patterson, R.L., 1965, Geology of part of the northeast quarter of the Mitchell Quadrangle, Oregon: Unpublished M.S. Thesis, Oregon State University, 97p.

Peacock, M.A., 1931, Classification of igneous rock series: Journal of Geology, V. 39, No. 1, p. 54-67.

Peck, D.L., 1960, Cenozoic volcanism in the Oregon Cascades: U.S.G.S. Professional Paper 400-B, p. 308-310.

_____, 1961, John Day Formation near Ashwood, north-central Oregon: U.S.G.S. Professional Paper 424-D, p. D153-D156.

_____, 1964, Geologic reconnaissance of the Antelope-Ashwood area north-central Oregon: U.S.G.S. Bull. 1161-D, p. D1-D26.

Peterson, D.W., 1970, Ash-flow deposits-their character, origin and significance: Journal of Geo. Ed., V. 18, No. 2, p. 66-76.

Phillips, W. Revell, 1971, Mineral optic principles and techniques: W.H. Freeman and Company, San Francisco, Calif., 240p.

Rensberger, John M., 1965, Subdivisions of the John Day Fauna; Preliminary report: G.S.A. Special Paper 82, p. 272.

Roberts, Miriam, 1966, Bibliography of thesis and dissertations on Oregon geology: Supplement to Miscellaneous Paper 7, Ore. Dept. Geo. Min. Ind. Bulletin, 11p.

Robinson, P.T., 1969, High titania alkali-olivine basalt of north-central Oregon, U.S.A.: Contributions to Mineral & Petrol., V. 22, p. 349-360.

_____, 1968, Facies changes in the John Day Formation, Oregon: G.S.A. Special Paper 101, p. 417 (abs.)

_____, 1973, Cretaceous and Cenozoic stratigraphy of north-central Oregon, John Day Formation: in "Geologic field trips in northern Oregon and southern Washington, Ore. Dept. Geo. Min. Ind. Bulletin 72, p. 19-22.

Rogers, J.J.W., 1966, Coincidence of structural and topographic highs during post-Clarno time in north-central Oregon: A.A.P.G. Bulletin, V. 50, No. 2, p. 390-396.

_____, and Novitsky-Evans, Joyce M., 1977, The Clarno Formation of central Oregon, U.S.A. - Volcanism on a thin continental margin: Earth and Planetary Science Letters, V. 34, p. 55-66.

Ross, C.S., and Smith R.L., 1961, Ash-flow tuffs: their origin, geologic relations and identification: U.S.G.S. Professional Paper 366, p. 81.

Schlicker, Herbert G., 1959, Bibliography of thesis on Oregon geology: Ore. Dept. Geo. Min. Ind. Misc. Paper 7, 14p.

Scott, R.A., 1954, Fossil fruits and seeds from Eocene Clarno Formation of Oregon: Paleontolographica, 96b, p. 66-97.

Snook, J.R., 1957, Geology of the Bald Mountain area, Richmond Quadrangle, Oregon: Unpublished M.S. Thesis, Oregon State College, 59p.

Sparks, R.S.J., Self, S. and Walker, G.P.L., 1973, Products of ignimbrite eruption: Geology, V. 1, p. 115-118.

Smith, R.L., 1960a, Ash flows: G.S.A. Bulletin, V. 71, p. 796-842.

_____, 1960b, Zones and zonal variations in welded ash flows: U.S.G.S. Professional Paper 354-F, p. 149-159.

Steere, Margaret L., 1954, Geology of the John Day country, Oregon: The Ore Bin, V. 16, p. 41-47.

Stirton, R.A., 1944, A rhinoceros tooth from the Clarno Eocene of Oregon: Journal of Paleontology, V. 18, p. 265-267.

Swanson, D.A., 1969, Reconnaissance geologic map of the east half of Bend Quadrangle, Crook, Wheeler, Jefferson, Wasco and Deschutes Counties, Oregon: U.S.G.S. Map I-568.

_____, and Robinson, P.T., 1968, Base of the John Day Formation in and near the Horse Heaven Mining District, north-central Oregon: U.S.G.S. Professional Paper 600D, p. D154-D161.

Swarbrick, J.C., 1953, Geology of the Sheep Mountain area and vicinity Mitchell Quadrangle, Oregon: Unpublished M.S. Thesis, Oregon State College, 100p.

Taubeneck, W.H., 1950, Geology of the northeast corner of the Dayville Quadrangle, Oregon: Unpublished M.S. Thesis, Oregon State College, 154p.

Taylor, E.M., 1960, Geology of the Clarno Basin Mitchell Quadrangle, Oregon: Unpublished M.S. Thesis, Oregon State University, 173p.

_____, 1977, Personal communication.

Tuttle, O.F. and Bowen, N.L., 1958, Origin of granite in the light of experimental studies in the system $MaAlSi_3O_8$ - $KAlSi_3O_8$ - SiO_2 - H_2O: Geological Soc. Amer. Mem., No. 74.

Vance, J.A., 1965, Zoning in igneous plagioclase and patchy zoning: Journal of Geol., V. 73, p. 636-651.

Walker, G.W.; Dalrymple, G.B. and Lanphere, M.A., 1974, Index to potassium-argon ages of Cenozoic volcanic rocks of Oregon: U.S.G.S. Miscellaneous Field Studies Map MF-569.

Waters, A.C.; Brown, R.E.; Compton, R.R.; Staples, L.W.; Walker, G.W. and Williams H., 1951, Quicksilver deposits of the Horse Heaven Mining District, Oregon: U.S.G.S. Bulletin, 969-E, p. 105-149.

_____, 1954, John Day Formation west of its type locality (Oregon) (Abs.): Geol. Soc. Amer. Bull., V. 65, No. 12, Pt. 2, p. 1320.

_____, 1966, Stein's Pillar area, central Oregon: The Ore Bin, V. 28, No. 8, p. 137-144.

Watkins, N.D. and Baksi, A.K., 1969, The age of the Picture Gorge Basalt at the type section and at Imnaha, and the maximum duration of a Miocene geomagnetic epoch: G.S.A. abstract for 1968, Special Paper 121, p. 312-313.

White, W.H., 1964, Geology of the Picture Gorge Quadrangle, Oregon: Unpublished M.S. Thesis, Oregon State University, 176p.

Wilkinson, J.F.G., 1968, The petrography of basaltic rocks: in "Basalts", V. 1, Interscience, New York, p. 163-214.

Wilkinson, W.D., 1932, The petrography of the Clarno Formation of Oregon with special reference to the Mutton Mountains: Unpublished PhD Thesis, University of Oregon, 180p.

Williams, Howell, 1948, The ancient volcanoes of Oregon: Ore. Supt. of Higher Education, p. 1-64.

_____, Turner, Francis J. and Gilbert, Charles M., 1954, Petrography, an introduction to the study of rocks in thin sections: W.H. Freeman and Co., San Francisco, Calif., 406p.

Wilson, P.M., 1973 Petrology of the Cenozoic volcanic rocks of the basal Clarno Formation, central Oregon: Unpublished M.A. Thesis, Rice University, Houston, Texas, 47p.

Wolf, J.A. and Hopkins, D.M., 1967, Climatic changes recorded by Tertiary land floras in northwestern North America: in "Tertiary correlation and climatic changes in the Pacific",Pacific Sci. Cong. 11th, Tokyo, 1966, Symposium 25 Tokyo, Sci. Council Japan, p. 67-76.

APPENDICES

Appendix A

Chemical Analysis of Clarno Igneous Rocks

Procedures

The samples were first slabbed and all visible alteration was trimmed away. They were then passed through a crusher, pulverizer and finally small amounts of each sample were reduced to powder in a ball mill. The samples were then heated at 650°C for about 45 minutes to render them anhydrous. They were then mixed with an anhydrous lithium metaborate ($LiBO_2$) flux in proportions of 3 to 1 (flux to sample). This mixture was placed into an oven for approximately one hour at 1100°C and fused. The melt was cast into a small glass button and after cooling one side was ground down to a smooth surface. The buttons were used in an x-ray florescence spectrometer to determine weight percent of TiO_2, CaO, K_2O, Al_2O_3 and total iron as FeO. The buttons were powdered again and the powders were taken into solution and used to determine Na_2O and MgO weight percent by atomic absorption spectrophotometry. Finally, values for SiO_2 were determined from the same solution using a visible light spectrophotometer. The weight percentages were determined with the following calculated accuracies:

FeO	$\pm$	0.1	K_2O	$\pm$	0.05
CaO	$\pm$	0.1	MgO	$\pm$	0.1
Al_2O_3	$\pm$	0.1	Na_2O	$\pm$	0.1
TiO_2	$\pm$	0.05	SiO_2	$\pm$	0.5

Appendix A. Chemical analysis of Clarno igneous rocks.

Sample	JWH-2	JWH-6	JWH-7	JWH-10	JWH-13	JWH-14
SiO_2	66.2	64.3	63.3	62.0	59.0	57.5
Al_2O_3	16.8	16.1	16.2	17.7	16.9	17.0
FeO	4.5	5.6	5.9	5.1	6.8	7.7
CaO	3.5	5.2	5.1	6.0	6.8	6.8
MgO	0.5	2.9	2.0	1.1	3.5	3.9
K_2O	3.00	1.80	1.75	1.65	1.05	1.00
NaO_2	3.7	4.1	3.8	4.1	3.9	3.8
TiO_2	0.75	0.80	1.00	0.80	1.00	1.00
Total	98.95	100.80	99.05	98.45	99.15	98.70

JWH-2 Dacite: elevation 1,800 ft., NE¼,SE¼, Sec. 1, T. 10 S., R. 20 E.

JWH-6 Dacite: elevation 2,000 ft., middle Sec. 1, T. 10 S., R. 20 E.

JWH-7 Porphyritic two-pyroxene bearing dacite: elevation 2,400 ft., middle SW¼, Sec. 1, T. 10 S., R. 20 E.

JWH-10 Andesite: elevation 1,720 ft., SE¼, NE¼, Sec. 1, T. 10 S., R. 20 E.

JWH-13 Two-pyroxene bearing andesite: elevation 1,560 ft., NE¼, NE¼, Sec. 2, T. 10 S., R. 20 E.

JWH-14 Two-pyroxene bearing basaltic andesite: elevation 1,560 ft., NE¼, NW¼, Sec. 2, T. 10 S., R. 20 E.

Sample	JWH-15A	JWH-15B	JWH-16	JWH-17	JWH-18	JWH-38
SiO_2	58.2	65.2	65.2	63.9	64.3	58.7
Al_2O_3	16.3	16.4	16.0	15.9	16.0	16.8
FeO	8.1	4.8	5.1	5.3	5.3	7.2
CaO	6.4	4.8	4.9	5.2	5.2	8.0
MgO	3.3	1.3	2.1	2.0	2.0	3.5
K_2O	1.25	1.90	1.90	1.80	1.80	0.80
Na_2O	4.0	4.3	4.1	4.3	3.9	3.1
TiO_2	1.30	0.75	0.70	0.80	0.75	1.20
Total	98.85	99.45	100.00	99.20	99.25	99.30

JWH-15A Two-pyroxene bearing andesite: elevation 1,600 ft., middle Sec. 2, T. 10 S., R. 20 E.

JHW-15B Porphyritic two-pyroxene bearing dacite: elevation 2,000 ft., NW¼, SE¼, Sec. 2, T. 10 S., R. 20 E.

JWH-16 Porphyritic two-pyroxene bearing dacite: elevation 2,100 ft., NW¼, SE¼, Sec. 2, T. 10 S., R. 20 E.

JWH-17 Augite bearing dacite: elevation 2,200 ft., NW¼, SE¼, Sec. 2, T. 10 S., R. 20 E.

JWH-18 Porphyritic two-pyroxene bearing dacite: elevation 2,360 ft., NW¼, SE¼, Sec. 2, T. 10 S., R. 20 E.

JWH-38 Quartz bearing andesite: elevation 1,950 ft., SW¼, NE¼, Sec. 11, T. 10 S., R. 20 E.

Sample	JWH-39	JWH-40	JWH-41	JWH-46	JWH-49	JWH-50
SiO_2	56.3	64.5	57.5	64.6	64.9	63.3
Al_2O_3	18.0	15.8	18.0	16.3	16.3	16.7
FeO	7.3	5.5	7.3	5.7	5.5	5.7
CaO	7.8	4.4	7.5	4.7	4.6	5.0
MgO	4.5	1.7	4.3	1.6	1.5	1.7
K_2O	0.65	1.90	0.95	1.95	1.85	2.30
Na_2O	4.0	4.3	3.7	4.4	4.5	3.8
TiO_2	1.10	1.00	1.10	1.00	1.00	1.00
Total	99.65	99.10	100.35	100.25	100.15	99.50

JWH-39 Porphyritic two-pyroxene bearing basaltic andesite: elevation 2,000 ft., NE¼, SE¼, Sec. 11, T. 10 S., R. 20 E.

JWH-40 Porphyritic two-pyroxene bearing dacite: elevation 2,100 ft., NE¼, SE¼, Sec. 11, T. 10 S., R. 20 E.

JWH-41 Porphyritic two-pyroxene bearing andesite: elevation 2,140 ft., NE¼, SE¼, Sec. 11, T. 10 S., R. 20 E.

JWH-46 Porphyritic two-pyroxene bearing dacite: elevation 2,120 ft., SW¼, SE¼, Sec. 1, T. 10 S., R. 20 E.

JWH-49 Porphyritic two-pyroxene bearing dacite: elevation 2,320 ft., SW¼, NW¼, Sec. 12, T. 10 S., R. 20 E.

JWH-50 Porphyritic two-pyroxene bearing dacite: elevation 2,360 ft., SW¼, NW¼, Sec. 12, T. 10 S., R. 20 E.

Sample	JWH-52	JWH-56	JWH-64	JWH-68	JWH-70	JWH-72
SiO_2	64.2	64.2	57.2	63.3	56.9	60.5
Al_2O_3	16.8	17.2	16.8	15.9	17.5	15.7
FeO	4.0	5.5	8.7	5.2	7.3	5.8
CaO	5.2	5.0	8.1	5.4	7.4	6.0
MgO	1.8	1.5	3.5	3.2	4.5	3.8
K_2O	1.80	1.65	0.80	1.60	0.95	1.55
Na_2O	4.5	4.6	3.5	4.1	4.0	3.9
TiO_2	0.70	1.00	1.20	0.70	1.05	0.75
Total	99.00	100.65	99.80	99.40	99.60	98.00

JWH-52 Porphyritic quartz bearing dacite: elevation 2,200 ft., NE¼, SE¼, Sec. 11, T. 10 S., R. 20 E.

JWH-56 Porphyritic two-pyroxene bearing dacite: elevation 1,880 ft., SE¼, NW¼, Sec. 13, T. 10 S., R. 20 E.

JWH-64 Basaltic andesite: elevation 1,840 ft., SW¼, SE¼, Sec. 11, T. 10 S., R. 20 E.

JWH-68 Porphyritic quartz bearing dacite: elevation 2,100 ft., center Sec. 14, T. 10 S., R. 20 E.

JWH-70 Porphyritic two-pyroxene bearing basaltic andesite: elevation 2,450 ft., NW¼, SW¼, Sec 14, T. 10 S., R. 20 E.

JWH-72 Porphyritic quartz bearing andesite: elevation 2,000 ft., NW¼, SW¼, Sec. 3, T. 10 S., R. 20 E.

Sample	JWH-73	JWH-74	JWH-76	JWH-77	JWH-78	JWH-80
SiO_2	59.3	58.0	55.1	59.3	58.5	58.0
Al_2O_3	15.8	16.8	14.9	15.9	16.8	16.9
FeO	6.2	4.9	7.6	5.3	7.4	7.4
CaO	6.1	7.0	8.9	6.1	8.1	7.9
MgO	4.3	4.2	6.7	4.5	3.9	3.7
K_2O	1.35	1.50	0.90	1.25	0.70	1.00
Na_2O	3.9	3.6	3.2	3.8	3.6	3.8
TiO_2	0.80	0.85	0.95	0.85	1.00	1.00
Total	97.75	96.85	98.25	97.00	100.00	99.70

JWH-73 Porphyritic quartz bearing andesite: elevation 2,050 ft., SW¼, SW¼, Sec. 3, T. 10 S., R. 20 E.

JWH-74 Porphyritic quartz bearing andesite: elevation 2,350 ft., NE¼, NE¼, Sec. 9, T. 10 S., R. 20 E.

JWH-76 Two-pyroxene basaltic andesite dike: elevation 1,900 ft., SW¼, SE¼, Sec. 3, T. 10 S., R. 20 E.

JWH-77 Porphyritic quartz bearing andesite: elevation 1,900 ft., SW¼, SE¼, Sec. 3, T. 10 S., R. 20 E.

JWH-78 Porphyritic two-pyroxene bearing andesite: elevation 1,850 ft., SW¼, SE¼, Sec. 3, T. 10 S., R. 20 E.

JWH-80 Porphyritic two-pyroxene bearing andesite: elevation 1,800 ft., SW¼, NW¼, Sec. 3, T. 10 S., R. 20 E.

Sample	JWH-81	JWH-83	JWH-86	JWH-90	JWH-91	JWH-93
SiO_2	60.8	56.7	61.2	55.0	56.7	58.8
Al_2O_3	15.4	16.9	16.1	16.1	15.9	17.6
FeO	6.5	7.7	6.0	8.7	6.9	6.4
CaO	6.0	6.7	5.9	7.5	7.6	7.0
MgO	3.8	3.5	3.9	4.7	5.1	4.1
K_2O	1.60	1.00	1.45	0.75	1.50	1.55
Na_2O	4.0	4.0	3.8	4.3	3.7	3.7
TiO_2	0.80	1.00	0.75	1.15	0.90	0.90
Total	98.90	97.50	99.10	98.20	98.30	100.05

JWH-81 Andesite: elevation 1,540 ft., NE¼, NW¼, Sec. 3, T. 10 S., R. 20 E.

JWH-83 Porphyritic two-pyroxene bearing basaltic andesite: elevation 1,560 ft., NW¼, NE¼, Sec. 3, T. 10 S., R. 20 E.

JWH-86 Porphyritic hypersthene and quartz bearing andesite: elevation 1,840 ft., SE¼, NE¼, Sec. 4, T. 10 S., R. 20 E.

JWH-90 Porphyritic two-pyroxene bearing basaltic andesite: elevation 2,600 ft., SW¼, NW¼, Sec. 9, T. 10 S., R. 20 E.

JWH-91 Porphyritic basaltic andesite: elevation 2,800 ft., NW¼, SW¼, Sec. 9, T. 10 S., R. 20 E.

JWH-93 Porphyritic augite and quartz bearing andesite: elevation 2,750 ft., SW¼, NE¼, Sec. 9, T. 10 S., R. 20 E.

Sample	JWH-99	JWH-100	JWH-102	JWH-103	JWH-105	JWH-110
SiO_2	65.8	62.4	61.7	60.5	61.3	60.0
Al_2O_3	16.4	16.4	16.4	17.4	16.2	17.7
FeO	3.5	6.0	5.2	5.9	5.7	4.2
CaO	4.3	5.2	5.6	6.0	5.4	7.0
MgO	1.3	3.0	2.8	2.3	1.9	4.3
K_2O	1.95	2.05	1.60	1.40	1.75	1.10
Na_2O	4.6	3.7	3.9	4.5	4.3	3.9
TiO_2	0.85	0.70	0.90	1.15	0.80	1.10
Total	98.70	99.45	98.10	99.15	97.35	99.30

JWH-99 Porphyritic hypersthene bearing dacite: elevation 2,400 ft., NE¼, SW¼, Sec. 10, T. 10 S., R. 20 E.

JWH-100 Porphyritic quartz and augite bearing andesite: elevation 2,400 ft., NE¼, SE¼, Sec. 9, T. 10 S., R. 20 E.

JWH-102 Porphyritic two-pyroxene bearing andesite: elevation 3,100 ft., NE¼, NW¼, Sec. 16, T. 10 S., R. 20 E.

JWH-103 Porphyritic hypersthene bearing andesite: elevation 3,100 ft., SE¼, NE¼, Sec. 16, T. 10 S., R. 20 E.

JWH-105 Epidote bearing andesite: elevation 1,800 ft., NW¼, SW¼, Sec. 11, T. 10 S., R. 20 E.

JWH-110 Porphyritic two-pyroxene bearing andesite: elevation 2,800 ft., SE¼, SE¼, Sec. 15, T. 10 S., R. 20 E.

Sample	JWH-113	JWH-119	JWH-123	JWH-134	JWH-138	JWH-140
SiO_2	56.4	57.9	60.5	57.8	57.5	62.5
Al_2O_3	17.3	17.3	17.2	17.8	16.8	15.5
FeO	7.6	8.2	6.0	6.1	7.6	7.8
CaO	7.5	6.6	6.2	7.5	7.0	4.7
MgO	4.3	3.9	2.8	4.3	4.6	1.7
K_2O	1.00	1.00	0.65	1.00	1.00	2.20
Na_2O	3.7	4.3	4.2	4.0	3.8	3.7
TiO_2	1.10	1.40	1.15	1.10	1.05	1.10
Total	98.90	100.60	98.70	99.60	99.35	99.20

JWH-113 Porphyritic two-pyroxene bearing basaltic andesite: elevation 2,200 ft., NE¼, NE¼, Sec. 15, T. 10 S., R. 20 E.

JWH-119 Porphyritic augite and quartz bearing basaltic andesite: elevation 2,760 ft., SW¼, SE¼, Sec. 21, T. 10 S., R. 20 E.

JWH-123 Porphyritic two-pyroxene bearing andesite: elevation 3,000 ft., NE¼, SE¼, Sec. 21, T. 10 S., R. 20 E.

JWH-134 Porphyritic two-pyroxene bearing basaltic andesite: elevation 3,100 ft., SE¼, SW¼, Sec. 21, T. 10 S., R. 20 E.

JWH-138 Porphyritic two-pyroxene bearing basaltic andesite: elevation 2,800 ft., SW¼, NW¼, Sec. 28, T. 10 S., R. 20 E.

JWH-140 Porphyritic two-pyroxene bearing andesite: elevation 2,960 ft., SE¼, NW¼, Sec. 28, T. 10 S., R. 20 E.

Sample	JWH-141	JWH-147	JWH-148	JWH-152	JWH-159	JWH-163
SiO_2	56.5	64.5	65.0	56.8	60.8	65.5
Al_2O_3	17.2	15.8	16.4	16.5	16.2	15.8
FeO	7.7	5.7	4.8	7.9	6.4	5.0
CaO	7.1	4.8	4.0	8.1	6.4	4.2
MgO	4.6	1.7	1.3	5.0	4.1	0.9
K_2O	0.95	1.85	1.90	0.85	1.30	2.15
Na_2O	3.9	3.9	4.3	3.6	3.9	4.5
TiO_2	1.10	1.00	1.00	1.25	0.85	0.85
Total	99.05	99.25	98.70	100.00	99.95	98.90

JWH-141 Porphyritic two-pyroxene bearing basaltic andesite: elevation 3,180 ft., NW¼, SW¼, Sec. 28, T. 10 S., R. 20 E.

JWH-147 Porphyritic two-pyroxene bearing dacite: elevation 2,700 ft., NE¼, SE¼, Sec. 28, T. 10 S., R. 20 E.

JWH-148 Porphyritic augite bearing dacite: elevation 2,650 ft., NE¼, SE¼, Sec. 28, T. 10 S., R. 20 E.

JWH-152 Porphyritic quartz bearing basaltic andesite: elevation 1,760 ft., NW¼, SE¼, Sec. 11, T. 10 S., R. 20 E.

JWH-159 Porphyritic two-pyroxene bearing andesite: elevation 3,600 ft., SE¼, NE¼, Sec. 32, T. 10 S., R. 20 E.

JWH-163 Porphyritic augite bearing dacite: elevation 2,850 ft., NW¼, NW¼, Sec. 34, T. 10 S., R. 20 E.

Sample	JWH-166	JWH-167	JWH-174	JWH-184	JWH-186	JWH-187
SiO_2	64.6	70.0*	61.6	59.2	71.3**	67.5
Al_2O_3	16.0	14.0	15.5	17.6	14.0	16.1
FeO	5.2	3.8	8.0	6.8	3.8	4.4
CaO	4.9	2.2	5.4	6.5	2.2	2.2
MgO	2.4	0.2	2.1	3.3	0.4	0.4
K_2O	1.75	3.08	1.70	1.20	3.20	3.90
Na_2O	3.9	4.8	4.1	3.9	4.4	3.9
TiO_2	0.85	0.60	1.45	1.05	0.50	0.50
Total	99.60	98.65	99.85	99.55	99.85	98.90

JWH-166 Porphyritic two-pyroxene bearing dacite: elevation 3,600 ft., SW¼, SW¼, Sec. 33, T. 10 S., R. 20 E.

JWH-167 Rhyodacite: elevation 3,400 ft., SW¼, SW¼, Sec. 33, T. 10 S., R. 20 E.

JWH-174 Porphyritic two-pyroxene bearing andesite: elevation 2,360 ft., NW¼, SW¼, Sec. 23, T. 10 S., R. 20 E.

JWH-184 Porphyritic two-pyroxene bearing andesite: elevation 1,820 ft., SW¼, NW¼, Sec. 25, T. 10 S., R. 20 E.

JWH-186 Porphyritic pyroxene bearing dacite: elevation 2,000 ft., NE¼, NE¼, Sec. 35, T. 10 S., R. 20 E.

JWH-187 Porphyritic pyroxene bearing dacite: elevation 2,200 ft., NW¼, SW¼, Sec. 36, T. 10 S., R. 20 E.

* minor secondary quartz
** large amounts of secondary quartz - should be similar to JWH-187

Appendix B

Harker variation diagrams for the Clarno rocks. Includes SiO_2, FeO, MgO, CaO, Al_2O_3, TiO_2, Na_2O and K_2O. (Compiled from data in Appendix A).

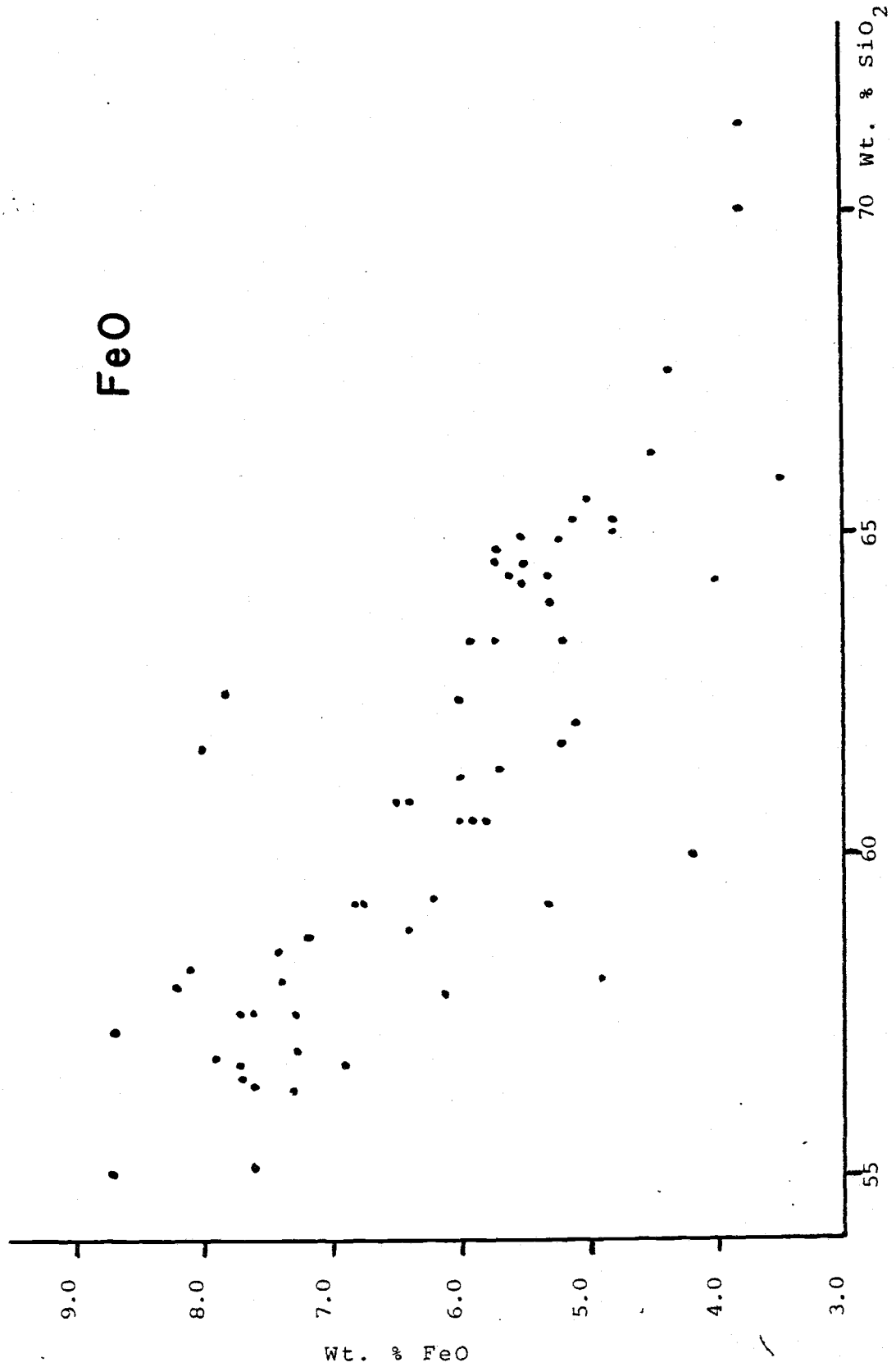
FeO
Wt. % FeO
9.0
8.0
7.0
6.0
5.0
4.0
3.0
55
60
65
70 Wt. % SiO2

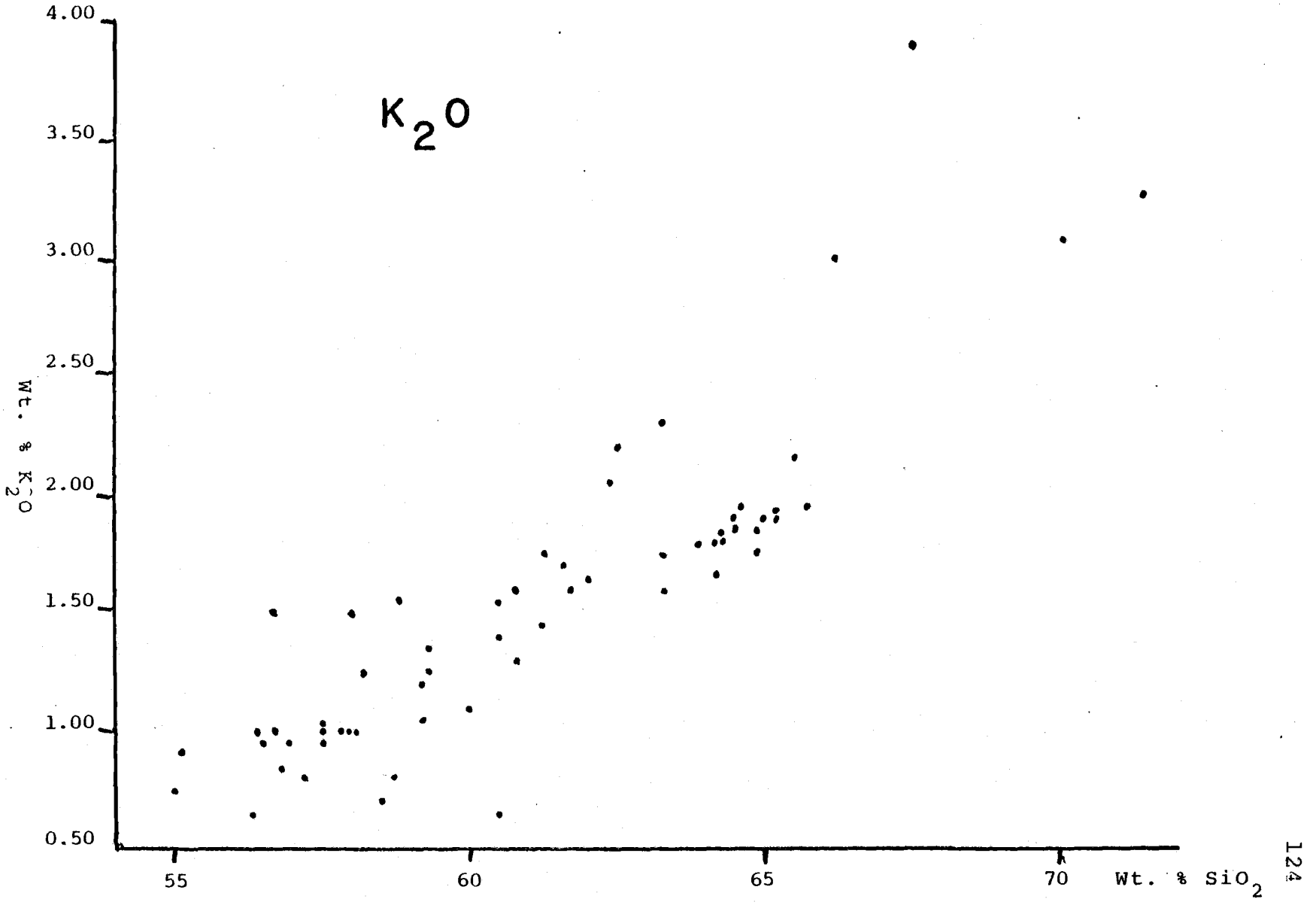
K_2O
4.00
3.50
3.00
2.50
2.00
1.50
1.00
0.50
Wt. % K_2O
55
60
65
70
Wt. % SiO_2

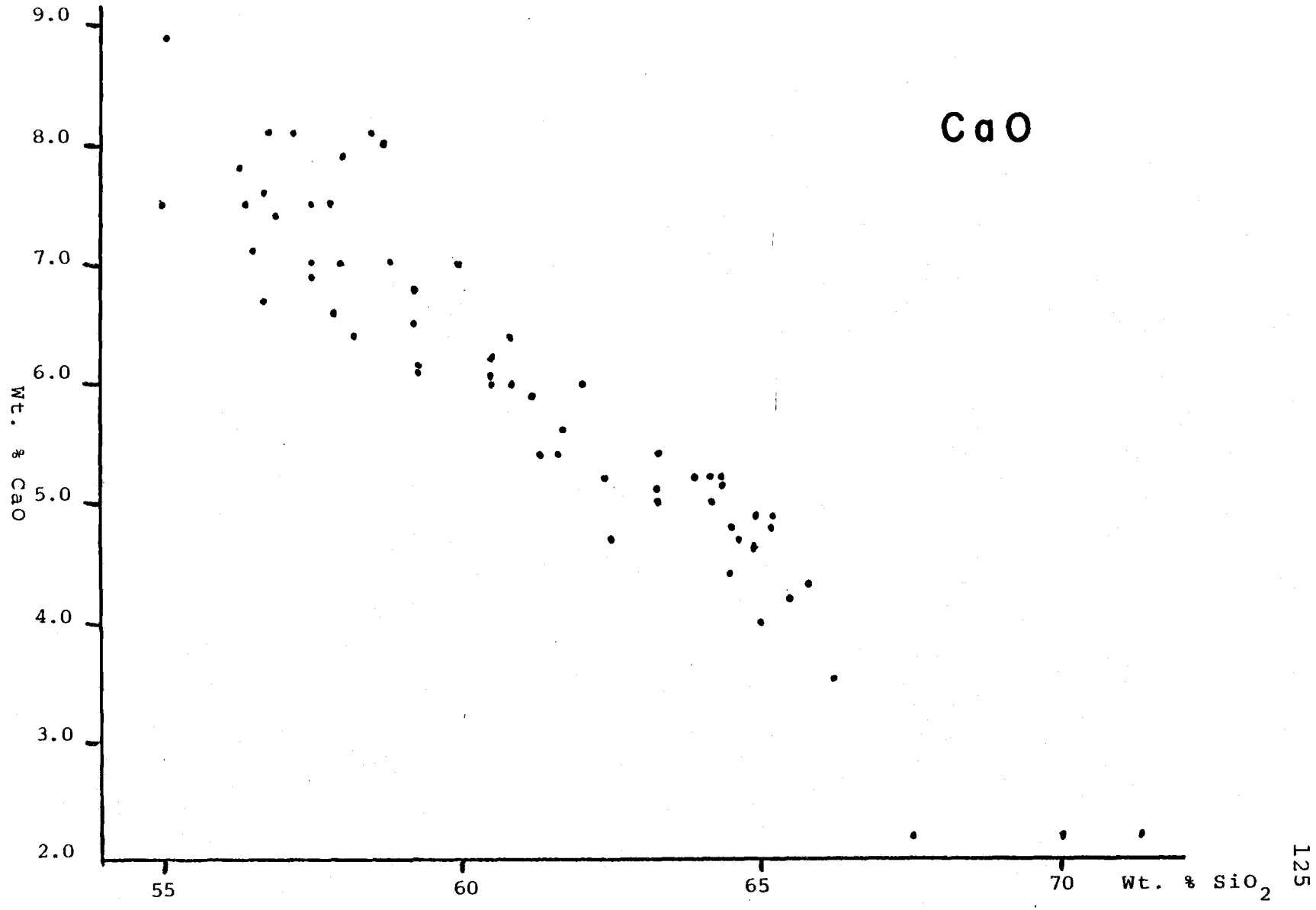
CaO
9.0
8.0
7.0
6.0
5.0
4.0
3.0
2.0
Wt. % CaO
55
60
65
70
Wt. % SiO2

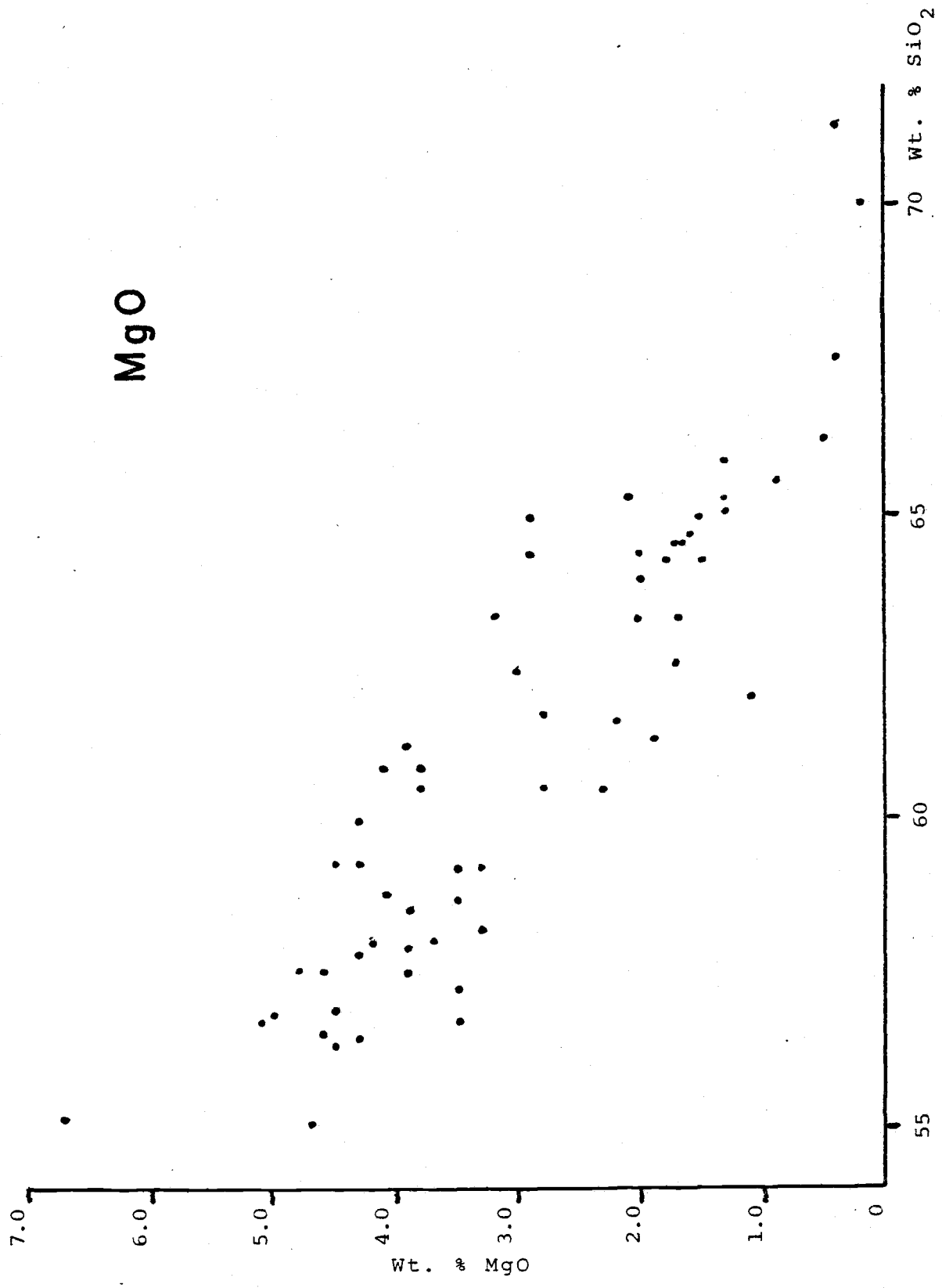
MgO
Wt. % MgO
7.0
6.0
5.0
4.0
3.0
2.0
1.0
0
55
60
65
70
Wt. % SiO2

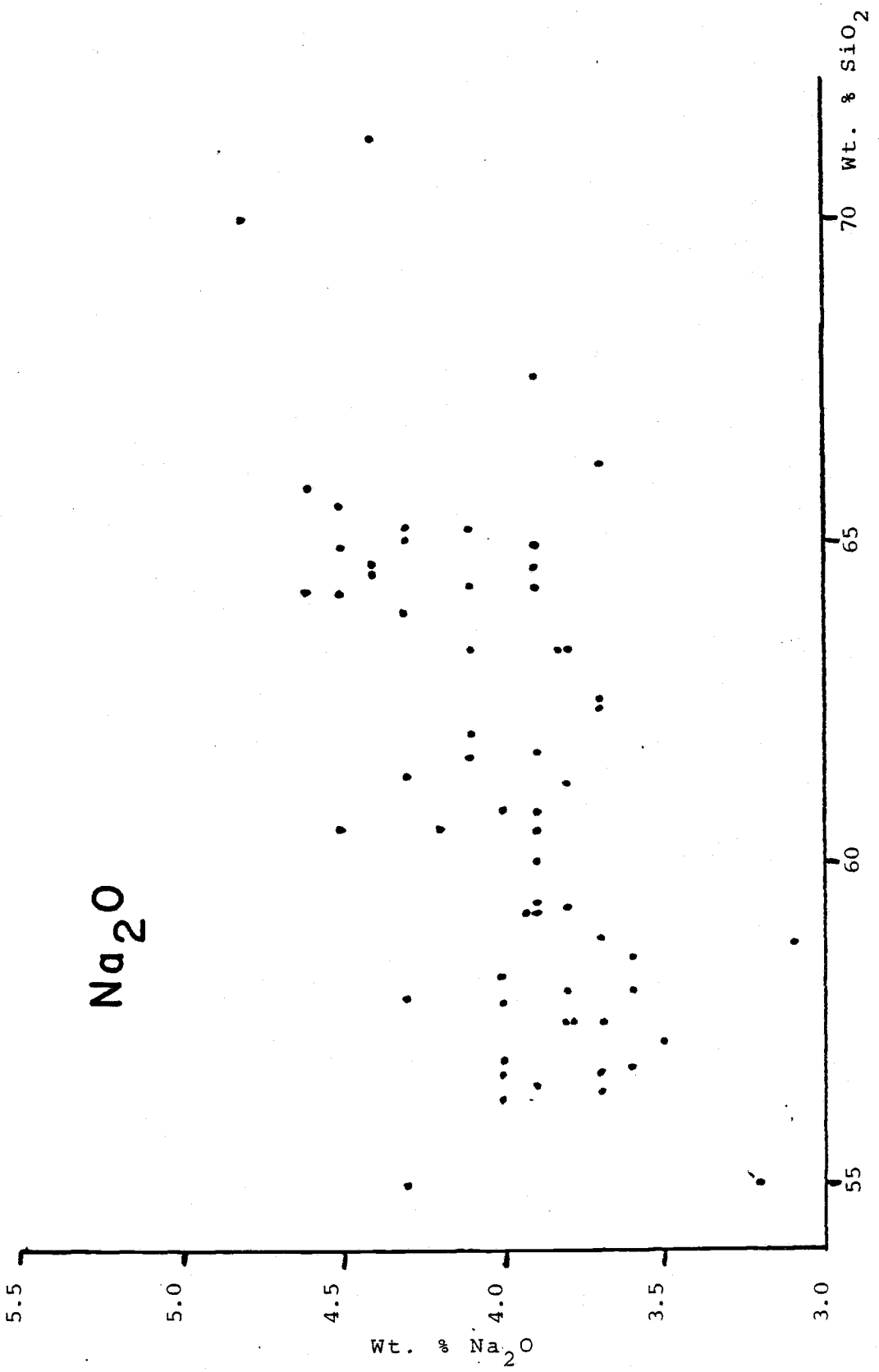
Na_2O
Wt. % Na_2O
5.5
5.0
4.5
4.0
3.5
3.0
55
60
65
70
Wt. % SiO_2

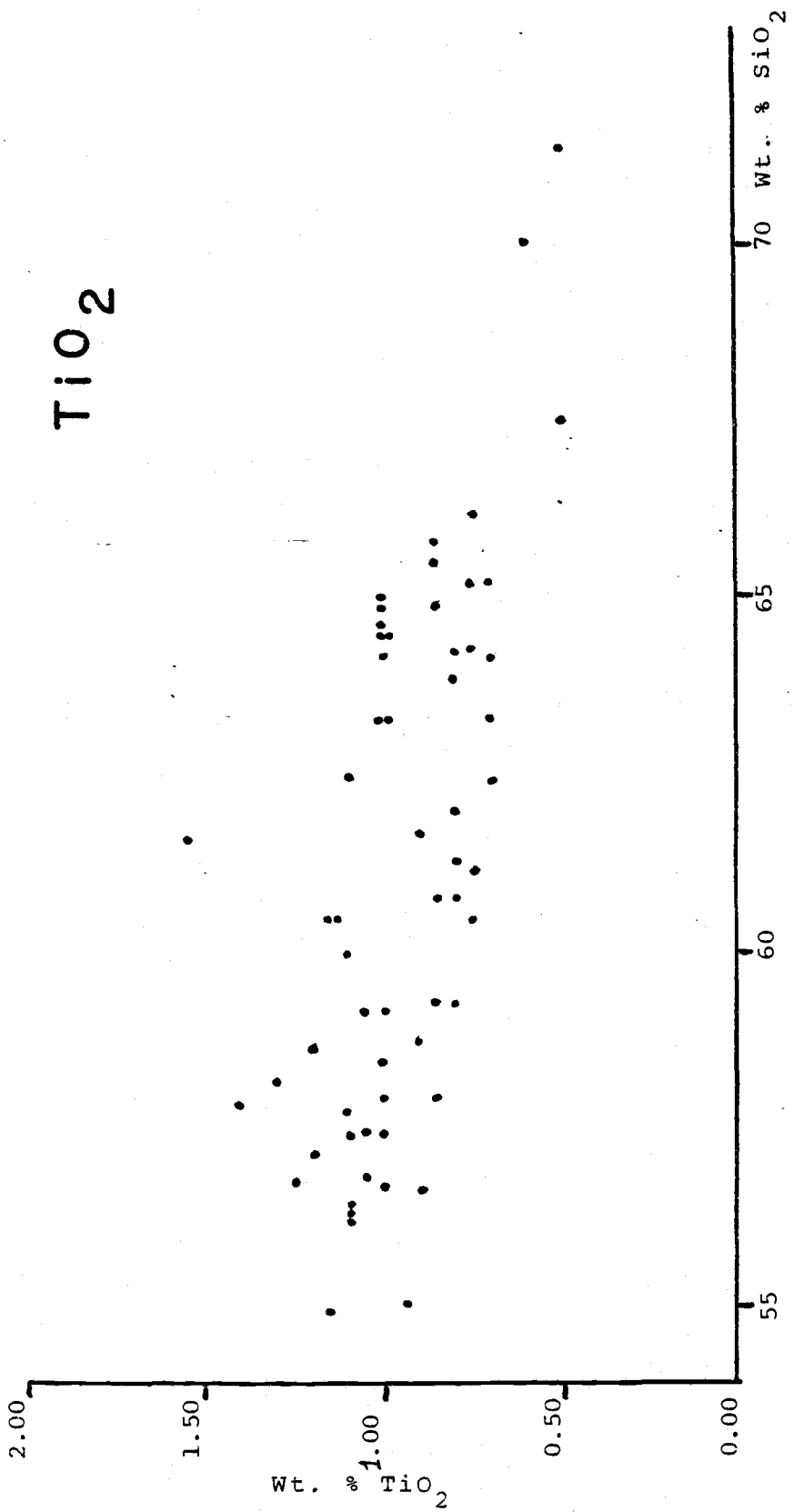
TiO2
Wt. % TiO2
2.00
1.50
1.00
0.50
0.00
55
60
65
70 Wt. % SiO2

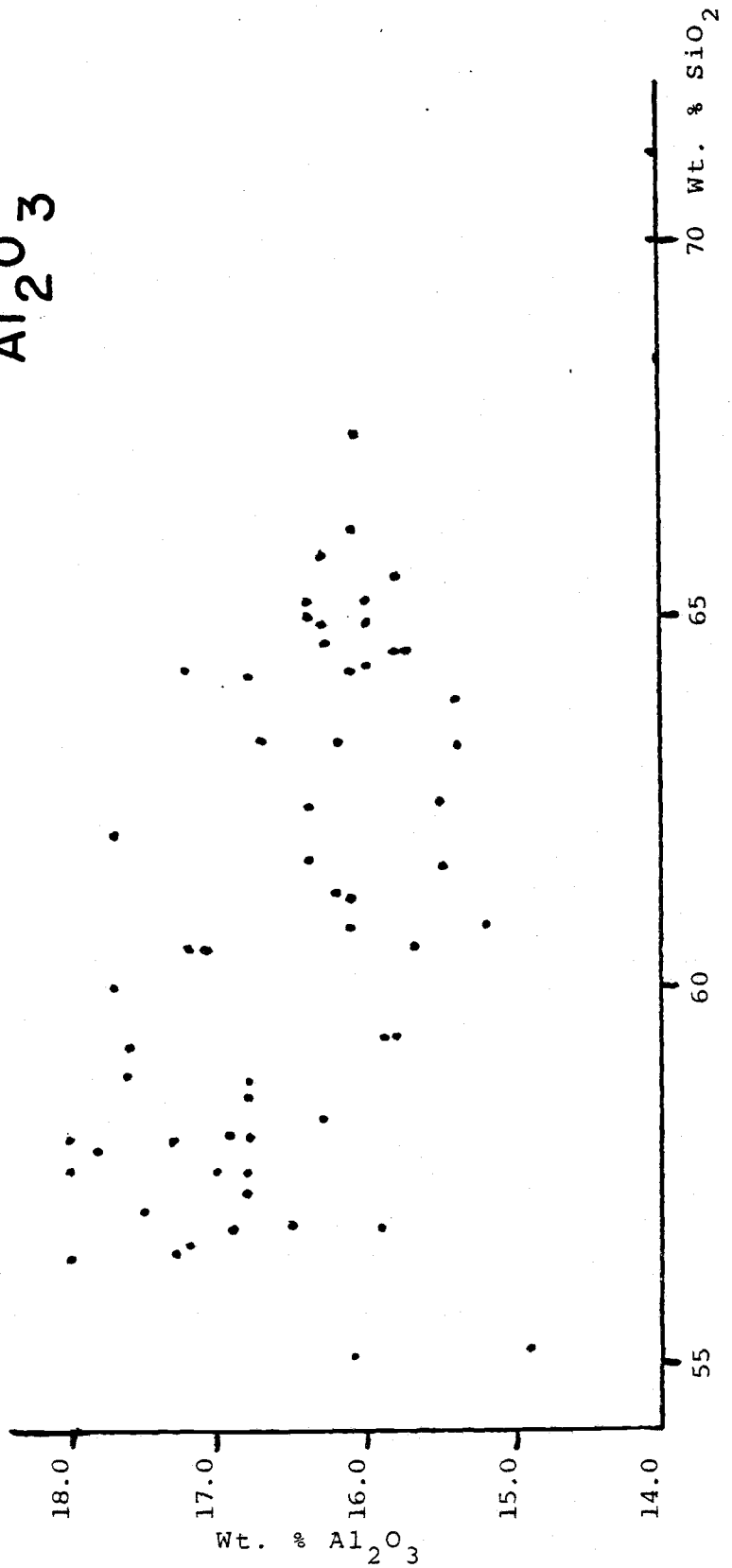
Al_2O_3
Wt. % Al_2O_3
18.0
17.0
16.0
15.0
14.0
55
60
65
70 Wt. % SiO_2